P-139

NASA Contractor Report 182168

Free-Piston Stirling Engine Conceptual Design and Technologies for Space Power

Phase I—Final Report

L. Barry Penswick and William T. Beale
Sunpower, Inc.
Athens, Ohio

and

J. Gary Wood, *Consultant*
Albany, Ohio

January 1990

Prepared for
Lewis Research Center
Under Contract NAS3-23885

Date for general release January 1992

National Aeronautics and
Space Administration

FREE-PISTON STIRLING ENGINE CONCEPTUAL DESIGN AND TECHNOLOGIES FOR SPACE POWER – PHASE I FINAL REPORT

Summary

As part of the SP-100 program, Sunpower, Inc. completed under contract for NASA Lewis a phase I effort to design a free-piston Stirling engine (FPSE) for a space dynamic power conversion system. SP-100 is a combined DOD/DOE/NASA program to develop nuclear power for space. This work by Sunpower was completed in the initial phases of the SP-100 program prior to the power conversion concept selection for the Ground Engineering System (GES). Stirling engine technology development as a growth option for SP-100 is continuing after this phase I effort.

Following a review of various engine concepts, a single-cylinder engine with a linear alternator was selected for the remainder of the study. The relationships of specific mass and efficiency versus temperature ratio were determined for a power output of 25 kWe. This parametric study was done for a temperature ratio range of 1.5 to 2.0 and for hot-end temperatures of 875 K and 1075 K.

Sunpower then completed a conceptual design of a 1080 K FPSE with a linear alternator producing 25 kWe output. This was a single-cylinder engine designed for a 62,000 hour life and a temperature ratio of 2.0. The heat transport systems were pumped liquid-metal loops on both the hot and cold ends. These specifications were selected to match the SP-100 power system designs that were being evaluated at that time. The hot end of the engine used both refractory and superalloy materials; the hot-end pressure vessel featured an insulated design that allowed use of the superalloy material.

The design was supported by the hardware demonstration of two of the component concepts – the hydrodynamic gas bearing for the displacer and the dynamic balance system. The hydrodynamic gas bearing was demonstrated on a test rig at Sunpower. The dynamic balance system was tested on the 1 kW RE-1000 engine at NASA Lewis.

Introduction

As part of the SP-100 program, Sunpower, Inc. completed under contract for NASA Lewis a phase I effort to design a free-piston Stirling engine (FPSE) for a space dynamic power conversion system. SP-100 is a combined DOD/DOE/NASA program to develop nuclear power for space.

The free-piston Stirling engine has been identified as having several very attractive features for space power applications. It has a high efficiency and can achieve that efficiency at low engine temperature ratios. Low temperature ratios and high efficiencies allow power system operation at high cold-end temperatures for lower radiator mass and area or possible use of a lower-temperature reactor. FPSE values of efficiency and specific mass allow minimizing overall system mass compared to other power conversion systems. Having only two to three moving parts per cylinder, utilizing noncontacting gas bearings on these moving parts, and using a hermetically sealed system give the potential for long life and high reliability. The FPSE can be dynamically balanced in either single-cylinder or opposed-piston configurations.

Stirling engine technology development under the SP-100 program began in the 1983 to 1984 time frame with contracted efforts at Sunpower, Inc., and Mechanical Technology, Inc. (MTI). MTI designed, fabricated, and tested the opposed-piston 25 kW Space Power Demonstrator Engine (SPDE) to show scaling to larger power levels and engine operation at a temperature ratio of 2.0. The SPDE had a hot-end temperature of 650 K. The SPDE is described in reference 1.

Sunpower, Inc. in their phase I effort, completed the conceptual design of a single-cylinder 25 kW FPSE with a linear alternator (LA) optimized for the lifetimes and temperatures appropriate for a space power system. This engine design used a temperature

ratio of 2.0 but with a hot-end temperature of 1080 K. The heat transport systems were pumped liquid-metal loops on both the hot and cold ends. These heat transport systems and the engine temperatures were chosen to correspond with the SP-100 Stirling engine power system designs that were being studied at that time. The hot end of the engine used both refractory and superalloy materials by employing an insulated pressure vessel design.

In support of the design, Sunpower demonstrated in hardware tests the feasibility of two key component technologies – hydrodynamic gas bearings and a dynamic balance system. Also completed were parametric analyses to define the FPSE/LA specific mass and efficiency for various temperature ratios. These phase I efforts are the subject of this report.

The phase I work ended with the selection of thermoelectrics as the power conversion concept for the SP-100 Ground Engineering System (GES). Free-piston Stirling engines were identified as a growth option for SP-100 offering increased power output and lower system mass and radiator area. Stirling engine technology development has continued under the NASA CSTI High Capacity Power Program on Conversion Systems for Nuclear Applications, a part of the SP-100 program. An overview of this work is given in reference 2. Sunpower modified their phase I design to use superalloy materials exclusively for the hot-end parts (no refractories) and to use heat pipes as the hot-end heat transport system. This design is reported in reference 3.

Task 1 Parametric Study

The basic input requirements for the Task 1 Parametric Study are shown in Table 1 and represent what was believed to be the range of operating requirements for the SP-100 power module. At the completion of the study, it was expected that the material shown in Table 2 would be made available to the NASA/Lewis project manager. After the start of the program, other issues were requested as a portion of the basic parametric results; these were growth potential of the current designs and modification of the results to a SPDE engine configuration.

TABLE 1: PARAMETRIC STUDY REQUIREMENTS

Power module power output	25 kW(e)
Power module thermal efficiency	> 25 %
Hot-end temperature	875 K and 1075 K
Temperature ratio	2.0 -- 1.75 -- 1.50
Operating life	62,000 hours
Working fluid	Helium
Pumped liquid-metal loop or heat pipe	
Balanced system	

TABLE 2: PARAMETRIC STUDY REQUIRED RESULTS

Percent Carnot efficiency vs. TH/TC

Specific mass vs. TH/TC

Optimized with respect to mass and efficiency

Operating conditions

Size

Principle loss mechanisms detailed

The basic approach taken in the parametric review was to investigate a number of Stirling engine concepts, select a specific configuration for review by NASA/Lewis, and after NASA approval, carry out the detailed analysis on this specific configuration. Throughout this effort a close NASA/ Sunpower interface was maintained to assure that the most relevant inputs from the ongoing system studies could be included in the designs.

Stirling Engine Concepts

During this phase of the program a wide ranging review of various Stirling engine concepts was carried out to see if any nonconventional concepts showed major advantages over the conventional free-piston linear alternator (FPLA) arrangement. The initial goal of this effort centered on the issue of potentially having a system with a rotary output driving a conventional high-speed rotary alternator. This required the investigation of a number of possible converters for the interface between the linear motion of the free-piston Stirling engine (FPSE) and the rotary input to the alternator. Based on this review, it was noted

that the introduction of this converter reduced the usable range of temperature ratios that could be attained with reasonable levels of Stirling engine and rotary alternator technology. Also, a number of component life issues concerning hydraulic and turbine converters were investigated. At the completion of this effort, it was evident that no clear advantage existed for the rotary output system over the more conventional FPLA arrangement.

Power Module Configuration

It was then decided that the effort should focus on the FPLA arrangements which had reached a relatively advanced level of development to maximize the applicability of the parametric results. A number of configurations were reviewed with the major criteria including not only the complexity of the design, but also the overall balance of the system to avoid excessive loads being transferred to the spacecraft. After this review, three arrangements remained as possible designs for the parametric studies. These are shown in Figures 1, 2, and 3. The conventional arrangement, shown in Figure 1, was selected for further review for the primary reasons listed below:

a. The major results of the parametric studies will have the highest accuracy with this arrangement since it has undergone considerably more hardware development than any other configuration.
b. With very simple changes in the hot-end heat exchanger portion of this concept, it can be modified into an SPDE configuration. This will allow the results to have wider applicability.
c. It has the least number of moving components of the concepts considered, which would improve reliability.
d. Active control schemes for the displacer and piston are more easily incorporated in this arrangement due to the reduced number of components and potential interaction between them.

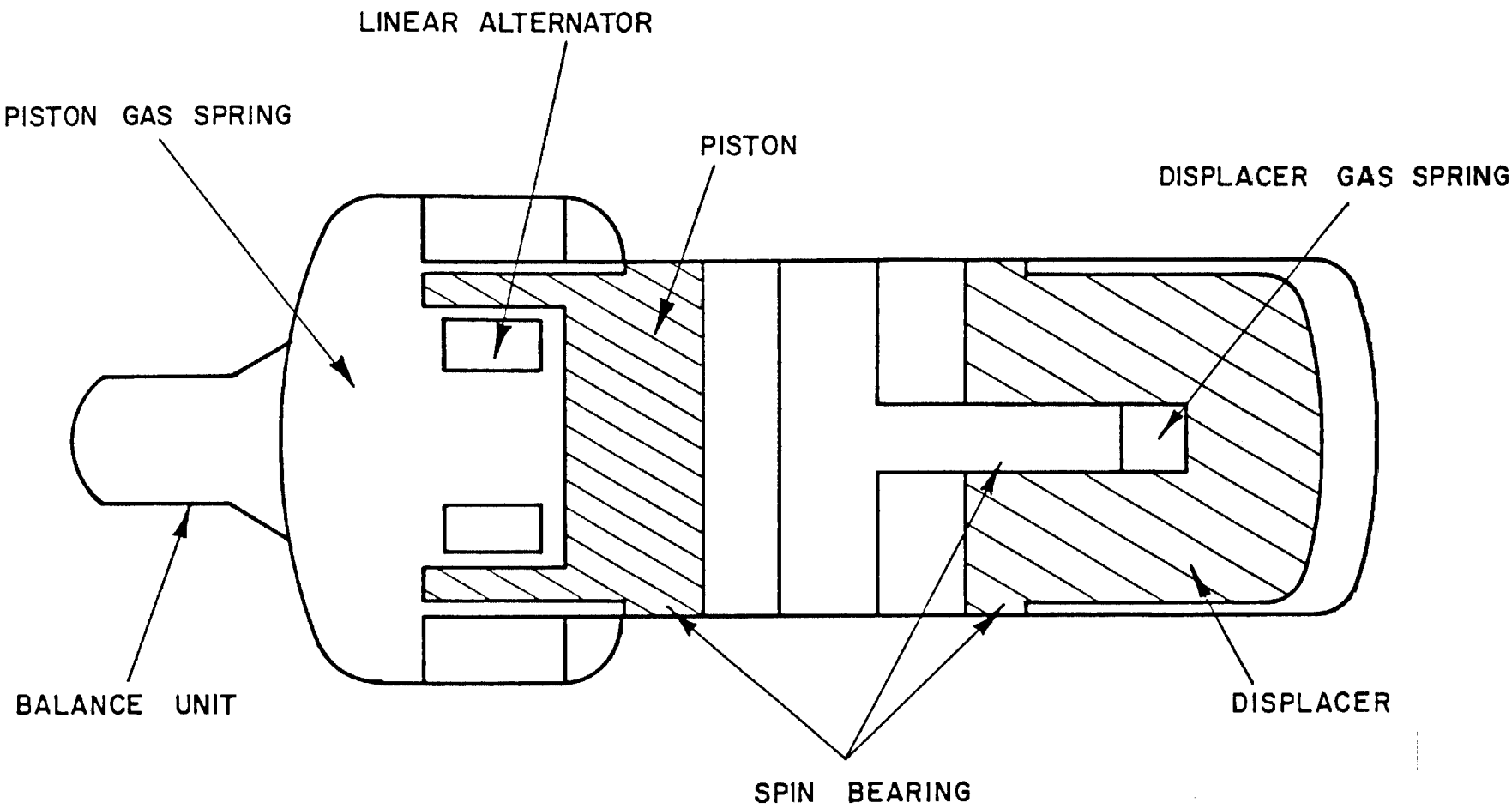

Figure 1: BASELINE ENGINE CONFIGURATION FOR PARAMETRIC REVIEW

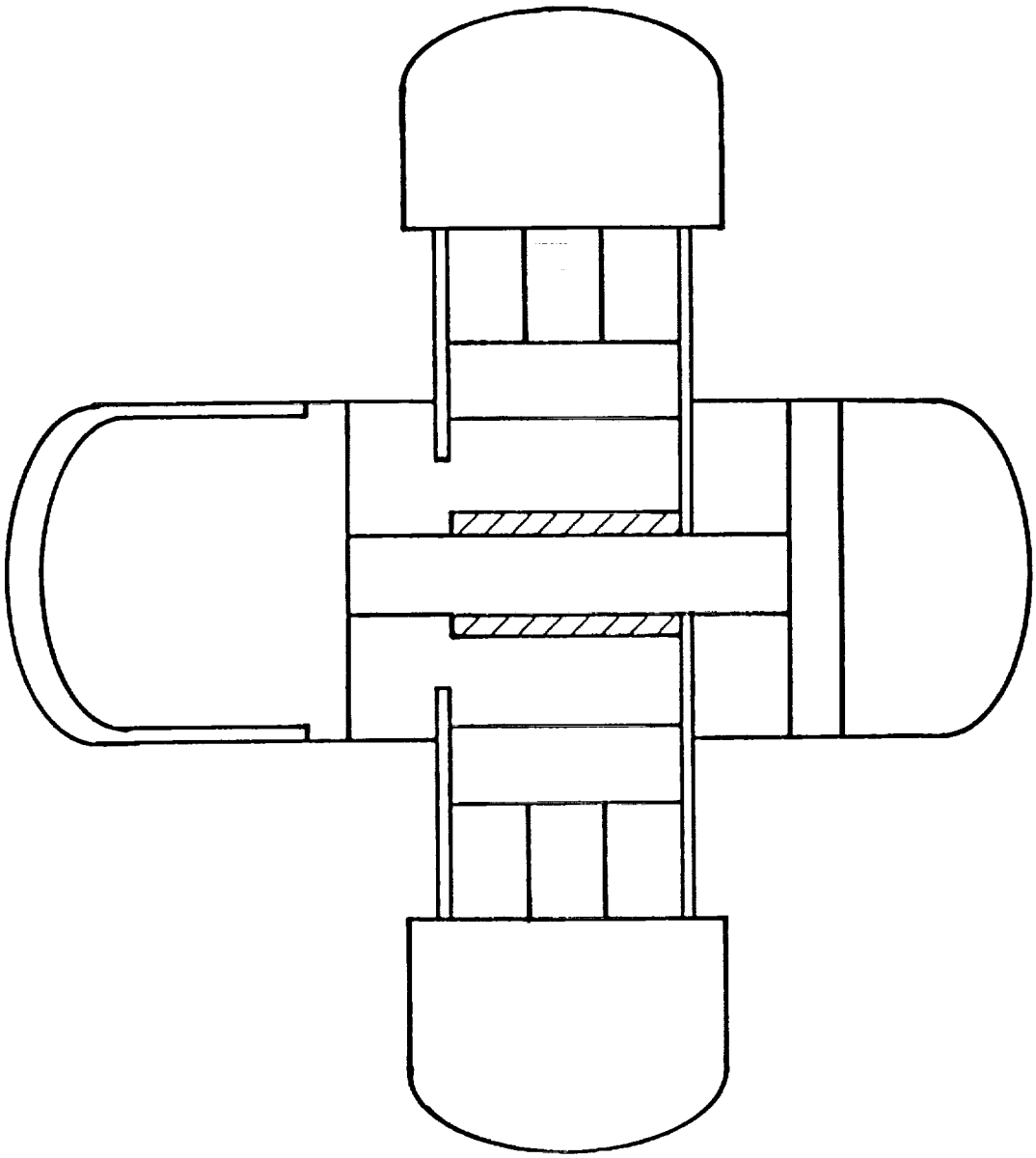

Figure 2: FPSE CONCEPT WITH TWO PISTONS AND ONE DISPLACER

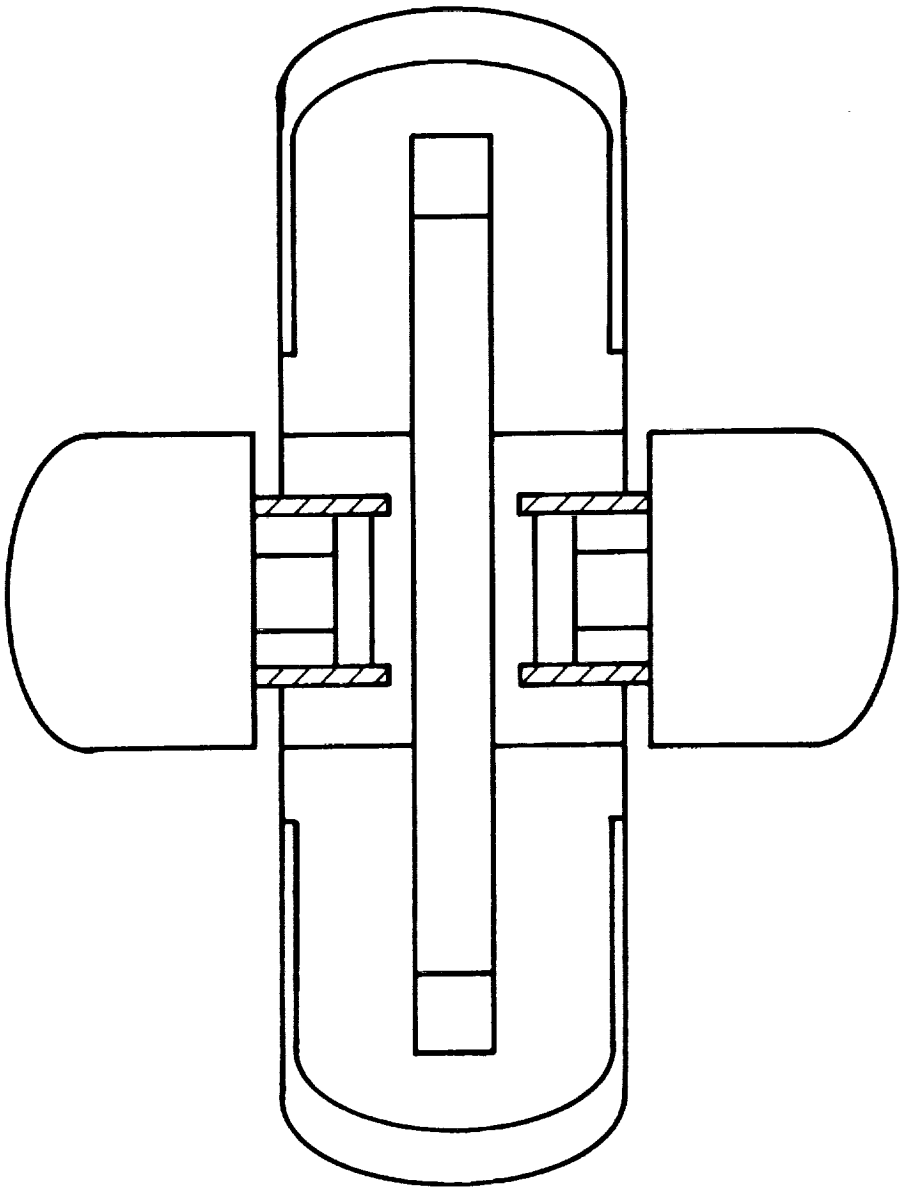

Figure 3: FPSE CONCEPT WITH TWO PISTONS AND TWO DISPLACERS

e. Results of Sunpower's very low temperature ratio heat pump work can be directly factored into the parametrics if this arrangement is employed.

f. The proposed dynamic balance system is directly applicable.

g. It is believed that considerable potential exists for refinement of this design from the viewpoint of structural arrangement, performance, and life potential.

Analytical Tools

To carry out the parametric studies, it was necessary to use a number of Sunpower's existing design programs or variants specifically tailored to the SP-100 effort. These modifications were required primarily to improve the accuracy of the specific mass calculations and to include the unique interaction of the pumped liquid-metal loop on the helium side heat exchanger assembly. The basic programs and their use in this study are briefly described below.

Scaling Program

The scaling program used in this effort is a major extension of the Sunpower scaling rules, which have been widely employed in hardware development programs. The changes were required to improve the overall accuracy of the specific mass calculations since in this task the combination of specific mass and performance were the key issues. Also, it was necessary to include into the scaling program the manifold and enhanced conductivity losses, so their impact could be seen when reviewing the large number of possible engine operating conditions. Gedeon Associates was used as a subcontractor to develop the necessary modifications and software changes.

To employ this program requires the development of a reference engine as a starting point for scaling. This engine need not be extremely detailed, but must have the same

general layout and heat exchanger types as the proposed parametric designs. A number of reference engine designs were developed once a specific configuration had been approved by NASA/Lewis. These differed primarily in the three heat exchanger types employed: simple shell-and-tube, monolithic heater, and a fin-tube design. It was during this early phase that it became evident that a variation on the shell-and-tube heat exchanger, shown in Figure 4, was superior to the others considered. Later refinement of this design resulted in the entire heater-regenerator-cooler being one unit (Figure 5), which allowed considerable freedom in design optimization of this critical component.

Since no stated trade-off existed between engine performance and specific mass, a very simplified model of the overall power system was developed and incorporated into the scaling program. The goal of this model was to show the trend in system mass as a function of the variables under investigation in the engine parametrics. The model inputs were based on preliminary system modeling provided to Sunpower by NASA/Lewis. While this model gives a reasonable indication of which direction to vary the parameters, it is not accurate enough to pick an optimum engine design.

Third-Order Simulation

Sunpower has a number of variants of its third-order Stirling engine simulation program that were employed in the parametrics effort. These programs have been used for all Sunpower designs for a number of years. This has allowed the programs to be refined and calibrated against actual running hardware; for example, the NASA RE-1000 has been modeled quite accurately in comparison to actual NASA test results.

In general the simulations are very good at determining overall power out of the engine in question and have proven to have reasonable accuracy in determining efficiency. The efficiency values generally fall above actual test results by 10 percent to 15 percent; however, as the engine model becomes refined, the accuracy improves. This is a key issue

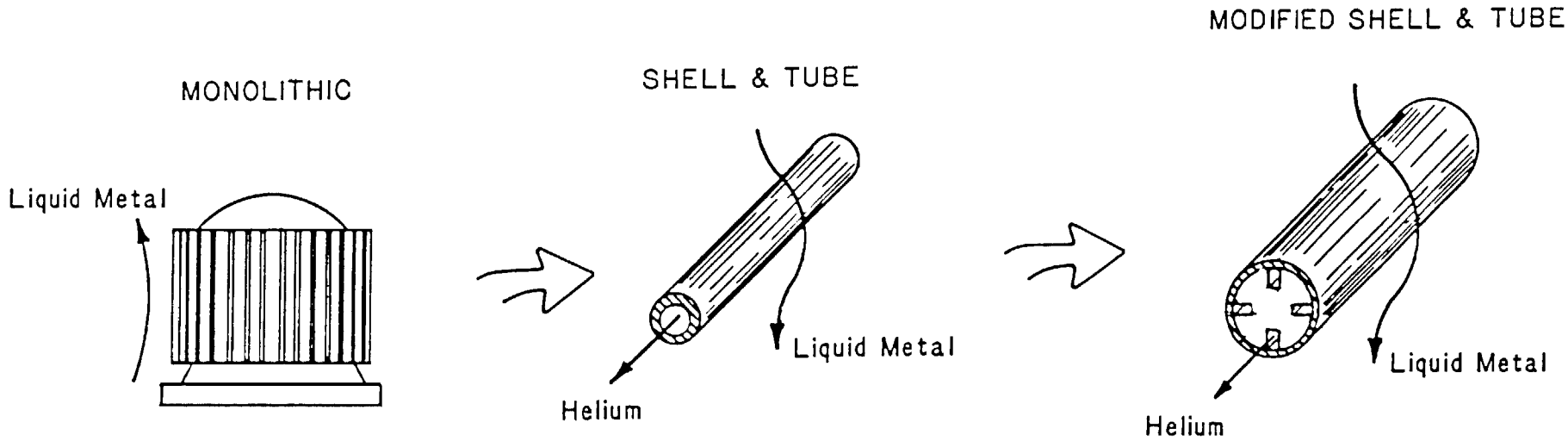

- Low Pressure / Very High Frequency Engines
- High Mass

- Low Mass
- Heat Transfer Areas "Reversed"
- Many Joints Required ($\sim 10^4$)
- Fabrication Limits
- Limited Material Selection

- Reasonable Mass
- "Matched" Heat Transfer Areas
- Few Joints ($\sim 10^2$)
- Optimized Passage Geometry
- Wide Material Selection

Figure 4: HEAT EXCHANGER EVOLUTION

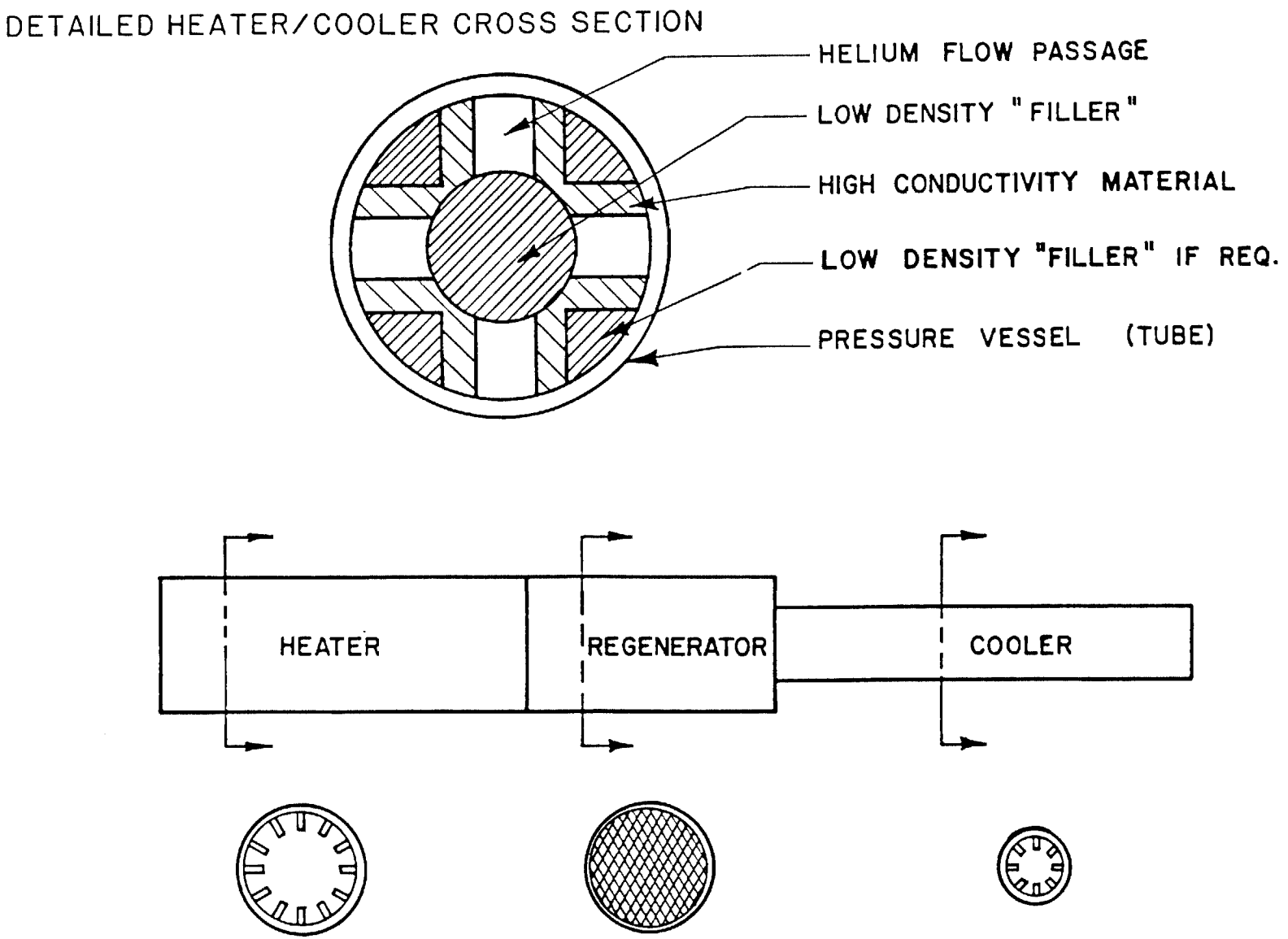

Figure 5: HEATER/REGENERATOR/COOLER MODULE

in using these programs in the SP-100 parametrics, since some of the operating conditions which maximize performance and minimize specific mass are well away from current engine conditions. To improve on the overall accuracy of these programs, a thorough review of the loss models and other internal thermodynamic issues was carried out at the start of the Task 1 effort. The prime areas investigated were the impact of high frequency operation on heat exchanger pumping losses, gas plenum or manifold losses, regenerator pressure drop, and enhanced conductivity effects in the regenerator.

After this review, it was evident that the existing models for the various loss mechanisms could be readily used as they existed or with slight modifications. This held for the unique loss mechanisms involving plenums and enhanced conductivity effects in the regenerator. However, it was evident that while the models employed to predict these losses were basically correct, the absolute value of the predicted loss was seriously in question. This was due to the fact that while both mechanisms had been investigated in detail in Sunpower's low temperature ratio ($T_H/T_C = 1.18$) heat pump program, the regime that this system operated in was radically different from those encountered in the SP-100 power module. This particular problem has not been fully resolved and will require further analytical work or actual experiments if the accuracy of these loss models are to be brought up to the status of those used for the more conventional losses. The impact of this issue is discussed in the section of this report concerned with growth potential of the designs developed in Task 1.

Procedure

The general approach was to use the fast running scaling program to direct the search for reasonable designs and then use the third-order programs to check for performance at that point. In most cases another set of scalings was done to further refine this point design prior to running limited optimizations with the third-order program. This particular

optimization program does not have as complete a loss model package as the performance predicting variants, so a final run was made of this optimized point using the higher accuracy model. For temperature ratios of 2.0 and 1.75, this process worked well; however, at 1.5 a considerable number of problems were encountered throughout the Task 1 effort. This effect was caused by the extreme sensitivity of these designs to minor changes in operating parameters.

Results

The primary results of the Task 1 effort are individually discussed in the following sections.

Efficiency vs. Engine Temperature Ratio

The variation of power module (defined as the free-piston Stirling engine and linear alternator) efficiency is shown in Figure 6 for the six points investigated. The power module efficiency (expressed in terms of percent of Carnot efficiency) is defined as net electric power out of the alternator divided by the heat input to the heater, and as such includes all engine and alternator losses. The selection of a particular point at any specific temperature ratio and hot-end temperature was complicated by the fact that no clear trade-off existed between power module performance and power module specific mass. The final selection process placed more emphasis on a realistic compromise between specific mass and performance rather than the highest possible efficiency. This is shown in Figures 7a through 7f, where the power module efficiency is cross-plotted against power module specific mass for the particular temperature ratio and hot-end temperature. The selected reference engine for each operating point is also indicated on these figures. Power module specific mass is defined as the total engine and alternator mass divided by the net electric output. The balance unit mass is not included in the power module mass for Figures 7a through 7f.

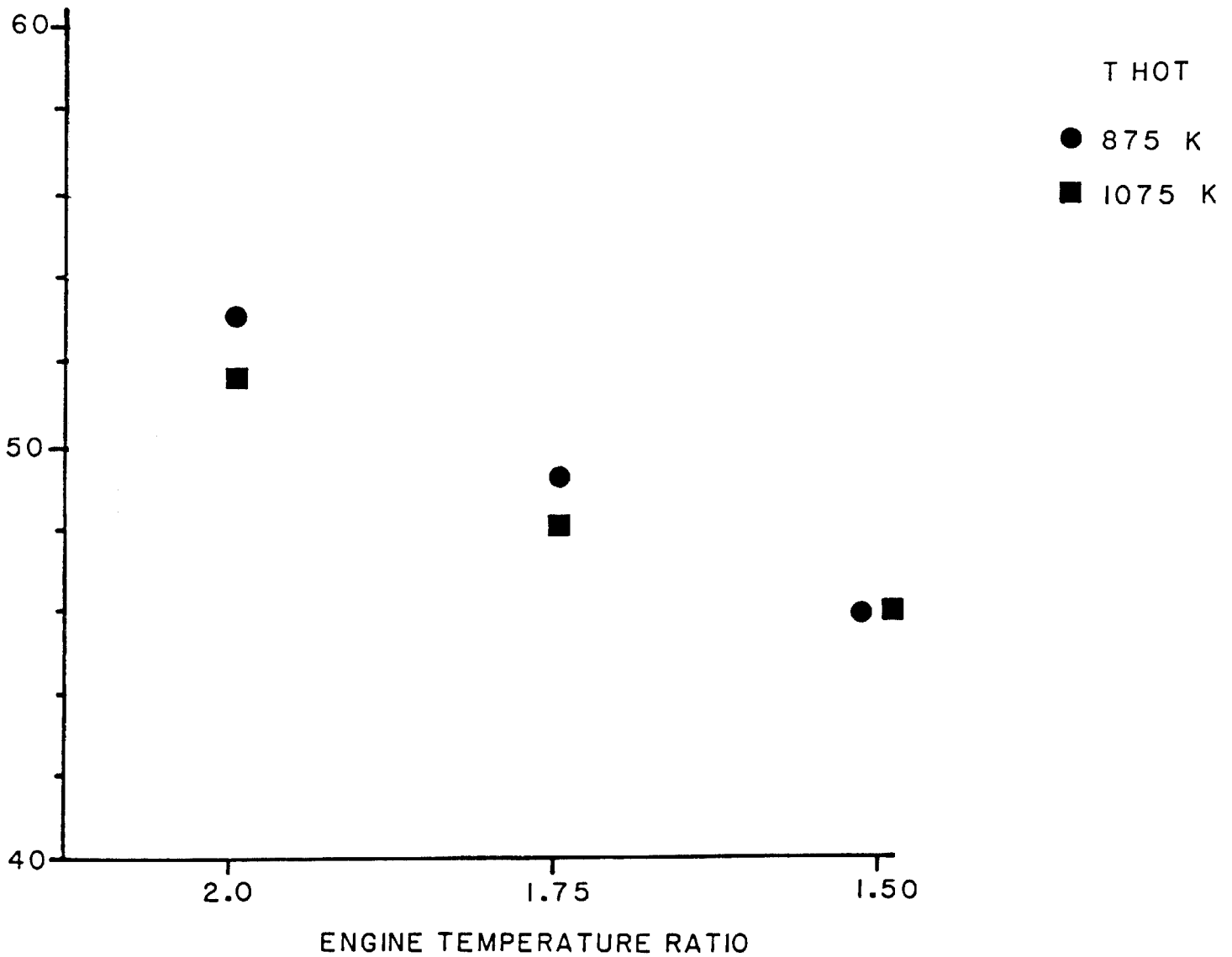

Figure 6: POWER MODULE EFFICIENCY VS. TEMPERATURE RATIO

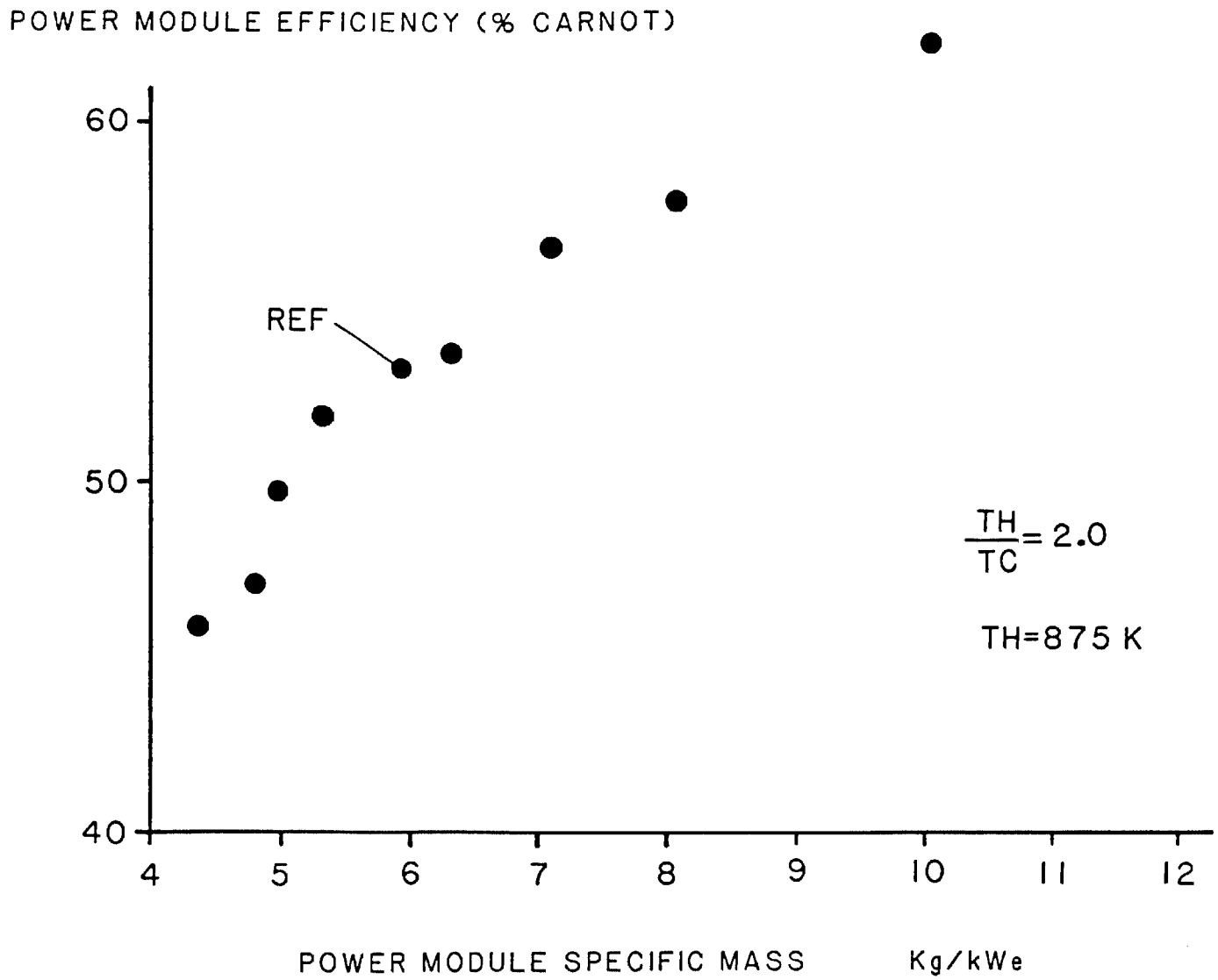

Figure 7a: POWER MODULE EFFICIENCY VS. SPECIFIC MASS

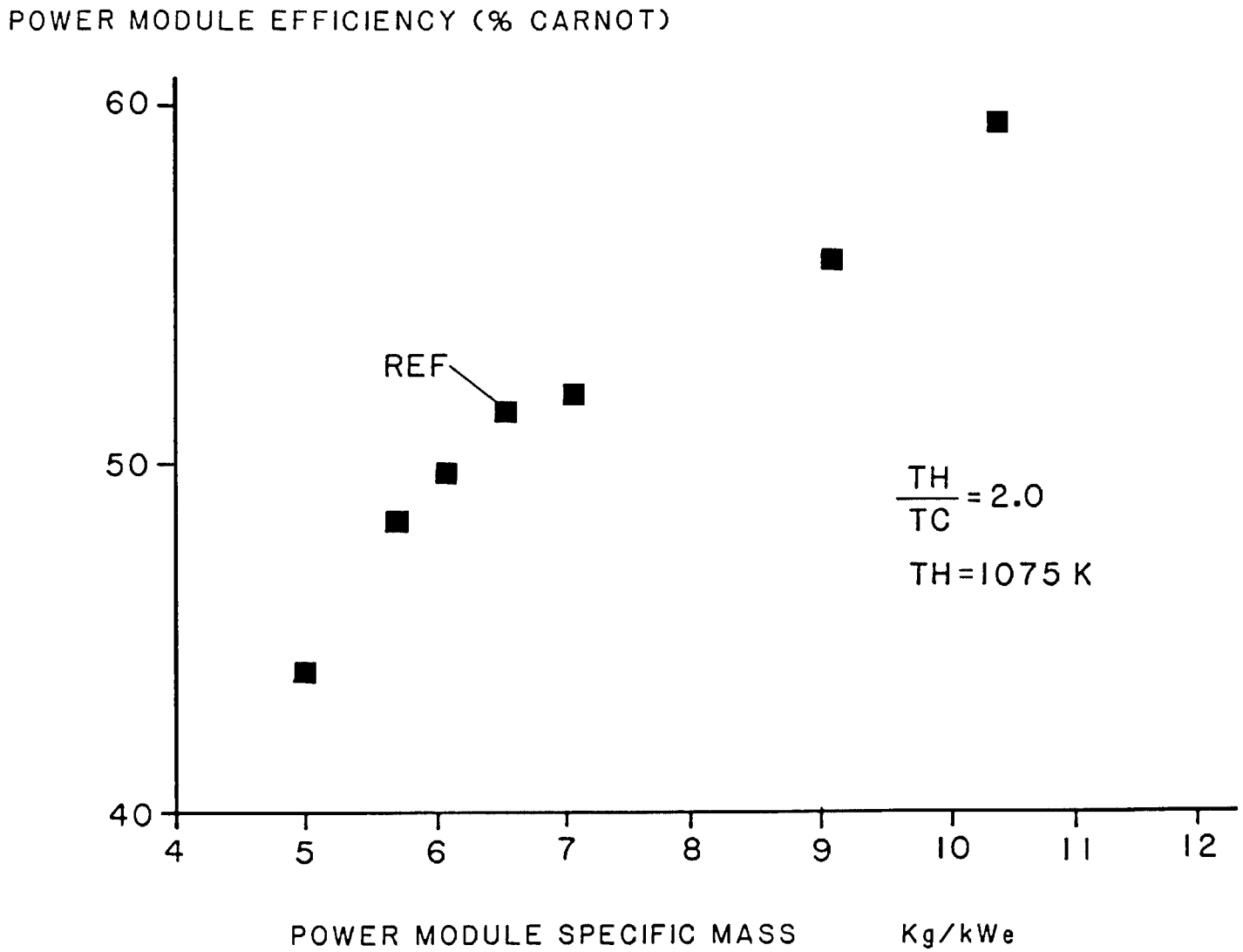

Figure 7b: POWER MODULE EFFICIENCY VS. SPECIFIC MASS

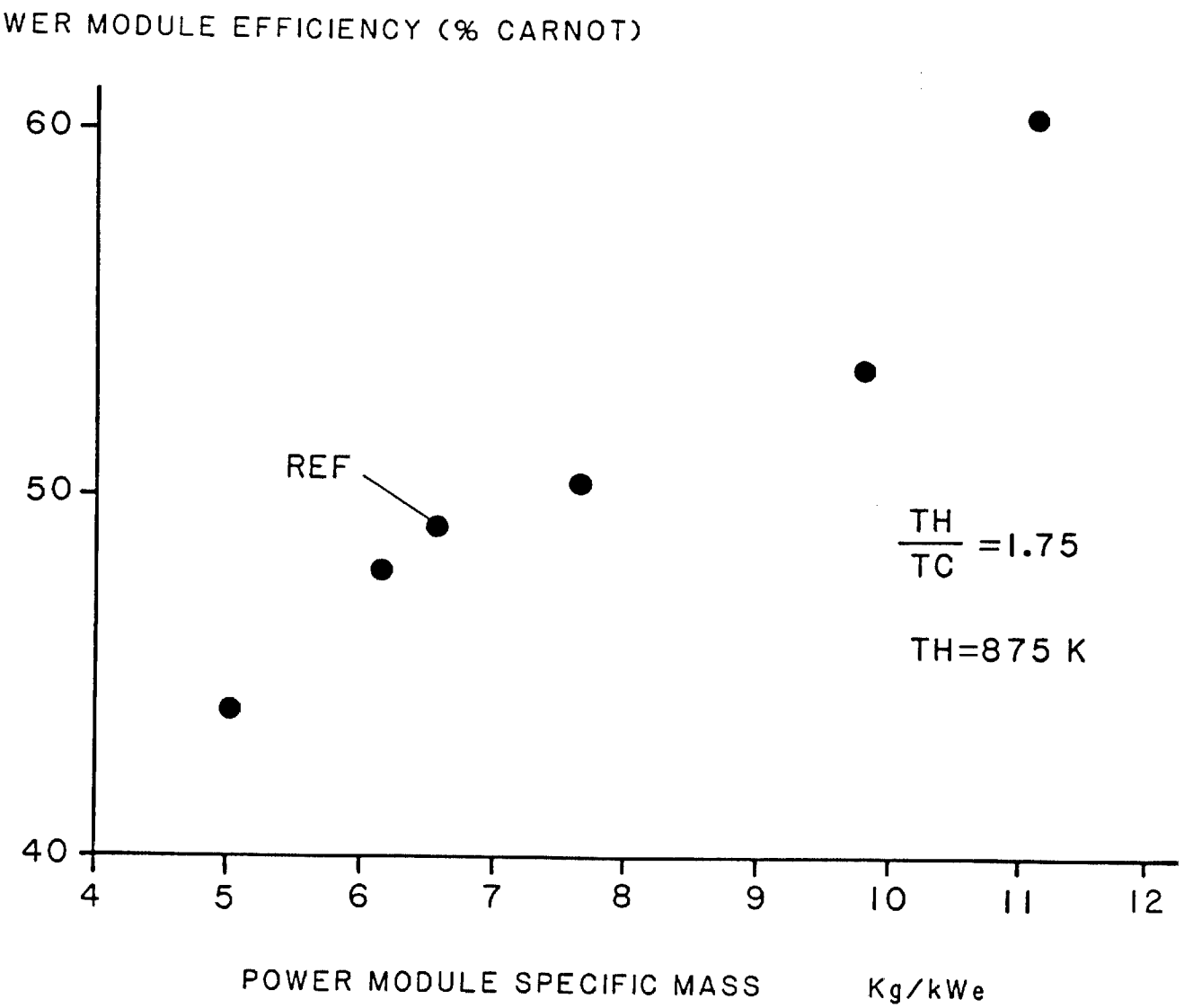

Figure 7c: POWER MODULE EFFICIENCY VS. SPECIFIC MASS

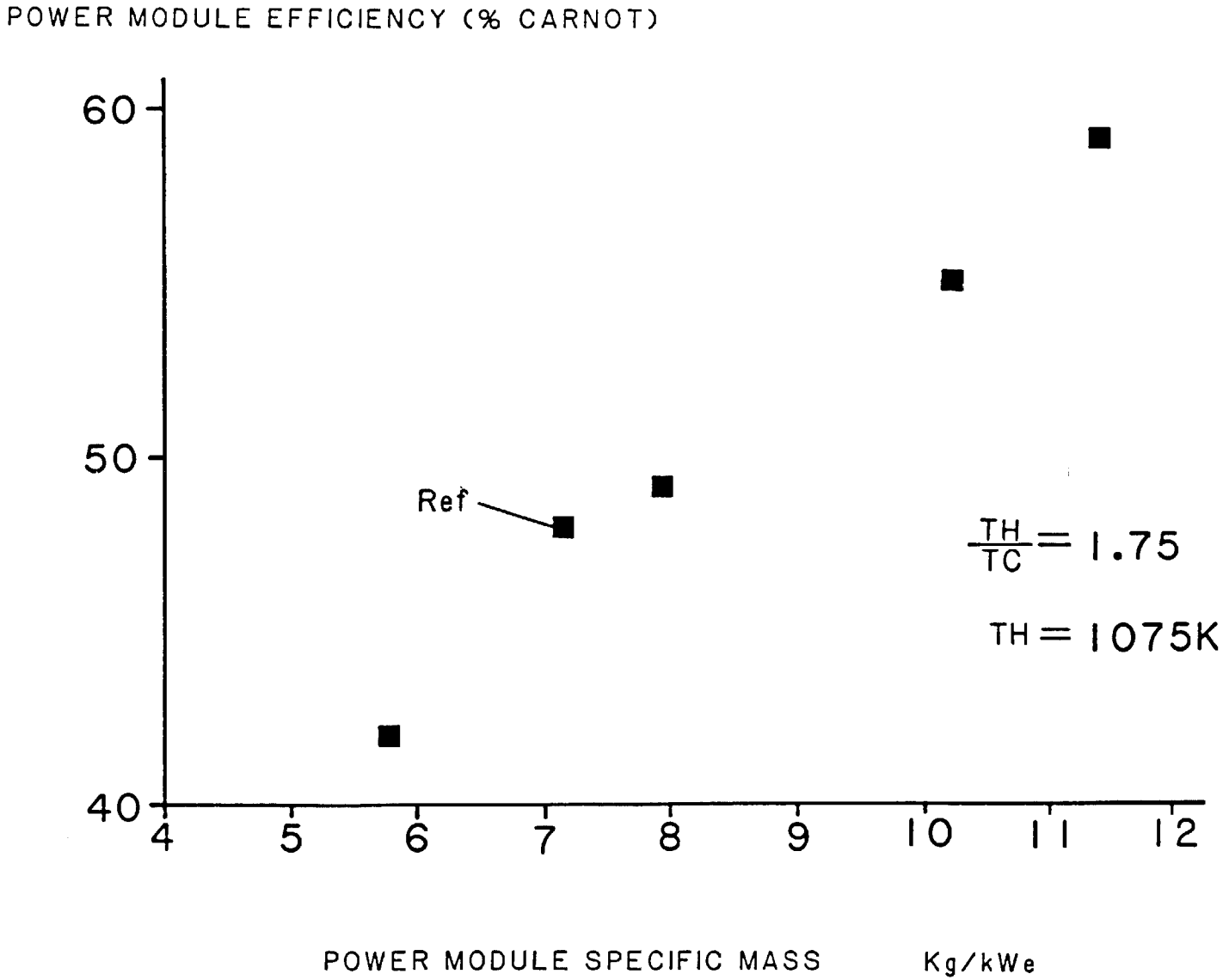

Figure 7d: POWER MODULE EFFICIENCY VS. SPECIFIC MASS

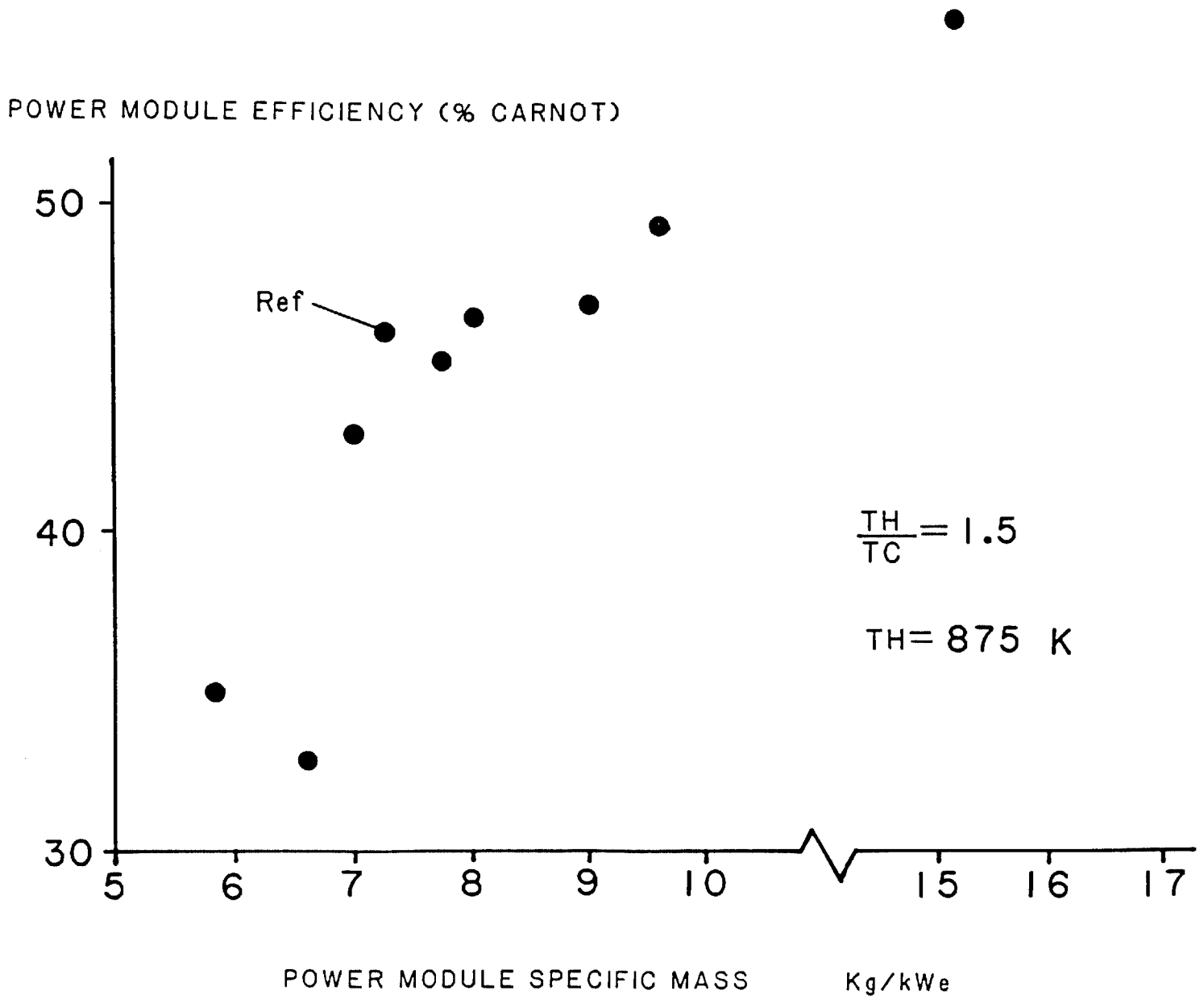

Figure 7e: POWER MODULE EFFICIENCY VS. SPECIFIC MASS

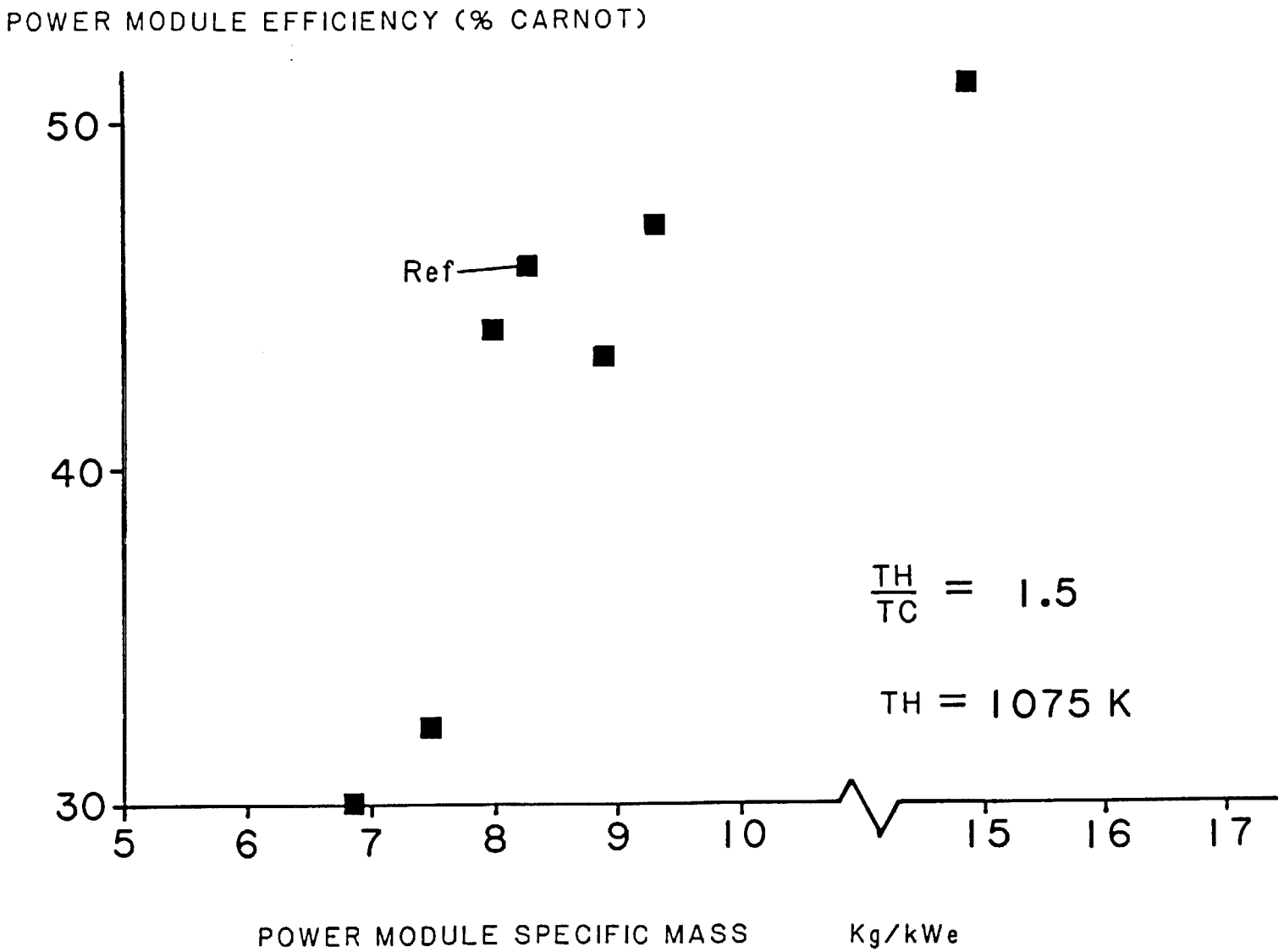

Figure 7f: POWER MODULE EFFICIENCY VS. SPECIFIC MASS

As is evident, considerably higher performance is available only at the price of much increased specific mass values, while a very rapid drop in performance occurs when specific mass values are reduced much below 5 kg/kW(e). The same general trend was seen for all the other points investigated, however, at $T_H/T_C = 1.5$ the scatter became very pronounced.

Little performance difference was noted between the higher and lower hot-end temperatures with the difference decreasing with decreasing temperature ratio. This must be tempered somewhat by the fact that with no clear trade-off between specific mass and performance, modifications of the "hot" system were governed by trying to keep its specific mass in line with that of the lighter "cold" system. With a more accurate trade-off model, it is possible that this slight performance disadvantage of the hot system could be eliminated by accepting the higher engine mass, due to the system savings caused by the higher radiator operating temperature.

Specific Mass vs. Engine Temperature Ratio

The variation of power module specific mass as a function of engine temperature ratio is shown in Figure 8. The issues concerning the selection of the reference engine from the viewpoint of specific mass are the same as that for performance, i.e., without the trade-off of specific mass and performance it is impossible to claim that the selected design is an optimum.

In all cases the lower temperature systems showed lower power module specific mass values with the difference increasing as the temperature ratio was decreased. This is caused by the increase in the average temperature of the heat exchanger assembly at low temperature ratios which reduces the operating strength of the cooler materials and/or requires the use of more advanced materials.

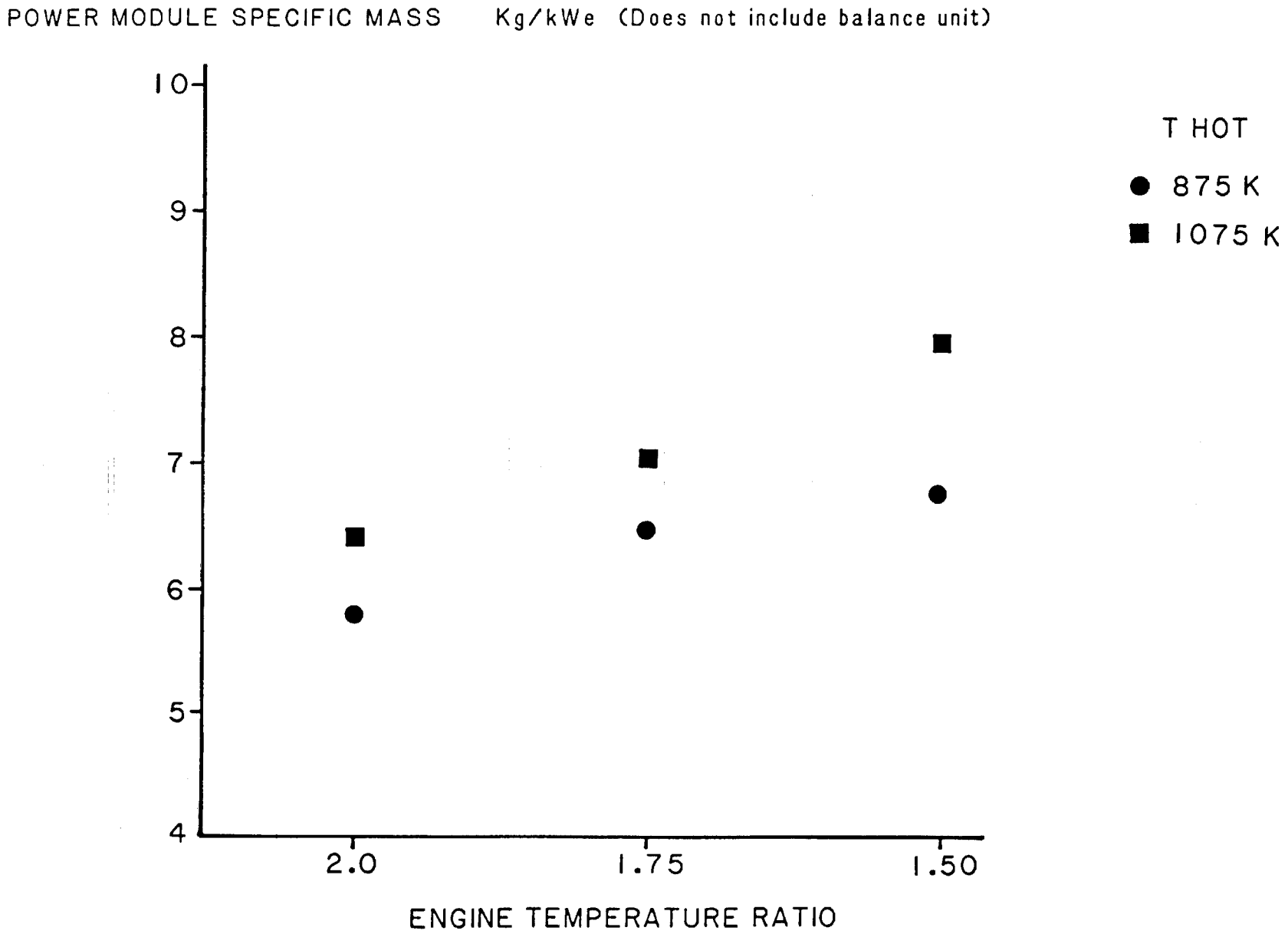

Figure 8: POWER MODULE SPECIFIC MASS VS. TEMPERATURE RATIO

For the materials employed (Table 3), no clear technology limitations were noted. To fully take advantage of the higher heater temperatures, some advancement in material joining technology may be required so an effective mix of refractory and nonrefractory materials can be employed.

TABLE 3: MATERIALS SELECTIONS

Stainless steel alloy	Pressure vessel, heat exchangers
Inconel 718	Pressure vessel, heat exchangers
Ultra high strength steel	Pressure vessel
Titanium	Internal components
Beryllium	Displacer and piston body
Copper	Heat exchanger, alternator
Plastics and fiber-reinforced composites	Alternator, magnet supports
For 1075 K Designs:	
Nickel-200	Heat exchanger
Niobium alloy (Nb-1Zr)	Pressure vessel, heat exchanger
Tantalum alloy (Ta-111)	Pressure vessel

The alternator mass, while contributing a significant fraction of the power module mass, probably cannot be reduced to any major degree below the values determined in Task 1. These designs employ the best current materials both for the iron and magnets components and use quite refined design techniques. While simply increasing the frequency may result in some decrease in specific mass, it is evident that the losses incurred in the engine will outweigh these gains.

The use of a passive balance unit increases the overall power module mass by between 6 percent and 14 percent, depending on the allowable forces the spacecraft can absorb. For engine power variations of 20 percent and reasonable casing motions, the specific mass increase can be assumed to be 10 percent and should be a representative value for all the systems developed in Task 1. This balance system mass is not included in the specific mass values shown in Figures 7a through 7f and Figure 8. The use of an active balance unit would reduce this specific mass penalty to less than 5 percent.

Power Module Operating Characteristics

The general operating characteristics of the engines developed in Task 1 are shown in Table 4, while the specific characteristics of the six design points are shown in Tables 5 through 10.

High operating pressures and reasonably high frequencies accurately describe the general characteristics of the designs developed. In all cases the use of pressures on the order of 200 bar resulted in engines with the best compromise of specific mass and performance. Attempts to reduce the pressure to any significant degree resulted in considerable increases in specific mass, as well as performance reductions due to increased manifold losses if the frequency was kept relatively constant. Radical increases in frequency, on the other hand, saved some mass in the alternator but tended to increase the

diameter of the heat exchanger, causing mass increases and increasing the potential losses due to enhanced conductivity occurring in the regenerator.

TABLE 4: GENERAL ENGINE CHARACTERISTICS

- High operating pressures
- "Medium to high" operating frequency
- Short and fat shape with heat exchanger determining maximum diameter
- Considerable external piston gas spring required
- Clear trade-off between efficiency and specific mass at lower temperature ratios
- Dynamic balance unit will increase specific mass by less than 10 % for a 20 % power change

The geometry of the engine systems are quite compact for the 25 kW(e) output with the maximum diameter determined by the heat exchanger assembly. This fact leads to engines of increasing diameter as temperature ratios are decreased (Figure 9) with the relative engine length remaining essentially constant. The impact of this is a clear trend to higher specific mass as temperature ratios are decreased.

TABLE 5: PARAMETRIC ENGINE DESIGN POINTS

Temperature ratio	2.0
Hot-end wall temperature	875 K
Power module efficiency	26.5 %
Efficiency-percent Carnot	53 %
Power module specific mass	5.8 kg/kW(e)
Power module specific mass with passive balance unit	6.4 kg/kW(e)
Alternator efficiency	93 %
Operating parameters	
Mean pressure	202.5 bar
Operating frequency	97 Hz
Displacer amplitude	10 mm
Piston pV power	26.8 kW
Electric power output	25 kW(e)
Component mass (percent of total)	
Alternator (stationary component)	31.3
Piston, Displacer (moving components)	9.5
Pressure vessel, internal structure	33.1
Heat exchanger assembly (heater-regenerator-cooler)	17
Passive balance unit	10

TABLE 5: PARAMETRIC ENGINE DESIGN POINTS (continued)

Basic dimensions		
Overall power module length		0.95 m
Maximum diameter		0.4 m
Piston diameter		0.16 m
Displacer diameter		0.16 m
Primary loss mechanisms		
Pumping power:		
	Cooler	1125 W
	Regenerator	2025 W
	Heater	900 W
Seal leakage		105 W
Spring hysteresis:		
	Displacer	345 W
	Piston	600 W
Appendix gap loss		735 W
Conduction:		
	Walls	1580 W
	Regenerator gas	2300 W

TABLE 6: PARAMETRIC ENGINE DESIGN POINTS

Temperature ratio	2.0
Hot-end wall temperature	1075 K
Power module efficiency	25.8 %
Efficiency-percent Carnot	51.5 %
Power module specific mass	6.4 kg/kW(e)
Power module specific mass with passive balance unit	7.0 kg/kW(e)
Alternator efficiency	93 %
Operating parameters	
Mean pressure	190 bar
Operating frequency	110 Hz
Displacer amplitude	9.3 mm
Piston pV power	26.8 kW
Electric power output	25 kW(e)
Component mass (percent of total)	
Alternator (stationary component)	25
Piston, Displacer (moving components)	8
Pressure vessel, internal structure	35
Heat exchanger assembly (heater-regenerator-cooler)	23
Passive balance unit	10

TABLE 6: PARAMETRIC ENGINE DESIGN POINTS (continued)

Basic dimensions		
Overall power module length		0.9 m
Maximum diameter		0.38 m
Piston diameter		0.16 m
Displacer diameter		0.16 m
Primary loss mechanisms		
Pumping power:		
	Cooler	1300 W
	Regenerator	2340 W
	Heater	1040 W
Seal leakage		115 W
Spring hysteresis:		
	Displacer	360 W
	Piston	800 W
Appendix gap loss		740 W
Conduction:		
	Walls	1605 W
	Regenerator gas	2620 W

TABLE 7: PARAMETRIC ENGINE DESIGN POINTS

Temperature ratio	1.75
Hot-end wall temperature	875 K
Power module efficiency	21 %
Efficiency-percent Carnot	49 %
Power module specific mass	6.5 kg/kW(e)
Power module specific mass with passive balance unit	7.1 kg/kW(e)
Alternator efficiency	93 %
Operating parameters	
Mean pressure	202 bar
Operating frequency	118 Hz
Displacer amplitude	9 mm
Piston pV power	26.8 kW
Electric power output	25 kW(e)
Component mass (percent of total)	
Alternator (stationary component)	26
Piston, Displacer (moving components)	8.4
Pressure vessel, internal structure	32
Heat exchanger assembly (heater-regenerator-cooler)	25
Passive balance unit	10

TABLE 7: PARAMETRIC ENGINE DESIGN POINTS (continued)

Basic dimensions		
Overall power module length		1.1 m
Maximum diameter		0.45 m
Piston diameter		0.158 m
Displacer diameter		0.171 m
Primary loss mechanisms		
Pumping power:		
	Cooler	1610 W
	Regenerator	2180 W
	Heater	920 W
Seal leakage		130 W
Spring hysteresis:		
	Displacer	345 W
	Piston	700 W
Appendix gap loss		525 W
Conduction:		
	Walls	1900 W
	Regenerator gas	3700 W

TABLE 8: PARAMETRIC ENGINE DESIGN POINTS

Temperature ratio	1.75
Hot-end wall temperature	1075 K
Power module efficiency	20.6 %
Efficiency-percent Carnot	48 %
Power module specific mass	7.1 kg/kW(e)
Power module specific mass with passive balance unit	7.8 kg/kW(e)
Alternator efficiency	93 %
Operating parameters	
Mean pressure	200 bar
Operating frequency	120 Hz
Displacer amplitude	9 mm
Piston pV power	26.8 kW
Electric power output	25 kW(e)
Component mass (percent of total)	
Alternator (stationary component)	24
Piston, Displacer (moving components)	7.7
Pressure vessel, internal structure	30
Heat exchanger assembly (heater-regenerator-cooler)	29
Passive balance unit	10

TABLE 8: PARAMETRIC ENGINE DESIGN POINTS (continued)

Basic dimensions		
Overall power module length		1.1 m
Maximum diameter		0.45 m
Piston diameter		0.16 m
Displacer diameter		0.175 m
Primary loss mechanisms		
Pumping power:		
	Cooler	1640 W
	Regenerator	2200 W
	Heater	930 W
Seal leakage		130 W
Spring hysteresis:		
	Displacer	380 W
	Piston	800 W
Appendix gap loss		600 W
Conduction:		
	Walls	2100 W
	Regenerator gas	3400 W

TABLE 9: PARAMETRIC ENGINE DESIGN POINTS

Temperature ratio	1.5
Hot-end wall temperature	875 K
Power module efficiency	15.3 %
Efficiency-percent Carnot	46 %
Power module specific mass	7 kg/kW(e)
Power module specific mass with passive balance unit	7.8 kg/kW(e)
Alternator efficiency	93 %
Operating parameters	
Mean pressure	128 bar
Operating frequency	126 Hz
Displacer amplitude	7.8 mm
Piston pV power	26.8 kW
Electric power output	25 kW(e)
Component mass (percent of total)	
Alternator (stationary component)	28
Piston, Displacer (moving components)	9
Pressure vessel, internal structure	21
Heat exchanger assembly (heater-regenerator-cooler)	32
Passive balance unit	10

TABLE 9: PARAMETRIC ENGINE DESIGN POINTS (continued)

Basic dimensions		
Overall power module length		0.95 m
Maximum diameter		0.57 m
Piston diameter		0.4 m
Displacer diameter		0.31 m
Primary loss mechanisms		
Pumping power:		
	Cooler	1550 W
	Regenerator	1660 W
	Heater	1240 W
Seal leakage		240 W
Spring hysteresis:		
	Displacer	230 W
	Piston	600 W
Appendix gap loss		680 W
Conduction:		
	Walls	1800 W
	Regenerator gas	3000 W

TABLE 10: PARAMETRIC ENGINE DESIGN POINTS

Temperature ratio	1.5
Hot-end wall temperature	1075 K
Power module efficiency	15.2 %
Efficiency-percent Carnot	45.6 %
Power module specific mass	8.1 kg/kW(e)
Power module specific mass with passive balance unit	9 kg/kW(e)
Alternator efficiency	93 %
Operating parameters	
Mean pressure	130 bar
Operating frequency	125 Hz
Displacer amplitude	7.5 mm
Piston pV power	26.8 kW
Electric power output	25 kW(e)
Component mass (percent of total)	
Alternator (stationary component)	24
Piston, Displacer (moving components)	9
Pressure vessel, internal structure	22
Heat exchanger assembly (heater-regenerator-cooler)	34
Passive balance unit	10

TABLE 10: PARAMETRIC ENGINE DESIGN POINTS (continued)

Basic dimensions		
Overall power module length		1 m
Maximum diameter		0.6 m
Piston diameter		0.42 m
Displacer diameter		0.35 m
Primary loss mechanisms		
Pumping power:		
	Cooler	1500 W
	Regenerator	1700 W
	Heater	1300 W
Seal leakage		250 W
Spring hysteresis:		
	Displacer	230 W
	Piston	600 W
Appendix gap loss		750 W
Conduction:		
	Walls	1800 W
	Regenerator gas	3000 W

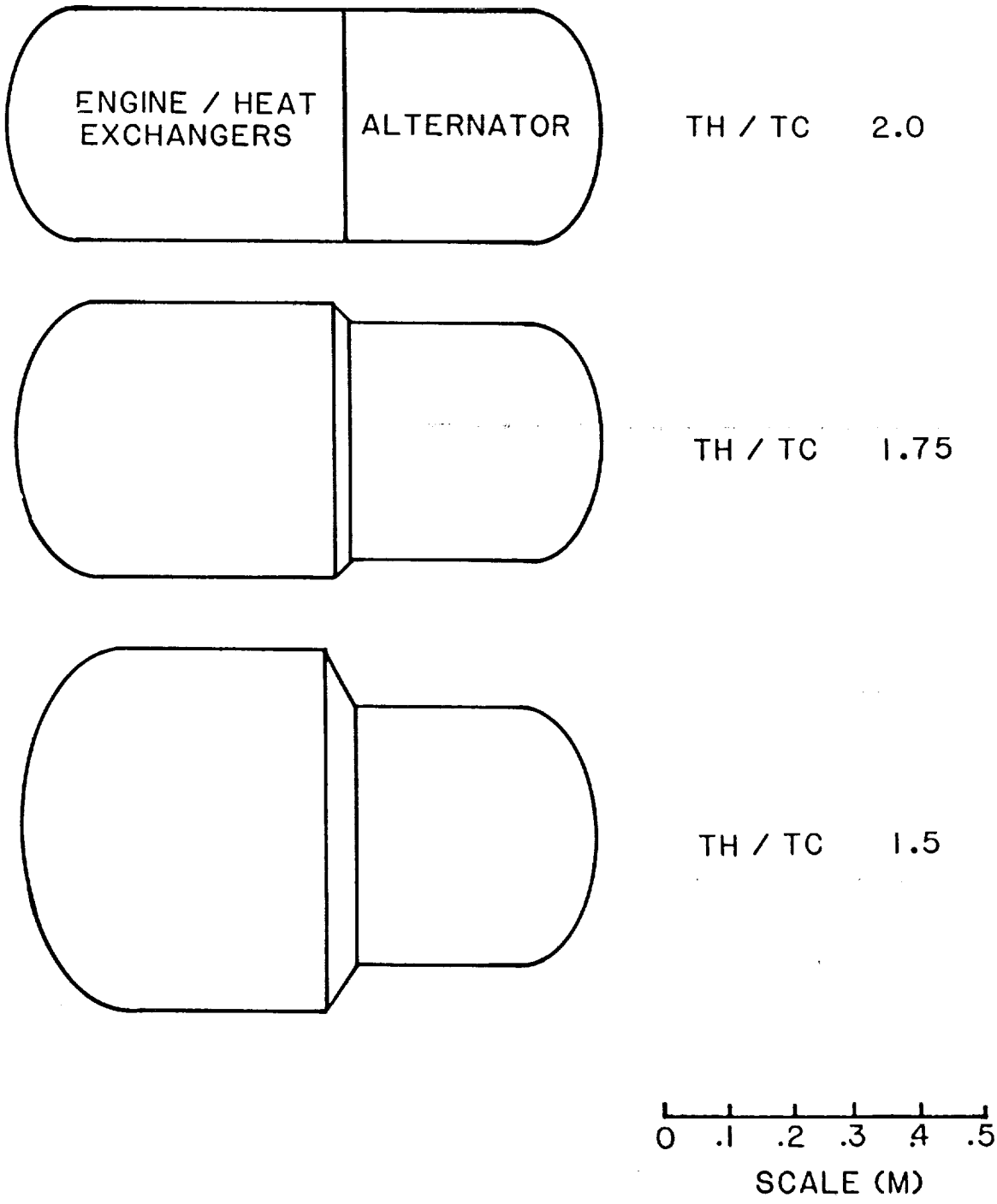

Figure 9: POWER MODULE GEOMETRY VS. ENGINE TEMPERATURE RATIO

During the review of various heater and cooler concepts, it became evident that no advantage could be seen in the application of a heat pipe system on the heater and only a marginal, if any, performance advantage if heat pipes are used on the cooler. This is primarily due to the large number of helium passages available with the modified shell-and-tube heat exchanger which provides for considerably better matching of the helium and liquid-metal heat transfer characteristics than a pure shell-and-tube design. Operating temperature drops then became very small and essentially nullified the heat pipe's prime advantage. The impact of auxiliary energy requirements necessary to drive an electromagnetic pump was factored into the design process by including the liquid-metal heat exchangers from the viewpoint of maximizing the engine net performance. For these Task 1 parametrics, the liquid-metal flow rates were not constrained to match values determined from an overall power system analysis. (These rates did not exist at this time.)

Accuracy Issues

During the development of the parametric modeling techniques, a number of assumptions were employed to simplify the search for optimum designs. This primarily affected specific mass of the designs investigated. In the designs at temperature ratios of 2.0 and 1.75, the difference between the specific mass values at T_H = 875 K and 1075 K are small enough that, for all practical purposes, they are equal in specific mass. This does not hold for the temperature ratio of the 1.5 case, where the requirements for employing higher operating temperature materials in the cooler portion of the engine does cause a significant specific mass variation between the 875 K and 1075 K design points.

Accuracy of the performance predictions from the parametric studies is hard to define. All of the classic losses are determined with the current Sunpower third-order simulation code which has consistently shown excellent correlation with hardware in the area of power prediction. Efficiency estimates based on this code are generally within 10 percent of actual

hardware results and tend to predict higher performance than actually occurs. The unique loss mechanisms involving plenums and enhanced conductivity effects are not fully understood at the present time and essentially only impact efficiency, not power output. The current feelings are that these losses do exist and the Sunpower correlations do track the trend in these losses as various parameters are changed. In the current parametrics a reasonable compromise was used between the worst case losses caused by these unique mechanisms and a situation where these losses do not exist. The net effect of this situation is shown in Figures 10 and 11 for temperature ratios of 2.0 and 1.75. As can be seen, there is the possibility that the engines could be lower in performance and have lower specific mass values than the current designs. The growth potential in power module efficiency due to a better understanding of the various loss mechanisms and further design refinement is discussed in the next section of this report.

Growth Potential of Parametric Study Engine Designs

During the process of developing the Task 1 results, it became evident that the performance values, in terms of fraction of Carnot efficiency, were falling below earlier expectations. While it was felt that the designs developed were realistic, both in specific mass and performance, it was realized that the potential growth of these designs would have to be investigated to provide a complete package for use in comparing the FPSE to other potential SP-100 power module concepts. The process employed in this effort was primarily directed at reviewing the major losses that existed in the Task 1 engine concepts and attempting to develop a rationale for reducing them.

This was carried out, not by radically changing the basic engine design, but rather by assuming that a better understanding of the particular loss mechanisms would allow the engine design to be modified to minimize these losses.

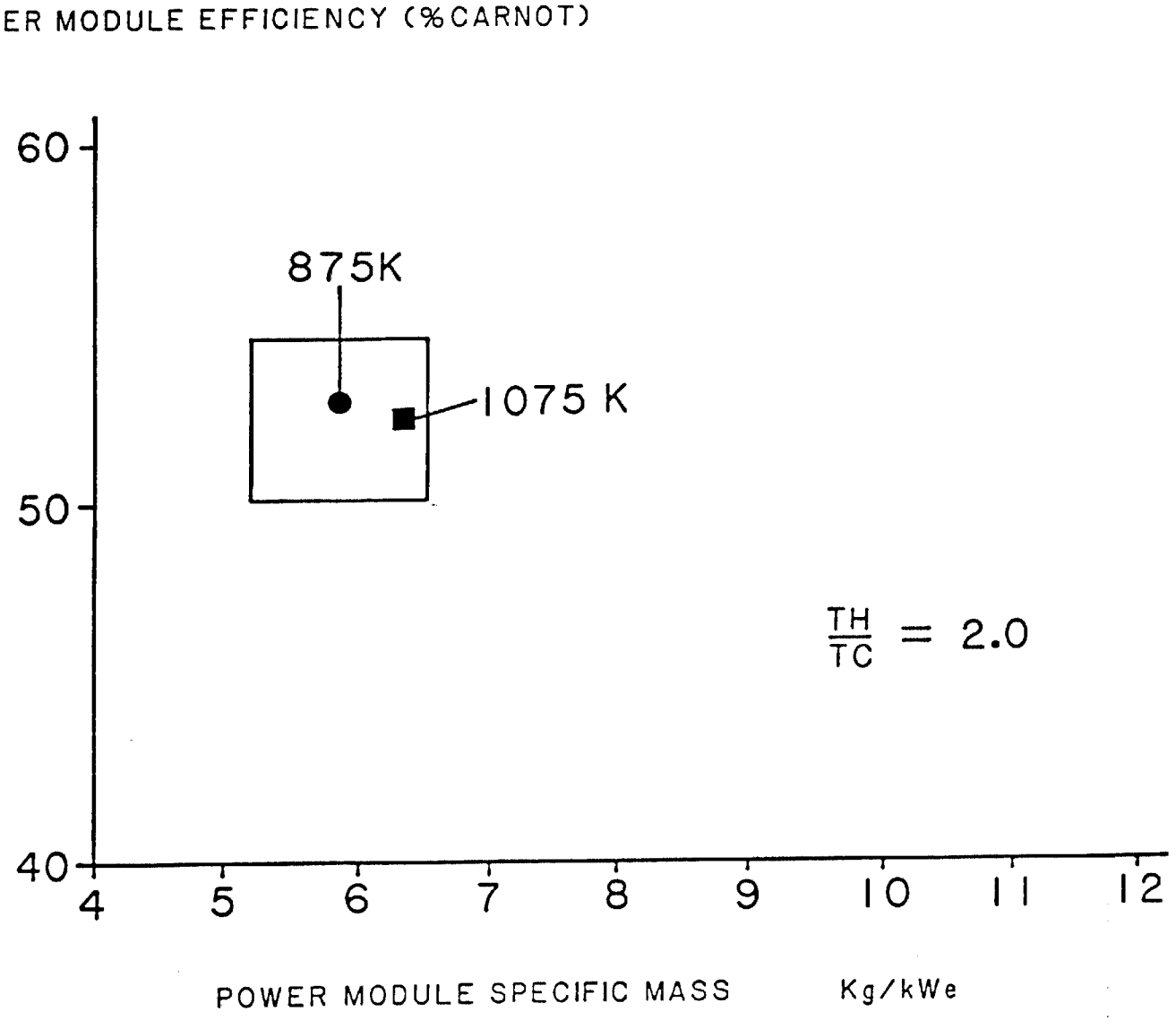

Figure 10: ACCURACY OF PARAMETRIC RESULTS

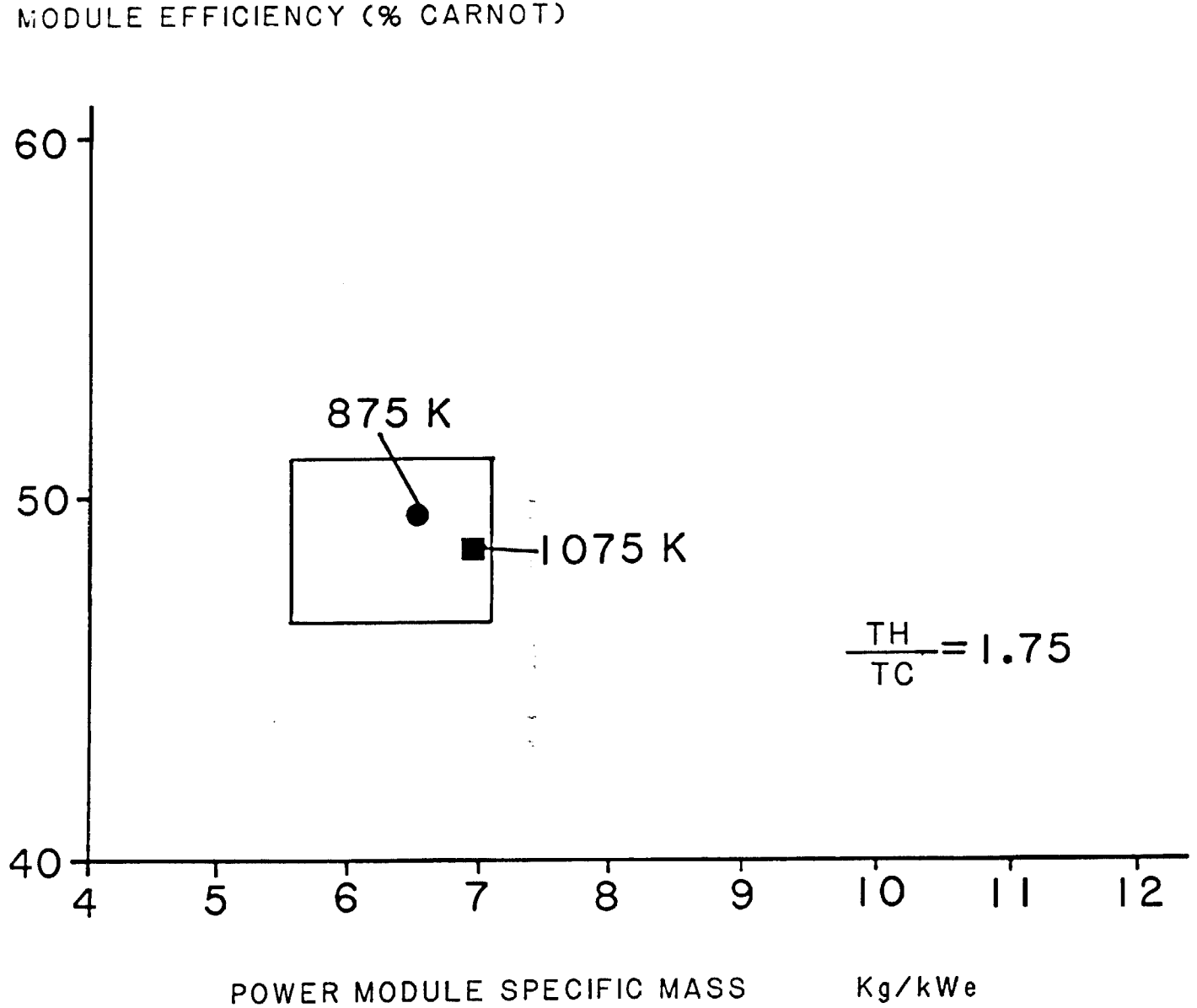

Figure 11: ACCURACY OF PARAMETRIC RESULTS

While engine performance was the key issue during the potential growth effort, it was also necessary to review the possible improvements in the specific mass of the engine since it is clear that the trade-off between both performance and specific mass is critical. Since a wide range of structural concepts and materials had been investigated in the earlier efforts in Task 1, it was deemed reasonable to push this technology so it would be representative of the level that could be obtained from a long-term development program. This was based on the general power module concept developed in Task 1 and as such emphasized the material and fabrication problems encountered in the designs employing high engine operating pressures.

After a thorough review of the potential growth issues it became evident that two general areas of investigation were involved. The first, Key Areas, emphasized the specific areas applicable to the type of engines developed during the Parametric Study while the second, Secondary Areas, addressed a much wider range of issues for improving the performance of the general FPSE concept. In this latter case some concepts were reviewed that do not, at present, satisfy the basic contract requirements, for example, the use of hydrogen as an engine working fluid. These areas are called out in Table 11 and are discussed in the following portions of this section.

TABLE 11: POWER MODULE GROWTH POTENTIAL

Key Areas

- Improved understanding of loss mechanisms
- Improved definition of specific mass vs. efficiency trade-off
- Refined structural concepts and material selections

TABLE 11: POWER MODULE GROWTH POTENTIAL (continued)

Secondary Areas

- Use of hydrogen
- Secondary gas for reduction of gas spring losses

It is important to note that the majority of this effort was directed at the basic design concepts developed in the Task 1 Parametric Study and as such are only applicable to this general type of design. It is not possible to simply assume that any other FPSE concept (such as the SPDE engine) will have the same level of improvement over its currently predicted performance.

1. Key Areas

Improved Understanding of Loss Mechanisms

The requirements of the Task 1 power module were such that the use of reasonably high operating frequencies and high engine pressures were required to attain the combination of performance and specific power levels desired. At the same time the use of a liquid-metal exterior heat exchange loop dictated the use of a shell-and-tube heat exchanger variant. The net result was that the designs developed require the use of relatively large gas manifolds to distribute the working gas from the work space to the heater/regenerator/cooler assembly. This can cause a number of problems to occur, as shown schematically in Figure 12, the net effect of which is a drop in overall system efficiency. This unique loss was first noted in the Sunpower/GRI duplex heat pump program (Figure 13) and a basic correlation was developed to describe it.

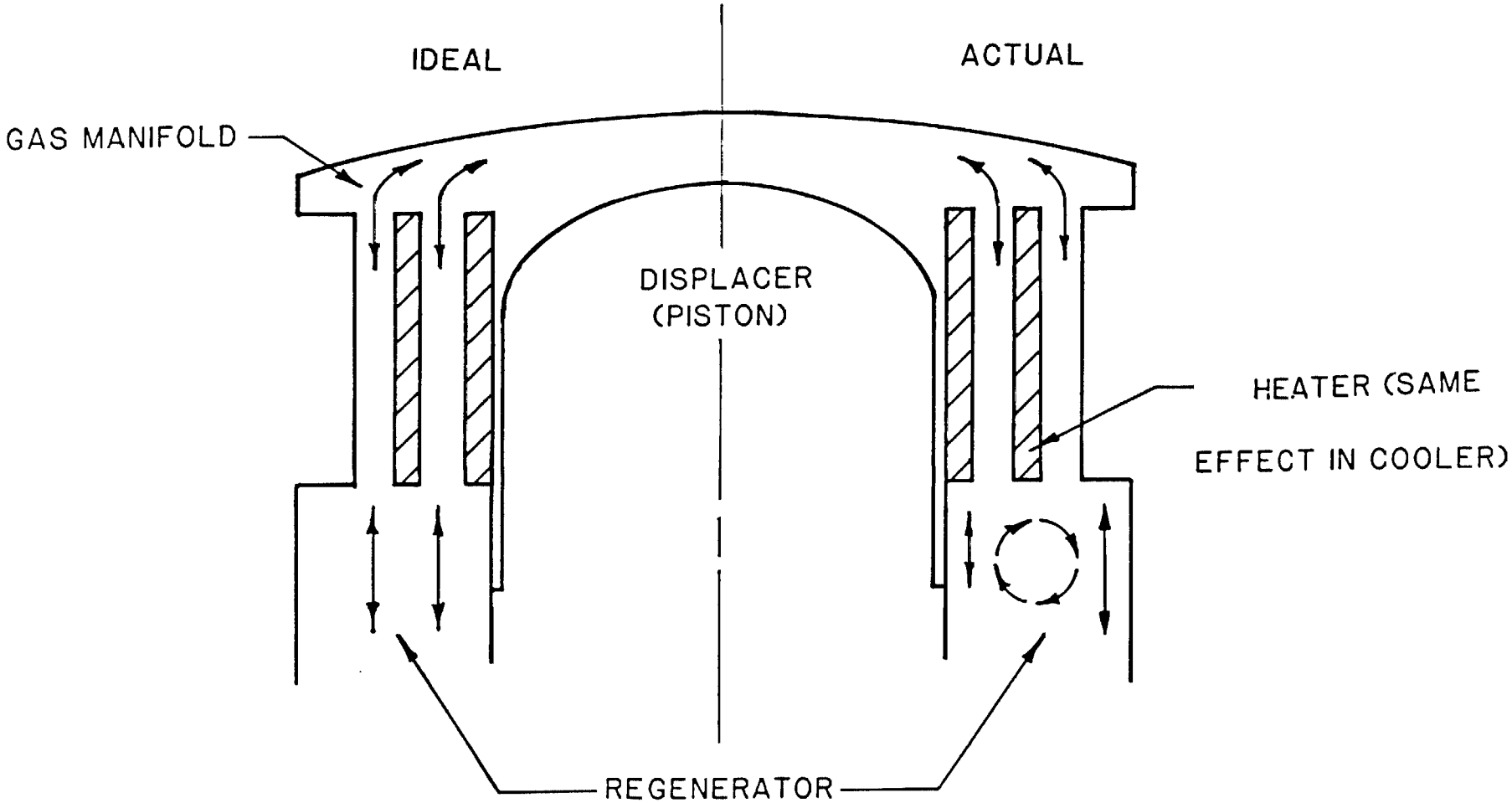

Figure 12: PLENUM OR GAS MANIFOLD LOSSES

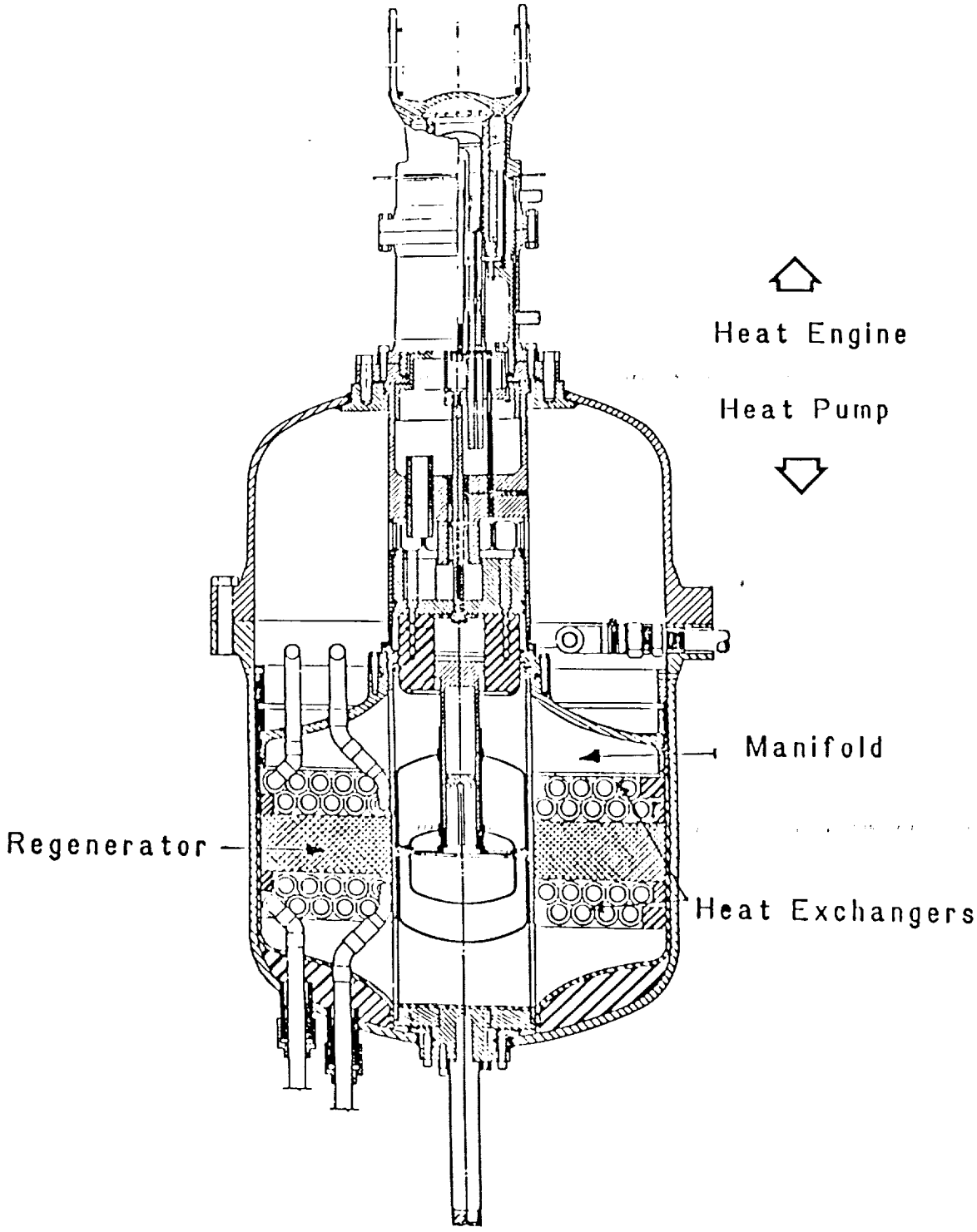

Figure 13: DUPLEX HEAT PUMP ASSEMBLY

There is, however, considerable doubt about the applicability of the specific coefficients employed in this correlation since they are based on operating conditions well away from those appropriate for the SP-100 application. To analyze this loss, it was assumed that the general form of the correlation was correct and that the key nondimensional grouping could be adjusted to minimize the flow maldistribution across the heat exchanger assembly. This will reduce the efficiency loss considerably at the expense of somewhat of an increase in dead volume and possible increase in structural mass of the engine. The net result is estimated to be an increase in the system's percent of Carnot efficiency by 1 to 1.5 percentage points compared to the specific design points developed in the parametric studies at T_H/T_C of 1.75 and 2.0. It is possible that further improvements can be made in this area with refined correlations and a re-optimization of the engine design; however, they are not expected to amount to a gain of more than 1 percentage point based on fraction of Carnot. It was also noted that the potential performance improvement due to reduction in this loss mechanism was higher for the lower specific mass designs.

The other unique loss mechanism encountered in the parametric study is related to enhanced thermal conductivity occurring in the regenerator. This would radically increase the quantity of energy that is lost between the heater and cooler due to the equivalent of a thermal short circuit through the regenerator. This particular loss mechanism is aggravated by the use of lower temperature ratios and high frequencies, both of which are required in the Task 1 power module. This loss was also noted first in the Sunpower/GRI duplex heat pump effort, and since that time a technical literature review has identified a number of papers related to flow in packed beds, which support the existence of this effect. The basic correlation developed at Sunpower was used in the Task 1 efforts for estimating the loss due to enhanced regenerator conductivity. The impact of this loss can be significant depending on the specific coefficients used in the correlation model. For designs at temperature ratios of 2.0 and 1.75, the resulting losses were on the order of 3 percentage points based on fraction of Carnot system performance. The use of less conservative models can result in losses of up to 4 to 6 percentage points under the same operating

conditions. It was assumed that the loss could be reduced by re-optimizing the regenerator assembly design once better correlations exist. Performance improvements by up to 2 to 3 percentage points may be possible in this case. It is very important to note that if experimental work were to show that this loss is higher than predicted with the current correlation, it would be necessary to re-optimize the entire engine design to reach higher performance levels.

Other more conventional loss mechanisms occurring in Stirling engines are reasonably well understood and further understanding of any one of them is not expected to significantly improve performance over the values determined in Task 1. However, refinement of the modeling techniques employed to define these losses could result in engine designs which tend to minimize the total losses. This is particularly true in the areas of gas spring losses, heat transfer and pressure drop in cyclic flows, leakage losses involving center ports, and flow maldistribution effects. The net effect could be a performance improvement on the order of 2 percentage points (based on fraction of Carnot system performance) for the reference designs. The improvements will impact the lower temperature ratio design point ($T_H/T_C = 1.5$) to a more significant degree, due to the extreme sensitivity of those designs to changes in loss models.

Performance vs. Power Module Specific Mass

Since no specific interrelationship between power module performance, power module specific mass, and overall system mass was available in the Task 1 effort, it is impossible to state that the six reference point engines represent true optimum designs. Initially, the primary driver for selection of a particular design was reasonable performance at specific mass values in the range of 5 to 8 kg/kW(e). This was later refined somewhat by the use of a very simplified model for the total system mass as a function of a few critical engine operating characteristics. With this model it was possible to see the trend in system mass when various changes were made in the engine.

The development of a more refined model may improve overall system performance since the trade-off between power module efficiency and specific mass could be better incorporated into the detailed design. This was an important issue for the Task 2 design effort since the push for higher power module efficiency was combined with a desire to reduce engine specific mass. This latter effort was complicated by a performance barrier which occurred when attempts were made to reduce engine specific mass to values below about 5 kg/kW(e) (not including the balance system mass) as shown in Figure 14. This characteristic was noted for the $T_H/T_C = 2.0$ and $T_H/T_C = 1.75$ design points, however, its presence at $T_H/T_C = 1.5$ was not clear.

Refined Structural Concepts

During the parametric study, it was necessary to use a number of generalizations concerning the structural layout and material selections for the engine concepts under consideration. To assure that the results were reasonable, it was decided early in the effort that relatively conservative design constraints would be employed. This, without question, has resulted in power module specific mass values which can be improved by further detailed design.

To attempt to estimate the potential reductions in specific mass values without a detailed review is somewhat risky since a number of fabrication effects play a major role in determining the possible improvements. This is due to the high operating pressures of the reference engine and the requirement for long operating life. For example, at operating temperatures of 1075 K, the refractory alloy Nb-1Zr has reasonably good stress rupture characteristics in comparison to the stainless steel and Inconel alloys, but at the same time has relatively poor characteristics compared to T-111 or TZM. Even though these latter alloys are quite dense they still could result in a lower overall hot-end structural weight. This introduces the question of should a higher-strength refractory alloy be used at

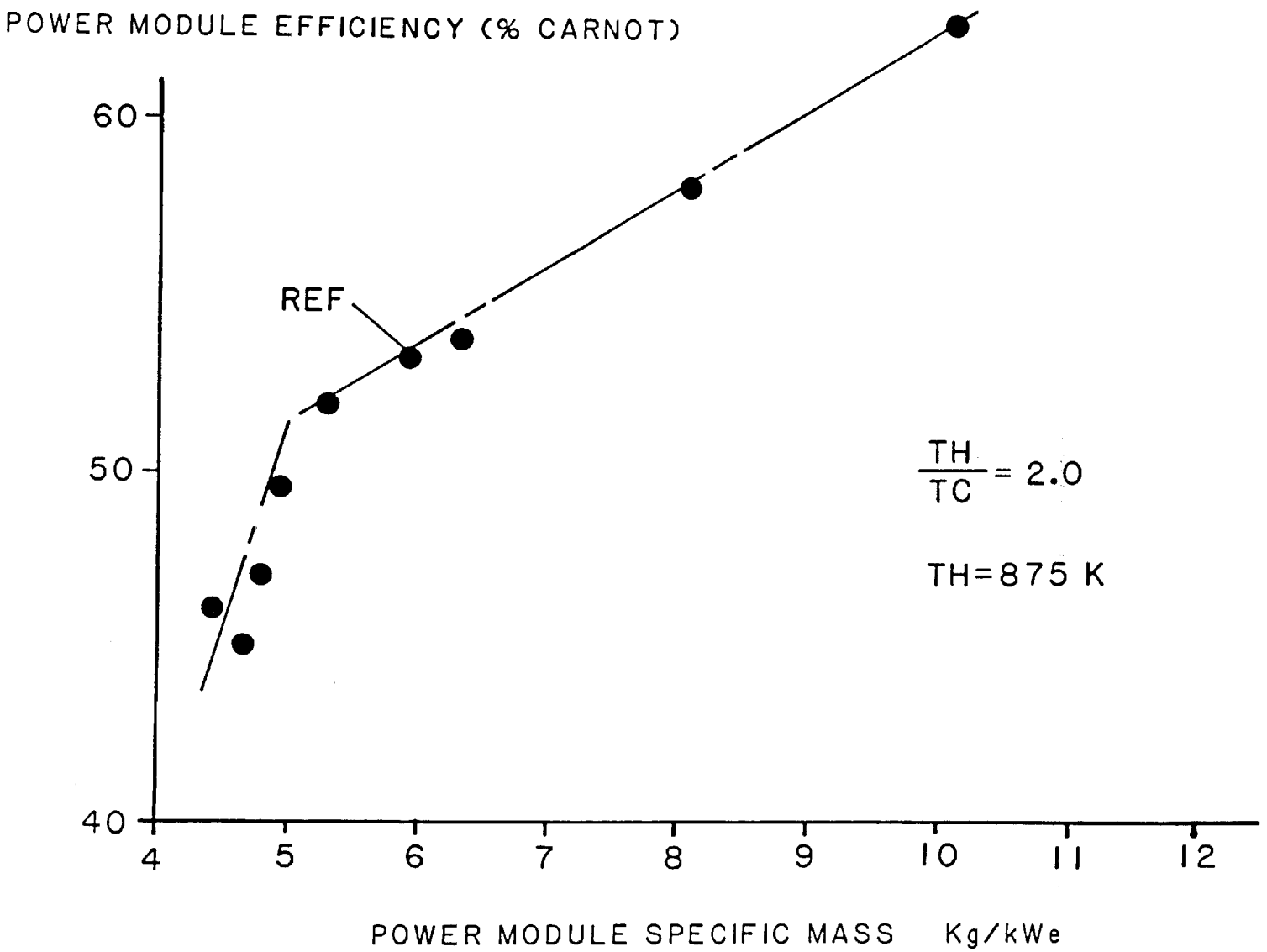

Figure 14: PERFORMANCE FALL-OFF AT LOW POWER MODULE SPECIFIC MASS VALUES

operating temperatures below the temperatures at which they are usually employed? Since the components under consideration are relatively simple rings or cylinders for the pressure vessel, complex fabrication schemes are not required for the individual parts, however, a number of dissimilar material joints will be required in the assembly. This could make joining technology a governing factor in the attainment of low specific mass systems, especially at the higher operating temperatures.

With these thoughts in mind, a review of the pressure vessel structure, heat exchanger assembly, and linear alternator was carried out from the viewpoint of potential major mass reductions. It quickly became evident that the alternator mass was just about at its lower limit unless frequency was radically increased. The cold-end pressure vessel/alternator support structure is assumed to operate at temperatures low enough that ultra high strength steels can be employed and, thus, its mass also will not decrease significantly below the values found in the parametric study.

The hot-end pressure vessel and, to a lesser degree, the hot-end heat exchanger represent the major areas where significant mass reductions are possible. Also, as the temperature ratio is decreased the potential mass savings increases since the higher cold-end temperatures can benefit from the use of more advanced materials. The use of an insulated hot end saves a considerable amount of pressure vessel mass, assuming the material joining technology is available for the high operating temperatures.

After reviewing a number of scalings with various material combinations, it was evident that specific mass reductions in the range of 10 percent to 15 percent are possible. It is expected that the changes introduced to improve the specific mass will not significantly reduce the performance of the engine module.

2. Secondary Areas

This group of modifications to the current parametric results represent major changes in the system design requirements or advances in the current FPSE technology base. They are briefly reviewed in this section so that first-order estimates can be made on their potential improvement to overall power module performance.

Use of Hydrogen

While helium was specified as the engine working fluid, the use of hydrogen (and its associated problems) would improve the engine performance. After a brief review, it is expected that the current engine designs would operate at 2 to 4 Carnot percentage points higher on hydrogen than helium. While not investigated in detail, it is believed that the specific mass reductions possible with a helium-charged engine (10 percent to 15 percent) can be somewhat exceeded with a hydrogen engine. This is due to the better heat transfer characteristics of hydrogen, which would allow some reduction in heat exchanger mass.

The key issue in this case is: Can hydrogen meet the system requirements? From the Stirling engine viewpoint, the problems with hydrogen are potential embrittlement of hot-end components and making up the inevitable leakage losses; both of these can probably be solved in a long-term development program. Other problems such as the hydrogen gas getting into the liquid-metal loop and, in turn, into the reactor may or may not be easily solved.

Secondary Gas for Gas Springs

In a number of the designs developed in the parametric analysis, rather large external piston gas springs were required to minimize specific mass. The corresponding gas spring hysteresis losses were on the order of 600 watts to 700 watts. Other potential FPSE

concepts may have substantially larger gas spring losses. The potential for employing another gas besides helium as the gas spring working fluid may have merit if a simple technique can be developed for maintaining separation between the gases.

A brief review of possible substitute gases indicated that nitrogen was a reasonable possibility due to its relatively inert characteristics and lower thermal conductivity. In this case, for similar gas spring requirements the losses with nitrogen would be about 1/5 to 1/6 that of helium. This could equate to 2 to 3 Carnot percentage points in engine performance for concepts with large gas spring losses.

The practicality of applying this concept to the current engine designs is highly questionable due to the relatively high operating frequencies and long-life requirements. At present the bellow type seal (Figure 15) is the only concept that would assure no migration of the helium into the gas spring space. The life requirement on the order of 10^{10} cycles may be beyond current capability in this area and, in turn, would require a major long-term development program. A potential negative impact of this concept could be caused by the lower heat transfer properties of the alternative gas spring fluid impairing the cooling of the alternator, which is also located in the gas spring space.

Potential Performance Growth - Summary

The results of the performance improvement review are shown in Figures 16, 17 and 18. Only the improvements listed in the Key Areas were included in these results and, as such represent logical improvements for the conventional engine design with a helium working fluid. The Secondary Areas may offer potential for even further improvements in a long-term development program. It is important to note that these improved performance levels represent upper bounds for the conventional engine arrangement with helium working fluid and can be expected to be attained only during a long-term development

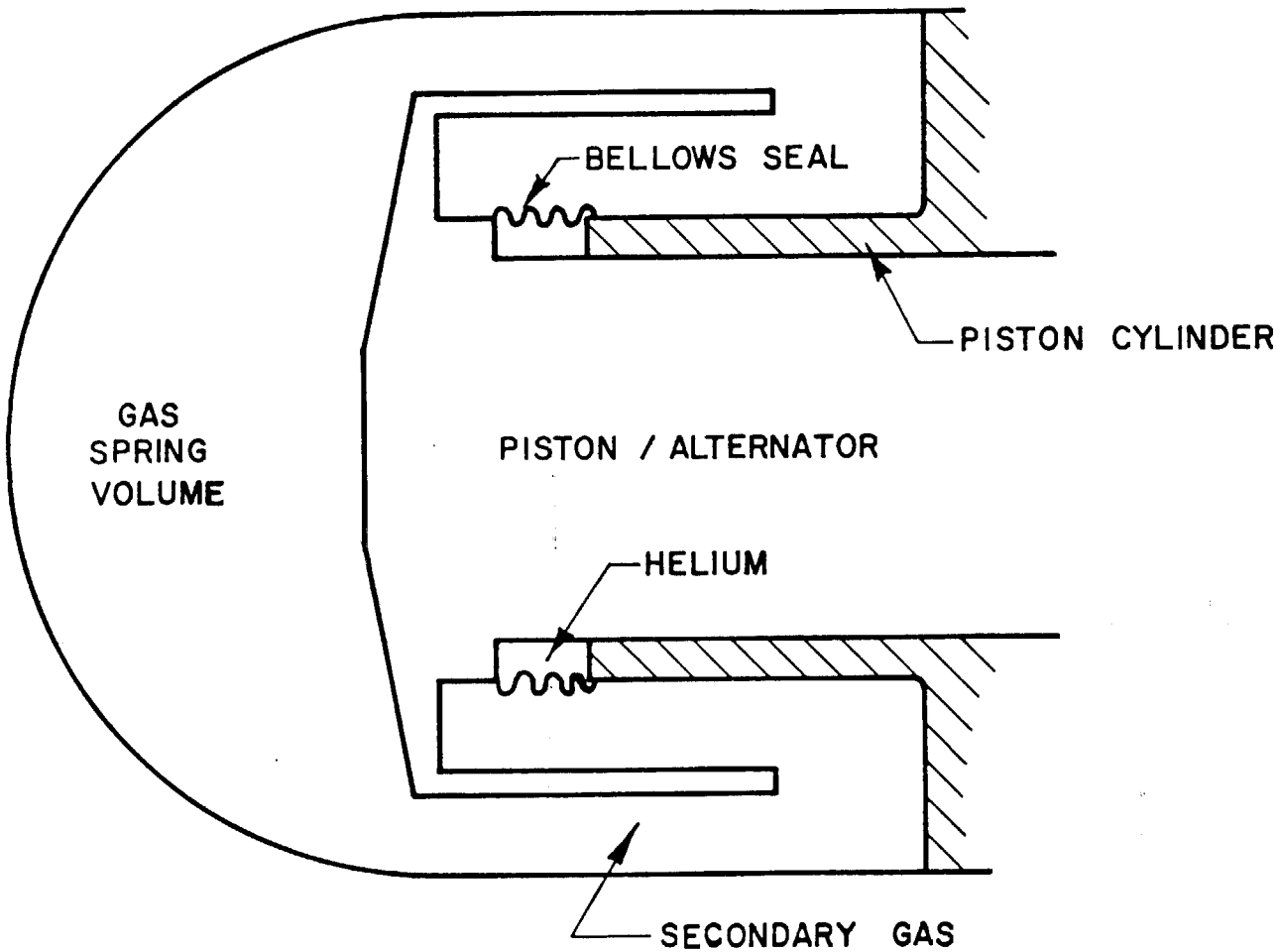

Figure 15: SEAL CONCEPT FOR USING AN ALTERNATIVE GAS IN THE PISTON GAS SPRING

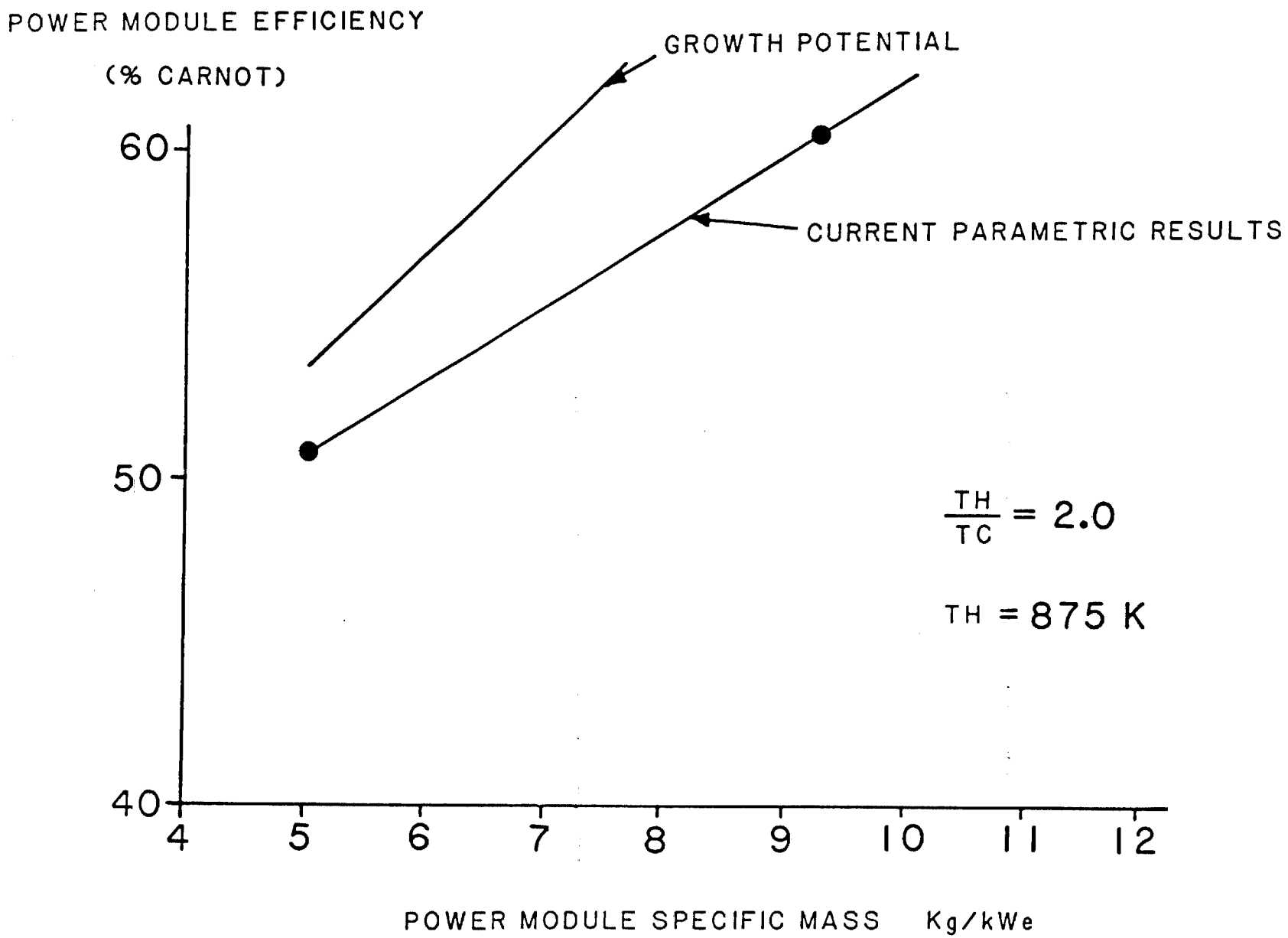

Figure 16: POTENTIAL PERFORMANCE IMPROVEMENTS

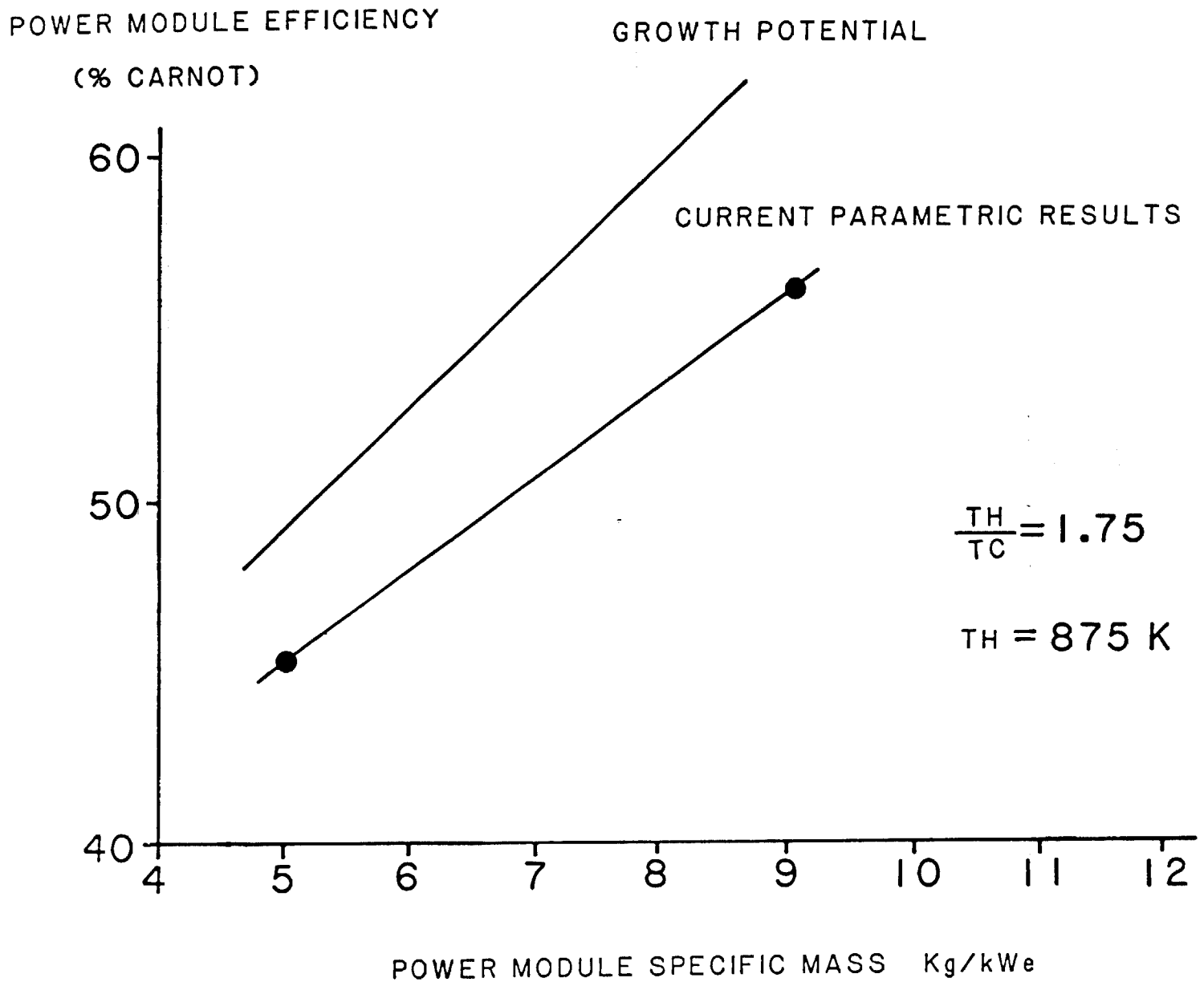

Figure 17: POTENTIAL PERFORMANCE IMPROVEMENTS

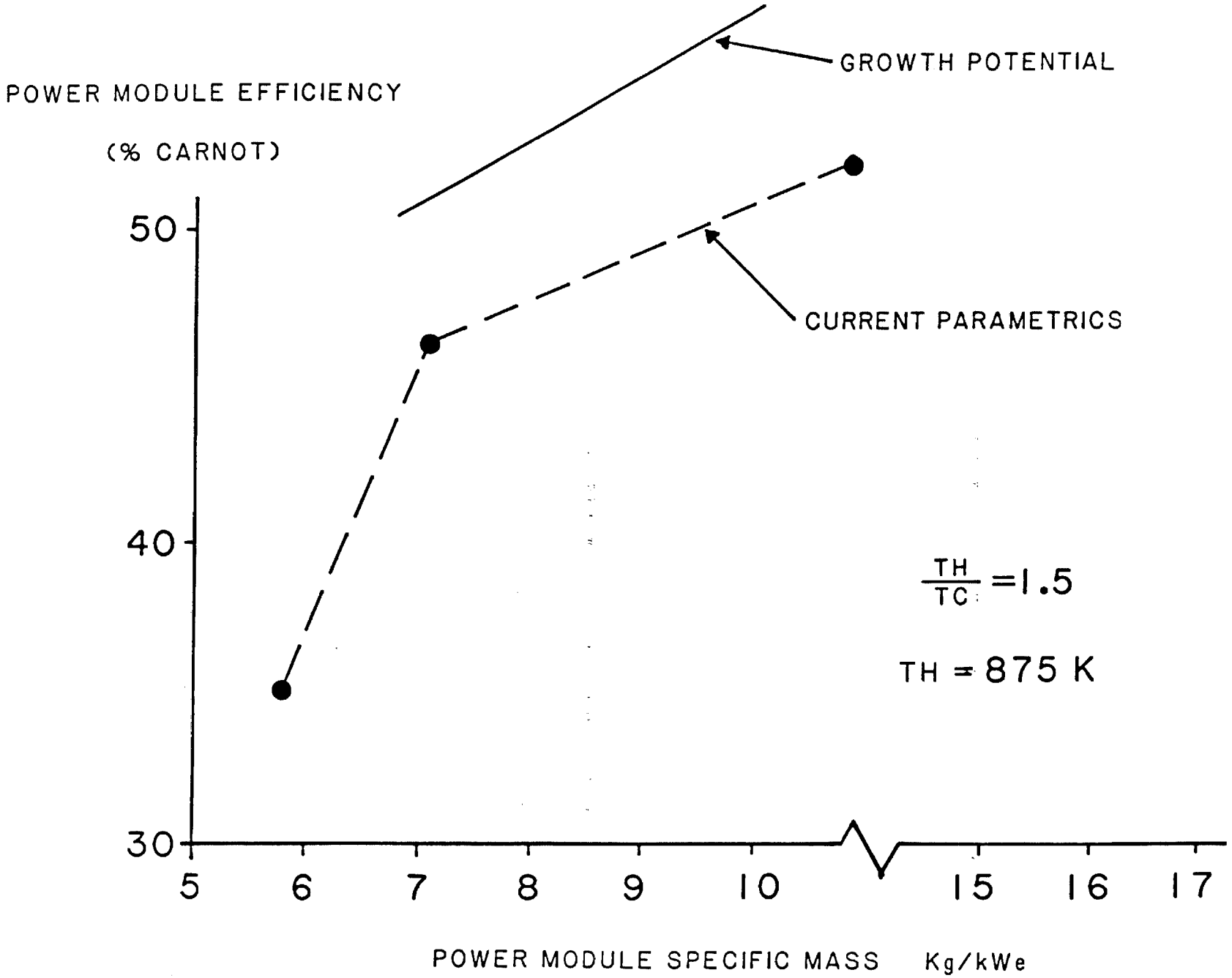

Figure 18: POTENTIAL PERFORMANCE IMPROVEMENTS

program. In all cases the maximum performance improvement was applied to a reference engine without changing its specific mass and the maximum specific mass reduction applied to the reference engine without affecting its performance. This tends to move the improved performance trend to its maximum limit. In reality an engine design undergoing improvements from the current parametric designs will tend to move in a north-west direction as shown in Figure 19 rather than simply west or north.

Table 12 lists the specific improvements considered and their magnitudes. These were applied to the reference engines developed in Task 1 and a few scalings were done at higher specific mass values to anchor the ends of the trend curve. Since more consistent information is available on the T_H = 875 K designs, they were used as the reference points.

TABLE 12: PERFORMANCE IMPROVEMENT ISSUES

ISSUES	PERFORMANCE GAIN OR CHANGE (Based on Fraction of Carnot Efficiency)
Manifold loss	3 % points
Enhanced conduction loss	3 % points
General losses	1 % to 2% points
Structural and material refinements	10 % to 15 % reduction in specific mass

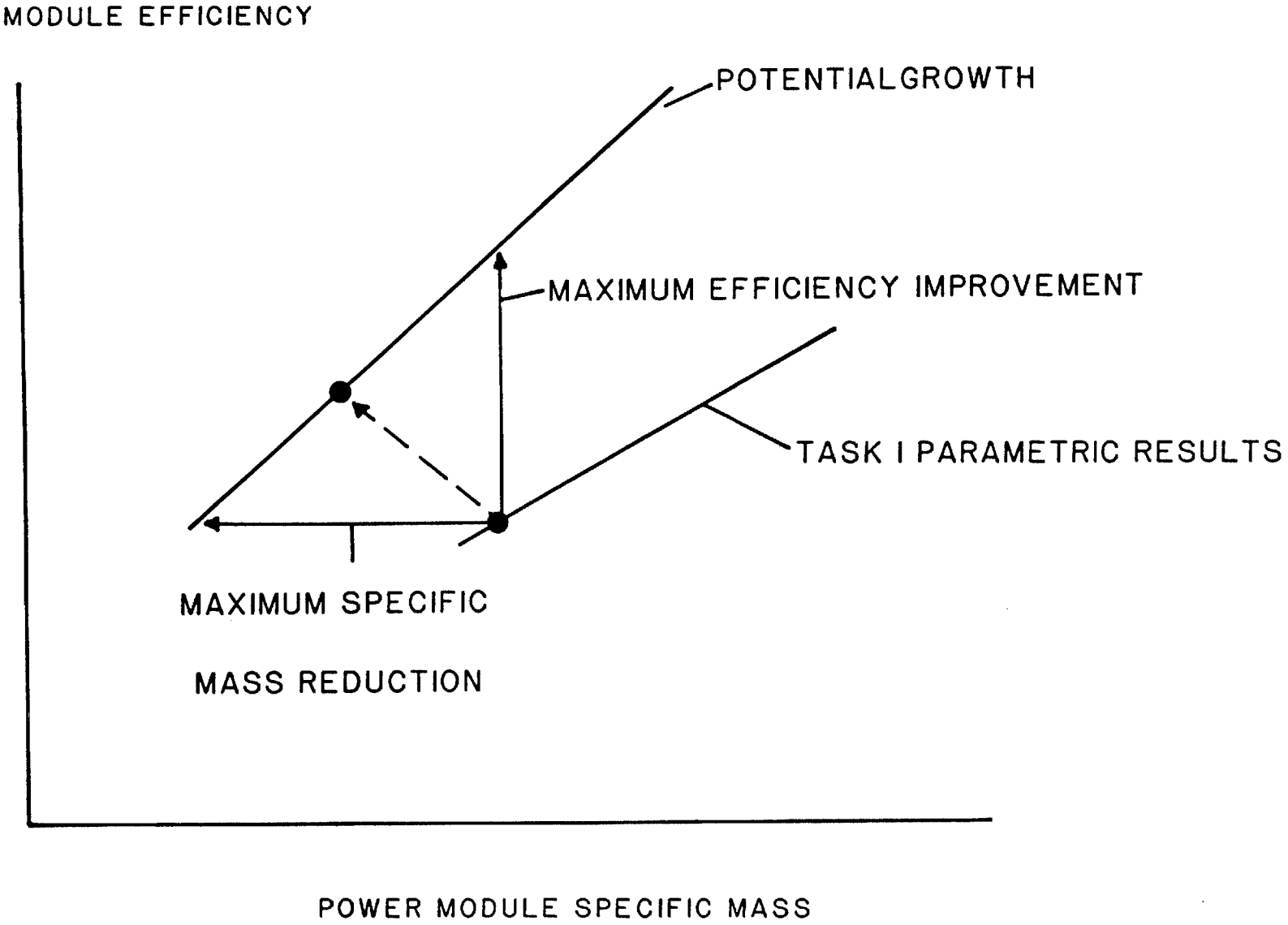

Figure 19: TREND IN POWER MODULE PERFORMANCE AND SPECIFIC MASS IMPROVEMENTS

No major differences are expected in the T_H = 1075 K case since, for all practical purposes, they are the same from the viewpoint of performance and specific mass. Caution should be used when considering the results at T_H/T_C = 1.5 due to the fact that the reference engines at this temperature ratio were quite sensitive to minor variations in their design characteristics.

Modification of Task 1 Parametric Results to an Opposed-Piston Configuration

An integral part of the Task 1 effort was to select a specific engine configuration for further parametric analysis. After considerable in-house review and discussions with NASA/Lewis personnel, it was decided that a conventional single-piston, single-displacer configuration (Figure 1) would be employed as the reference engine for the Task 1 parametrics. Due to the requirement for minimization of the forces transmitted to the spacecraft structure, it was necessary to employ a dynamic balance concept. The use of the balance system adds extra mass to the basic engine/alternator assembly which would not be present in an opposed-piston (SPDE-type) configuration. To evaluate the impact of this added mass and make the results of this effort as widely applicable as possible to the groups investigating the overall SP-100 system, NASA/Lewis requested that a correction factor be developed which would allow the results of Task 1 to be applied to an engine of the SPDE configuration.

The scheme employed to determine this factor is outlined in Figure 20. Basically, the process was to first select a number of specific engine arrangements developed in the parametric analysis, all of which are 25 kW(e) single-cylinder designs. Each of these designs were then scaled down to 12.5 kW(e) at the same basic engine operating characteristics (pressure and frequency). At this point it was necessary to run a number of subscalings of the individual engines to assure that the same geometrical relationships were retained between the 25 kW(e) and 12.5 kW(e) designs. This particular issue is discussed under the "Limitations" heading later in this section.

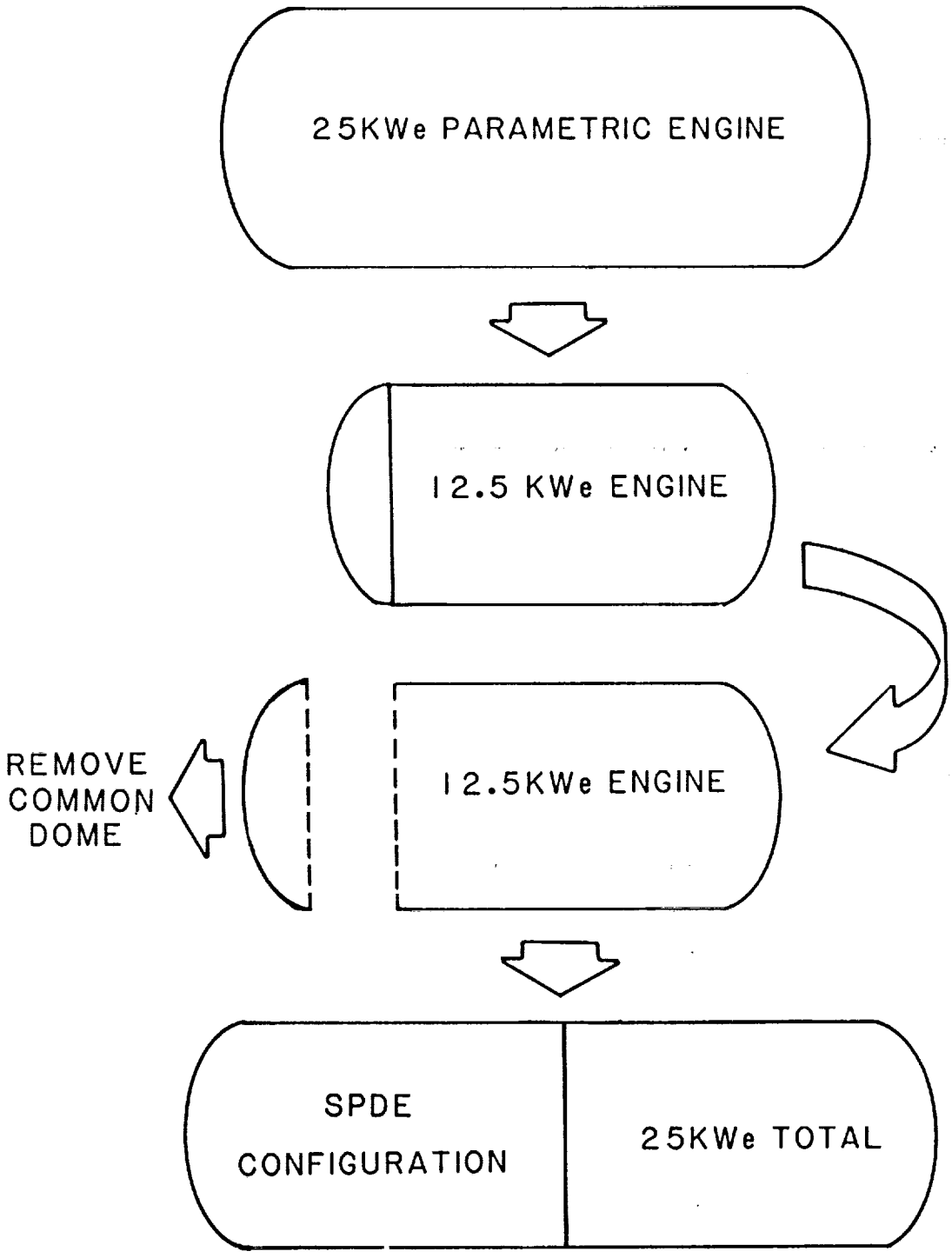

Figure 20: PROCESS EMPLOYED TO MODIFY PARAMETRIC RESULTS FOR AN OPPOSED-PISTON (SPDE TYPE) CONFIGURATION

The common components of the 12.5 kW(e) engine hot ends were then removed and the resulting specific mass considered to be representative of that of a SPDE configuration. The mass of the dynamic balance system for the 25 kW(e) single-cylinder configuration was determined such that both configurations have the same casing motion relative to the spacecraft. These specific masses can then be used to compare the relative advantages of the two configurations. It is important to note, however, that the process employed does not optimize the performance of each 12.5 kW(e) half of the opposed-piston configuration.

1. Results

A number of cases were investigated at each of the following operating temperature ratios: T_H/T_C = 1.5, 1.75, and 2.0. For the two higher temperature ratios, a reasonably consistent correlation could be developed relating the parametric results to the SPDE configuration. However, at the lower temperature ratio (1.5), no clear relationship can be developed. This was due to the performance of the scaled 12.5 kW(e) being radically off that of the starting 25 kW(e) reference point. This effect was not unexpected due to the extreme sensitivity of the low temperature ratio designs noted during the previous parametric review.

In all cases at T_H/T_C = 1.75 and 2.0, the performance and specific mass of the combined SPDE configuration was somewhat better than the single 25 kW(e) design with its dynamic balance unit attached. While there was some variation on each design point investigated, the relative improvements in performance fell within the band of 5 percent to 7 percent, which equates to about 1.5 percentage points in efficiency. The higher improvement values were for the lower specific mass engines, i.e., when starting with a low specific mass 25 kW(e) engine as the reference engine, the 12.5 kW(e) scaled version had the higher relative performance improvement as compared to starting with a higher specific mass 25 kW(e) reference point.

From the viewpoint of specific mass, all scaled individual 12.5 kW(e) modules had higher specific mass values than the reference 25 kW(e) engine (without dynamic balance unit). The magnitude of this increase was on the order of 8 percent for the engines investigated. The common portion of the engine pressure vessels that was removed to mate the two 12.5 kW(e) designs represented approximately 4 percent of the engine specific mass for the particular design employed in the parametrics. For other pressure vessel designs or heater configurations that cannot employ the insulated head concept, the relative change in specific mass could be higher. (See following section, Limitations.)

The result of the components' removal brings the specific mass of the equivalent SPDE engine configuration to about 4 percent greater than the 25 kW(e) unbalanced engine.

The dynamic balance unit for the 25 kW(e) single-cylinder engine was assumed to be a passive balance unit, that is it did not employ an active control scheme to vary its tuning. For equivalent casing motions for both systems (assumed to be 0.003 in. amplitude) the balance unit made up 10 percent to 12 percent of the specific mass of the 25 kW(e) engine. Therefore, when the single 25 kW(e) balanced engine is compared to an equivalent SPDE configuration, the specific mass of the SPDE configuration will be 6 percent to 8 percent less.

In summary, the overall performance of the SPDE configuration can be expected to be, at best, 5 percent to 7 percent (about 1 to 1.5 percentage points of efficiency) greater than the equivalent Task 1 parametric designs and have specific mass values about 6 percent to 8 percent less when a passive absorber unit is employed. The use of an active absorber eliminates this specific mass advantage of the SPDE configuration. The potential performance advantage (See next section, Limitations.) must be weighed against the complexity of the SPDE concept and its impact on system reliability.

2. Limitations

During the process of converting the 25 kW(e) Task 1 designs to the SPDE configuration, a number of steps were employed which impact the results. These are called out in the following paragraphs and should be reviewed prior to simply using the results reported above.

Scaling Process

The scaling system developed for the Task 1 Parametric Study was used to convert the 25 kW(e) engines to 12.5 kW(e) modules. This technique has shown itself to be quite accurate within specific limits dictated by the mathematics employed in the development of the scaling rules. For the range employed in this analysis, the accuracy is on the order of the differences noted in specific mass and performance. However, in the area of showing trends, which they were specifically developed to do, scaling results clearly indicate a trend toward the results shown above, i.e., somewhat higher performance and lower specific mass than compared to a single 25 kW(e) balanced engine module employing a passive absorber unit. To further improve the accuracy of these results would require a process akin to that used in the main Task 1 parametrics.

Engine Operating Characteristics

During the scaling process employed, no attempt was made to vary the key engine operating characteristics (pressure and frequency) from those employed in the Task 1 designs. This is without doubt a limitation on the results since there is no assurance that these engine characteristics are optimum for the 12.5 kW(e) modules.

Geometrical Considerations

During the Task 1 Parametric Study, it was noted that the specific mass of an engine module was a strong function of a particular geometrical ratio once frequency and pressure had been selected. This parameter relates the piston diameter to the alternator reference diameter. In all cases it was found that values close to 1 minimized power module specific mass. During the process of scaling from 25 kW(e) to 12.5 kW(e), this ratio changed to a lower value than desired from a minimum specific mass viewpoint. To improve the specific mass of the 12.5 kW(e) module required a modification to the amount of piston external gas spring employed to drive the ratio closer to 1 (and to those used in the 25 kW(e) design). This was done by employing the scaling rules and represents the only change made to the 12.5 kW(e) scaled engine.

Dynamic Balance Unit

The balance unit employed in this analysis technique did not use any form of active control system. A fully automated system would, without question, be less massive than the current system and it can be expected to nullify the specific mass advantage of the SPDE configuration.

Pressure Vessel Modification

The baseline engine developed during the Task 1 Parametric Study employed an insulated dome on the hot end of the pressure vessel. This arrangement had considerable advantages from a mass viewpoint by reducing the impact of the relatively large diameters caused by the heat exchangers employed. This dome represents the portion of the engine removed when forming the SPDE configuration from two 12.5 kW(e) modules. Thus, if some radically different heat exchanger were employed and the insulated hot end were not applicable, the amount of mass removed could be considerably different than the 4 percent assumed in this analysis.

Relative Performance

As was previously noted, it was necessary to modify the external piston gas spring on the 12.5 kW(e) engine module to minimize the specific mass. This was done by using the scaling rules and varying the amount of piston external gas spring employed. In the process the gas spring losses were reduced along with the relative piston stroke. These effects cascaded through the system causing changes in other losses. The net effect was a small performance increase over the 25 kW(e) design. While it is believed that the trend to higher performance is real, the absolute magnitude is harder to gauge. A few higher order simulations were run of a scaled engine ($T_H/T_C = 2.0$) to attempt to better define this performance advantage and in all cases the performance improvements ranged between 1 percent and 5 percent (about 1 percentage point in efficiency). While this somewhat confirms the trend, it is based on an extremely limited number of cases. It is recommended that caution be employed if this potential performance advantage is used to justify the SPDE configuration over the single 25 kW(e) module. The reduced number of components in the single-cylinder design and its higher level of development improves the potential power module reliability over the SPDE concept.

Task 2 25 kW Design

At the completion of the Task 1 effort, it was felt that an excellent justification existed for further refinement of the basic power module concept developed.

At the same time it was evident that the original power module specifications would need modification to reflect the results of the completed parametric analysis as well as the information developed by the various SP-100 system integrating contractors. From both efforts it was evident that the temperature ratio and heater temperature should be increased. From discussions with NASA personnel, it was agreed that the Task 2 effort should be oriented toward a higher temperature ratio design with a maximum heater temperature such that a refractory-based alloy would be required. It was assumed that one of the niobium-based alloys, preferably the niobium-zirconium alloy, Nb-1Zr, would be used at least in the hot-end heat exchanger elements which are exposed to the liquid metal. Further, the operating temperature distributions and mass flow rates of the liquid metal (NaK) for the heater and cooler were also defined, based on values determined from the SP-100 systems integration studies.

While no specific guidelines for engine forces transmitted to the spacecraft were available, it was believed at the start of the Task 2 effort that the adaptive balance unit could reduce these loads to values well below 100 newtons with significantly reduced balance mass requirements compared to the passive unit investigated earlier. Due to this factor, no compelling reason could be made to radically change the basic engine configuration from that developed in the Task 1 effort.

Power Module Description

The FPSE linear alternator power module designed during Task 2 represents a relatively straightforward extension of the technology developed at Sunpower over a number of years. While the required operating conditions are reasonably advanced by current FPSE standards, only the operating life requirement of seven years represents a major departure from demonstrated technology. At the same time it is important to note that there are no particular problems in the development of the seven year life SP-100 engines which are not already under active review due to the life requirement of the commercial market place. It is agreed by many groups that the refinement of the existing various noncontact bearing and seal concepts will essentially eliminate engine operating life as a major issue. This is not to say that considerable engineering work is not needed, rather that the basic concepts of noncontact component life has been demonstrated in other dynamic systems and now these must be implemented in the FPSE. In the case of the SP-100 power module, it is believed that the issues revolving about the use of refractory alloys and their unique compatibility and joining characteristics are more critical to the potential success of the current design than any other issue.

The general configuration of the 25 kW power module is shown in Figure 21 with its major subcomponents called out. This design represents the culmination of the information developed in the parametric study portion of this effort and the SP-100 system requirements placed on the power module via the reviews carried out by the system integrating contractors. The key goals and system constraints used in the design are shown in Table 13 and the resulting power module operating characteristics are given in Table 14.

In the following sections of this report, the overall characteristics of the current power module are further discussed, the key components described and any unique design concepts or requirements reviewed.

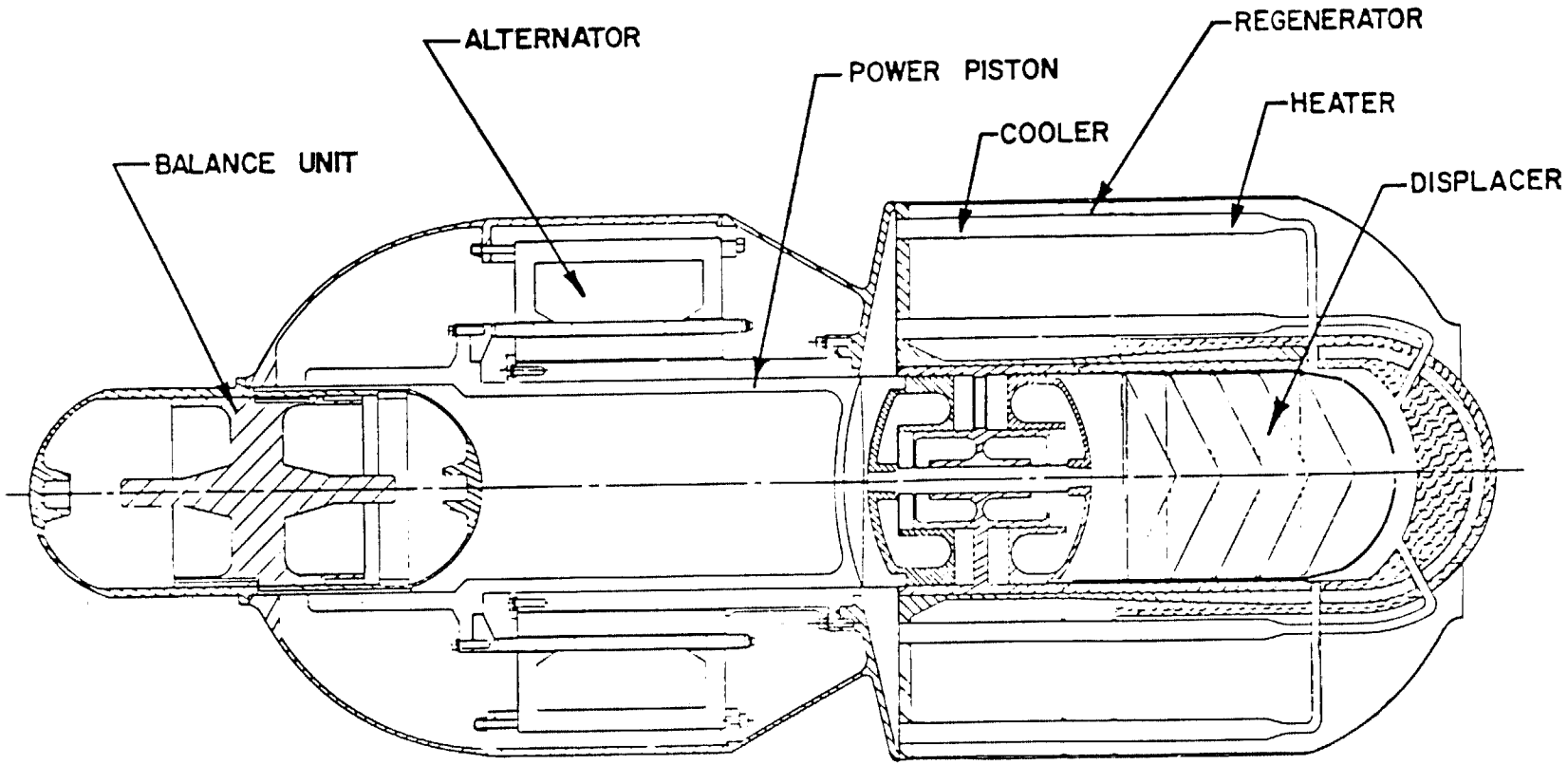

OVERALL LENGTH 1.25 M
MAXIMUM DIAMETER .46 M
MASS 145 Kg

Figure 21: SPACE POWER MODULE

TABLE 13: NASA INPUT REQUIREMENTS FOR TASK 2

Pumped liquid-metal loops	
Reactor NaK outlet temperature	1150 K
NaK inlet temperature to power module	1130 K
Average heater wall temperature	1080 K
Average cooler wall temperature	540 K
Temperature ratio	2.0
Specific mass	5.5 kg/kW to 6 kg/kW
Power module efficiency	> 55 % Carnot
Heater material	Refractory (Nb-1Zr)

TABLE 14: TASK 2 DESIGN POINT

Mean pressure	176 bar
Piston amplitude	15 mm
Displacer amplitude	11 mm
Operating frequency	95 Hz
Engine efficiency	30.3 %
Alternator efficiency	93 % to 94 %
Power module efficiency	28.5 %
Percent Carnot	57
Module specific mass	5.8 kg/kW(e)
Transmitted force	80 N
Overall length	1.25 m (49 in)
Maximum diameter	0.46 m (18 in)

General Characteristics

As can be seen in Figure 21, the current power module employs a conventional single-cylinder design common to the majority of existing free-piston Stirling engines. Due to the

unique operating requirements, an adaptive balance unit is employed to minimize the forces to the spacecraft. Its mounting on the rear of the power module pressure vessel allows it to serve also as a support for the piston gas spring seal. The main axis of the engine is occupied by the piston and displacer which are essentially of constant diameter. The power piston supports the magnet assembly for the linear alternator which is wrapped around the piston cylinder. The cylindrical magnet assembly is composed of a fiber composite encasing the magnets themselves attached to a titanium support structure which is joined to the beryllium piston body. The inner and outer alternator laminations are fabricated from a high cobalt content alloy to maximize the allowable saturation current. The copper coil is surrounded by the outer lamination set which is actually made up of a number of individual stacks (Figure 22) rather than a continuous lamination ring as used on the inner lamination set. This portion of the power module is enclosed in a pressure vessel fabricated from ultra high strength steel which also supports the outer lamination assembly.

At the interface between the piston and displacer, the cold-end gas manifold directs the working gas periodically at small turbines located on both the piston and displacer. These are shown schematically in Figure 23. These induce a spinning motion to the displacer and piston as they reciprocate, causing the components to self-pump a gas film between the moving component and its respective wall. This action will provide the necessary noncontact operation of critical piston and displacer bearings and seals to assure the seven-year operating goals can be reached.

The displacer is made of a beryllium structure in the area of its double-acting gas springs and seals, with an Inconel alloy used for its other high temperature components. To allow the necessary power change from 80 percent to 100 percent should another power module fail (system includes five 25 kW(e) engines producing 100 kW(e) total output), a single-shot control valve is installed in the displacer gas spring assembly. When open, the unit provides enough additional damping to detune the engine; when closed, this damping is removed and the engine operates at the higher power point. While the scheme is the

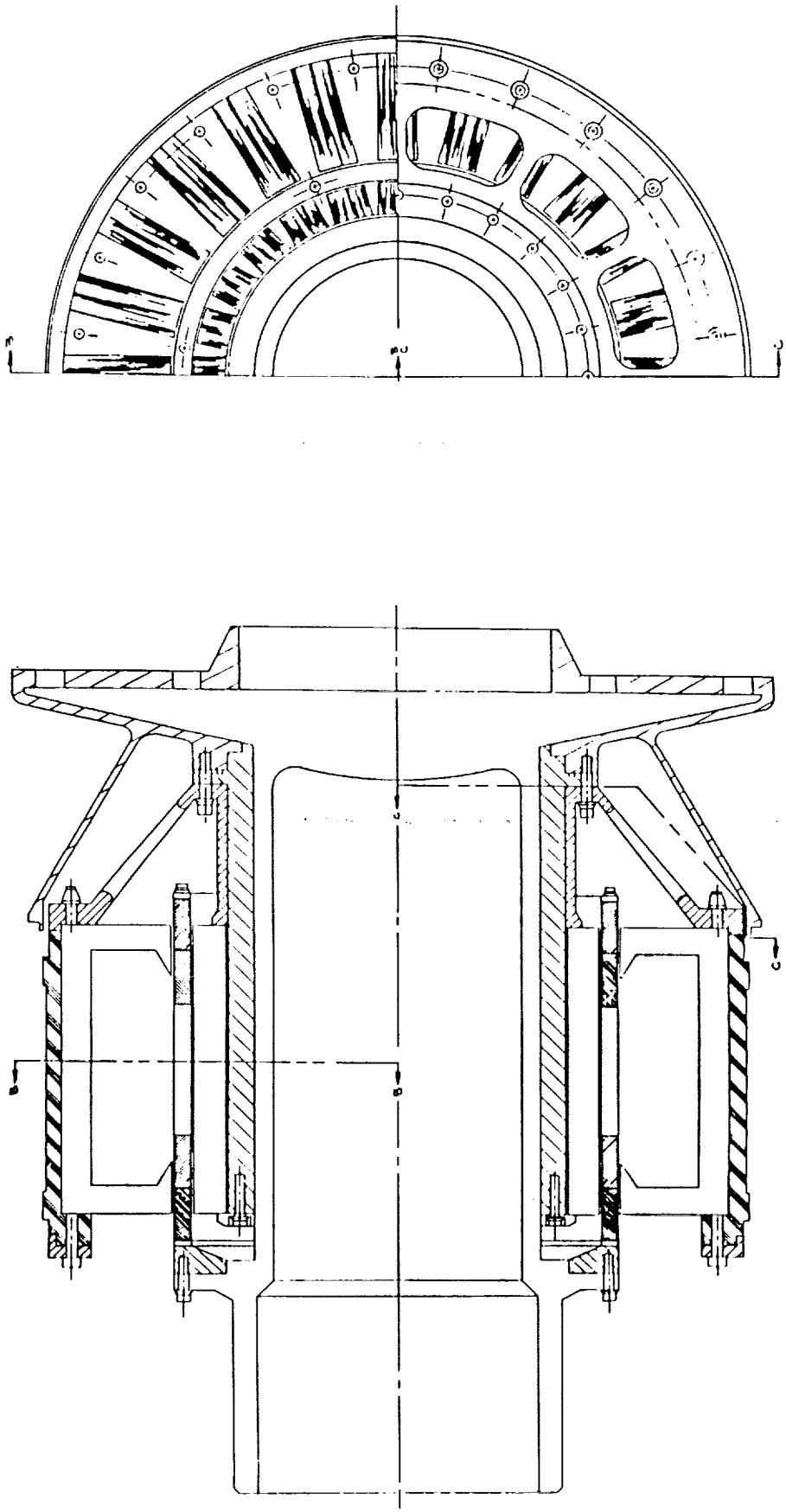

Figure 22: ALTERNATOR ASSEMBLY

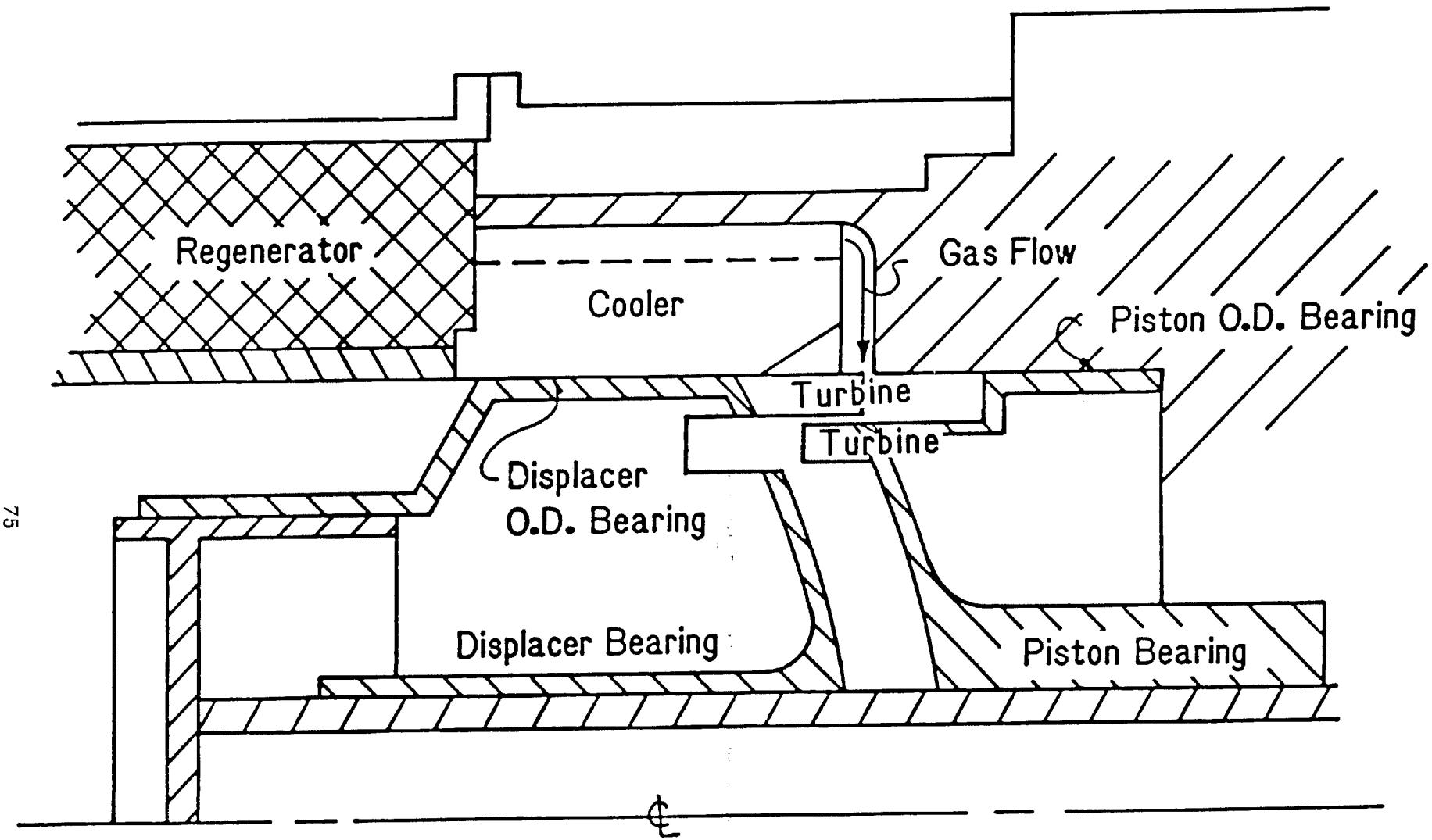

Figure 23: SPIN BEARING ARRANGEMENT IN STIRLING ENGINE

primary one considered, a fall-back unit employing a single-acting spring was also investigated. In this type of system, a one-time change in the displacer gas spring volume is made during the power change and as such does not suffer from the power loss caused by the damper in the double-acting spring case; however, the sealing requirements are more critical.

The heat exchanger assemblies are unique in that they are made up of 178 individual modules each of which contains its own heater, regenerator, and cooler. These are fabricated from a continuous refractory alloy tube (Nb-1Zr) with a hollow niobium insert forming the working gas passages in the heater and a composite copper and beryllium insert forming the equivalent passages in the cooler. Between these is a regenerator module made of layers of woven metal screens. Each module can be fabricated and fully tested before being assembled into the power module, greatly improving the reliability of the heat exchanger unit. A second advantage of this concept is the relatively small number of joints (500) that are formed when the heat exchanger joins the basic pressure vessel. In comparison a conventional shell-and-tube unit would have more than 10,000 joints.

The liquid-metal working fluid (NaK), used in both the heater and cooler assembly, is forced to flow at right angles across the heat exchanger assembly through baffles which also support the individual modules. The heat exchangers are further partitioned into four longitudinal assemblies to assure uniform heating of the modules. This will require four discrete inlets and outlets for the heater and cooler. The cylindrical regenerator section is separated from the individual liquid-metal flows by bulkheads on each end. Radiation shields and vented multi-foil insulation surround the regenerator assembly, minimizing the heat transfer from the heater and cooler bulkheads. Axial conduction down the pressure vessel walls surrounding each regenerator module represents a significant thermal loss to the unit caused primarily by the relatively thick wall necessary when only Nb-1Zr is employed. To reduce this loss, a refractory alloy sleeve of TZM is placed over the

regenerator tube wall which is fabricated of Nb-1Zr with a thickness necessary for the colder end of the regenerator. Since TZM has excellent working strength at the temperatures used, the composite wall can be considerably thinner and, in turn, reduces the conduction loss by nearly a factor of 2. The performance gained by this arrangement is equivalent to raising the hot-end temperature by about 50°C and requires only a relatively simple refractory to refractory brazed joint in an area that is not exposed to the liquid-metal heat transfer fluids.

The primary hot-end pressure vessel wall represented a unique design problem due to the relatively low useful strength of the niobium alloys and the tube perforations required in the high temperature end. For adequate strength in this area, the pressure vessel wall thickness (and overall mass) became excessive and possible substitute materials and fabrication techniques were considered. The final approach eliminated the complexity of an all-refractory pressure vessel by employing a conventional Inconel pressure vessel with an internal and external insulation layer to reduce the wall temperatures by approximately 250°C below the maximum gas temperatures. This concept has been proposed in a number of designs. However, in the past the goal was to reduce the pressure vessel operating temperature to essentially ambient conditions so that low cost, high strength steels could be employed. To attain these goals, extremely advanced internal insulation schemes were required. In the current power module, the temperature reduction is relatively small so that the internal insulation requirements can be provided by the helium working gas itself. This is accomplished by placing a felt-metal insulation (very similar to the engine regenerator) layer, which is covered with a thin metallic shell, in the critical areas. The space between this shell and the pressure vessel wall is maintained at mean engine pressure by a controlled leak to the work space of the engine, thus forming a quiescent layer of helium which provides the actual insulating characteristics. The basic technique has been widely employed in current free-piston Stirling engines as an insulating sleeve between the expansion space/displacer wall gap and the regenerator assembly, so no radically new fabrication concepts are required. The primary failure mode for this type of arrangement is

a gradual increase in the size of the leak to the trapped helium space; this will not significantly decrease its insulation characteristics but will cause a change in the power of the engine due to the volume of this space now being involved in the thermodynamics of the basic engine cycle.

The necessary exterior insulation for the pressure vessel is provided by a multi-foil, vacuum insulation blanket with a thin niobium shell which is exposed to the hot liquid metal. This insulation is only required in the upper portion of the pressure vessel, however, it will represent a complicated installation issue since it must surround the heat exchanger tubes where they enter the pressure vessel. A number of schemes have been considered, with the most practical being the integration of the insulation with the reinforcement employed at the refractory metal to Inconel joint (Figures 24 and 25). This would allow the complete fabrication and checkout of the insulation prior to the installation of the heat exchanger modules. While not specifically addressed in the current design, it is assumed that the entire heat exchanger assembly is further insulated over its exterior surface to minimize thermal losses from the liquid-metal filled heater and cooler.

Material Selection Issues

It was evident from the start of this power module effort that the FPSE/LA system would employ a considerable mix of materials if the ambitious specific mass goals were to be reached. Figure 26 shows the general materials considered for the basic power module at the start of the Task 2 design effort and their possible areas of application. For the lower temperature systems of the Task 1 parametric studies (< 1000 K), no particular materials problems were expected other than those common to the development of long-life high temperature structures. This latter issue was of primary importance to the internal system components since long-term distortion could lead to interference with the moving components, rapidly causing failure. The external pressure vessel and heat exchanger

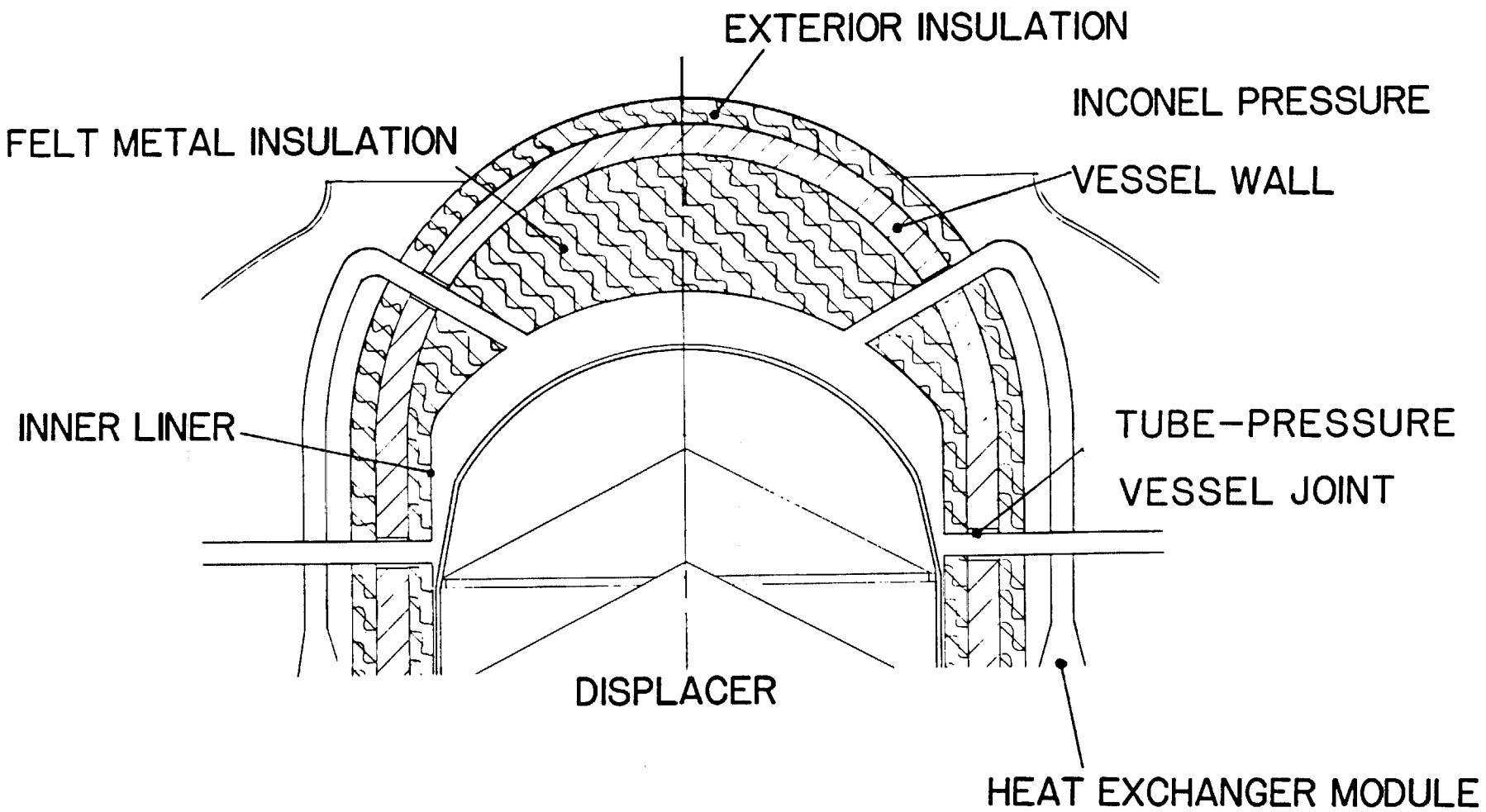

Figure 24: INSULATED WALL CONCEPT

(INSULATED WALL CONCEPT ONLY)

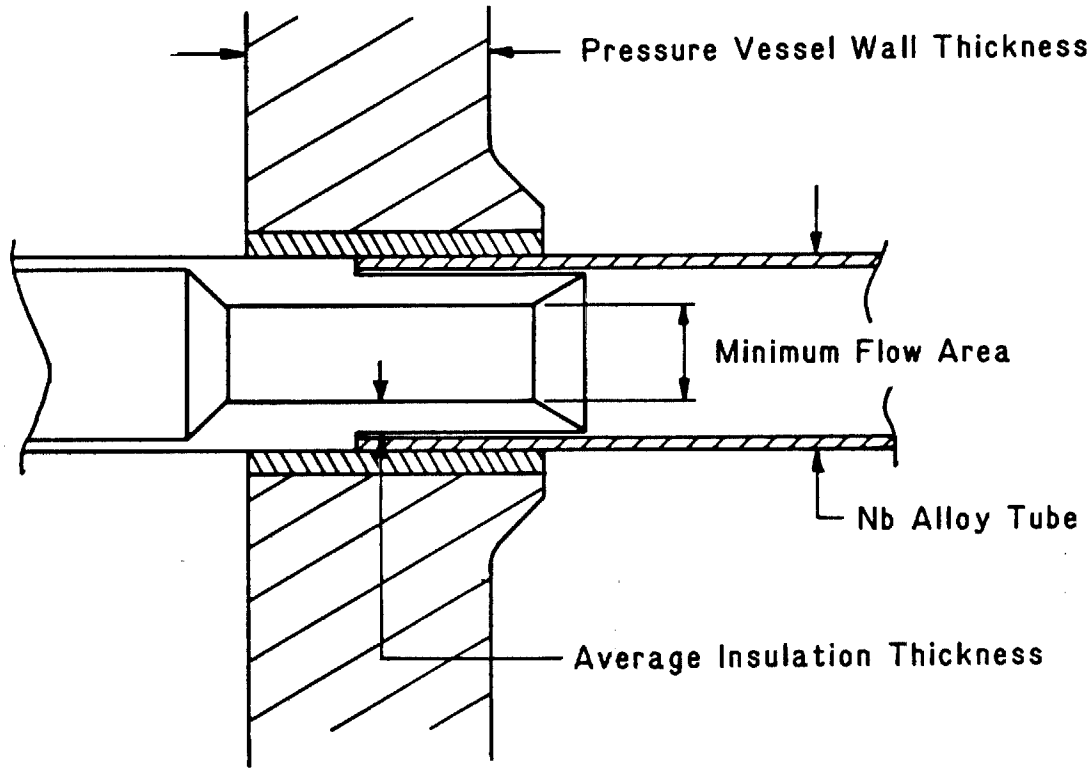

Figure 25: HEATER TUBE TO PRESSURE VESSEL JOINT

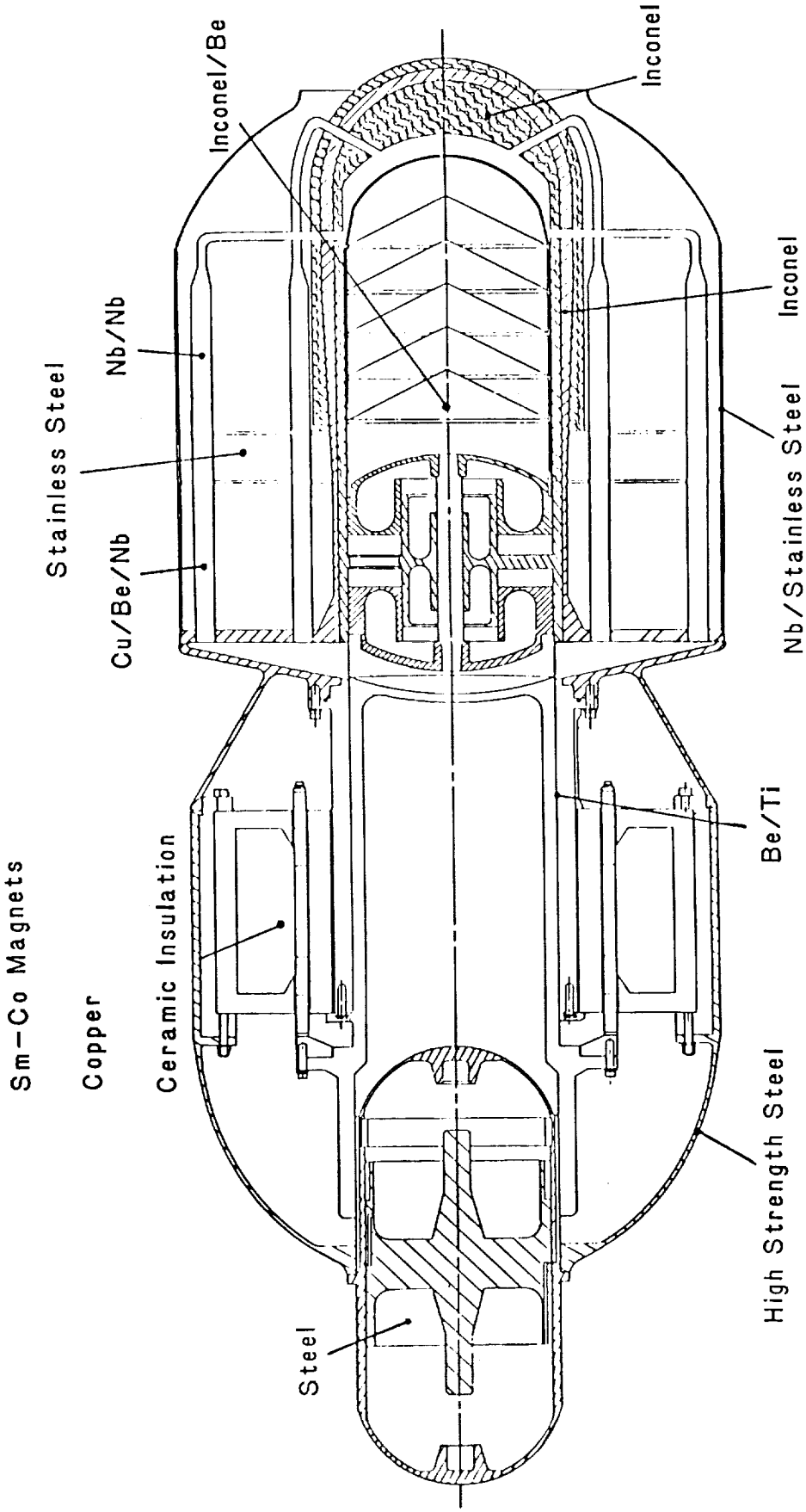

Figure 26: SPACE POWER MODULE MATERIALS

components were relatively conventional and quite tolerant to some permanent distortion over the operating life of the system. Joining technology for these materials was also well established and would only possibly eliminate a few of the harder to fabricate superalloys from application in the relatively complex heat exchanger components.

The introduction of the requirements for higher heater operating temperatures and, in turn, the use of a refractory alloy was not expected to change the basic materials picture since only a relatively small fraction of the overall power module needed to be fabricated from this material. This relatively optimistic view was quickly changed when it became evident that considerable variation existed within the refractory metal community on the sensitivity of the potential alloys to contamination from various sources within the power module.

Initial design requirements indicated that the driving criteria for the selection of the refractory alloy for use in the FPSE application were at odds with those of other components in the SP-100 system. From the reactor viewpoint, reasonable strength levels and good corrosion resistance to the liquid metal would play a major role in alloy selection, along with the unique material requirements of the nuclear reactor assembly. The FPSE, on the other hand, is a dynamic system which is required to operate at quite high pressures if the specific mass goals are to be attained. This places considerable emphasis on the high strength-to-density ratio materials for fabrication of the higher temperature components. However, since one of the significant loss mechanisms in the Stirling engine is thermal conduction from the hotter to cooler portions of the various components, the combination of high strength-to-density ratio and low thermal conductivity defines the best material in many cases. In the temperature range of interest a number of refractory alloys provide reasonable performance from the viewpoint of strength-to-density ratio and thermal conductivity (Figure 27). It is evident that to best meet the Stirling engine requirements the selection of an alloy generally associated with much higher temperature operation would be

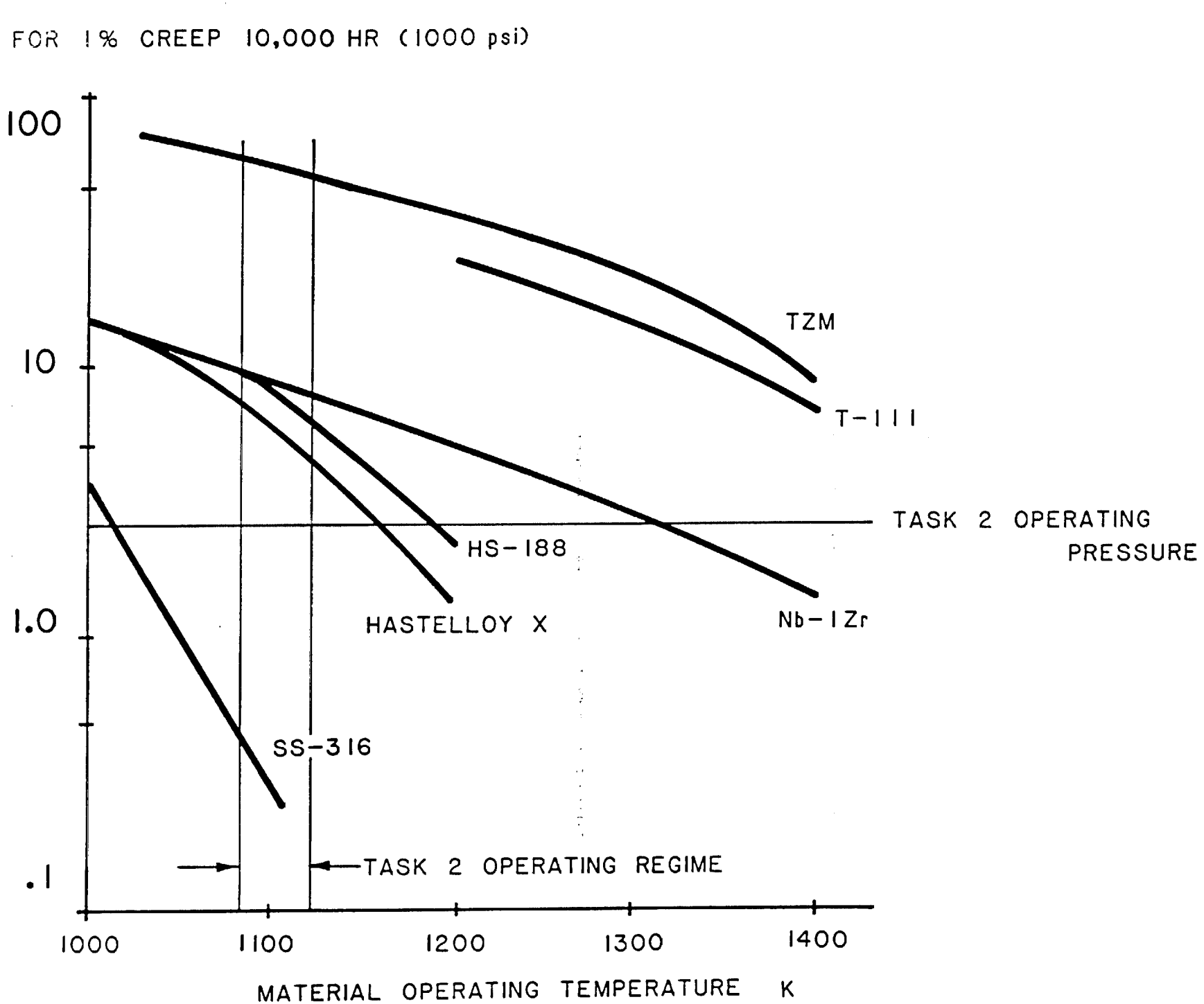

Figure 27: CANDIDATE HIGH TEMPERATURE ALLOYS

recommended, for example, TZM. The niobium alloys, on the other hand, provide an excellent choice at the temperatures of interest when relatively low operating pressures allow the use of structures that are so thin that in many cases manufacturing limits rather than strength limits govern the material thickness requirements.

Based on considerable review of the potential alloys available and discussion with both NASA and industry personnel, it was agreed that the primary refractory alloy to be employed in the design would be of the niobium family, preferably the niobium-zirconium alloy Nb-1Zr. However, it was also agreed that higher strength niobium-based alloys would be considered along with application of other higher-strength refractory alloys in selected portions of the primarily niobium structural components.

The primary unanswered question concerning the use of the refractory alloy became one of contamination by materials transported from other parts of the engine. This could occur via the helium working gas or through direct contact at the various points within the engine where joints between the refractory and nonrefractory materials occurred. This latter issue was investigated primarily through an in-depth review of past and current efforts in the fabrication and joining of niobium-based alloys and is discussed in the sections of the report concerning the design of specific engine components.

The potential for working gas-carried contamination was never completely resolved during this study. It is expected that materials testing under the direction of NASA/Lewis will provide the first clear design guidelines concerning this issue. Two possible approaches were considered during the latter portion of the program and, as such, are not included in the current design per se. The first, and least likely to be possible, is the simple process of building the engine entirely from niobium or from a single material which is known to not contaminate the niobium-based alloys. This would eliminate the contamination issue but is clearly unworkable in many components, such as the alternator

where niobium does not meet the basic electrical requirements. The second approach is to clad, plate, or in some other manner encapsulate specific components within the engine in a compatible material. This may have considerable advantages if a high temperature resistant process can be developed; cladding the interior of the current niobium-based heat exchanger modules to effectively block off the contact of the contaminated working gas could allow conventional fabrication materials to be used throughout the remainder of the design. While no specific process was defined, the simple, relatively large diameter refractory metal tubes employed in the heat exchanger modules are considerably more adaptable to such a scheme than the large number of extremely small diameter tubes present in a conventional shell-and-tube heat exchanger. This coating process would result in a considerably lighter heater which would also be somewhat more efficient since materials with better thermal properties could be employed as inserts. It is recommended that this concept be given further detailed review since it would essentially eliminate the sensitive compatibility issue if it were possible.

Material Limitations

At the onset of the Task 2 design of the power module, a review of various material design issues was undertaken to develop a consistent set of criteria for determining material useful-strength characteristics. This was necessary due to the long-life requirements of the SP-100 system, seven years of continuous operation, and the extremely large number of cycles the various moving components had to withstand.

The basic pressure vessel structure and heat exchangers are primarily limited by creep distortion limits over the desired life time. Since the structures are exposed to a relatively high mean pressure, as well as a cyclic pressure with an amplitude of approximately 10 percent of the mean pressure, the technique described in (reference 4), was used to determine the effective stress rupture life of these components. For the pressure variation described, the cyclic stress component decreases the time to rupture by a factor given by:

$$\frac{T_0}{T_C} = \left(1 - \frac{\sigma_C}{\sigma_0}\right)^3$$

where: T_C is the cyclic creep rupture time, T_0 is the static rupture time, and σ_C and σ_0 are the cyclic and static stress levels, respectively. In the proposed design the pressure variation induces a value of σ_C/σ_0 of approximately 0.10 and, in turn, a factor of T_C/T_0 of about 0.75. Therefore, to arrive at a design creep rupture life of about 62,000 hours with a cyclic loading it is necessary to design the structure to be capable of 85,000 hours to rupture with a static load. This basic criterion was further modified to limit the distortion to 1 percent during this time period, rather than rupture. The useful strength of the material for design purposes was limited to 90 percent of this stress level. These basic criteria, as well as other material operating issues, are listed in Table 15.

TABLE 15: MATERIAL DESIGN CRITERIA

- System operating life
  - 62,000 hours
- Hot-end heat exchanger material operating stress limited to 90 % of stress producing 1 % creep in 85,000 hours
  - To account for cyclic pressure stress
- Compatibility with NaK at temperatures between 1100 K and 500 K
- Easily joined by welding or brazing

The above criteria primarily apply to the higher temperature components of the power module. The vast majority of the remaining components are relatively straight forward designs which employ high strength materials primarily for weight reduction. Two exceptions are the rare-earth magnets employed in the linear alternator and the beryllium alloy components making up the majority of the piston assembly and portions of the displacer.

To attain the desired performance from the linear alternator, it is necessary to employ rare-earth magnets to produce the flux levels required. To date only magnets from the samarium-cobalt family have proven to have the necessary magnetic characteristics. These magnets do, however, suffer from a gradual degradation if operated at temperatures much above 150°C (Figure 28). While this characteristic has been noted in a number of programs there is no clear description of the process occurring during this degradation. To counter this effect, it is necessary to cool the linear alternator space, since even with efficient alternators 6 percent to 7 percent of the power generated will end up as heat in this area. This does not consider the other processes, such as gas spring losses and thermal conduction from the hotter portions of the engine, which will further increase the temperature in this area.

The magnet support structure operates in a highly stressed environment from the viewpoint of mechanical loads and the potential of failure by fatigue. In most designs to overcome these problems, the actual structure is made up of a metallic frame supporting a nonmetallic structure which, in turn, supports the brittle magnets. The entire assembly is overwrapped with a high strength, nonmetallic fiber-reinforced composite to create a single assembly of minimum weight. One unique problem encountered with this type of fabrication is rejection of heat from the magnets themselves. This thermal load is generated internally within the magnet due to various secondary effects, eddy currents, etc., and if not removed, can cause excessive temperatures. Since the nonmetallic components are generally reasonably good insulators, the overwrap tends to trap the generated heat. To

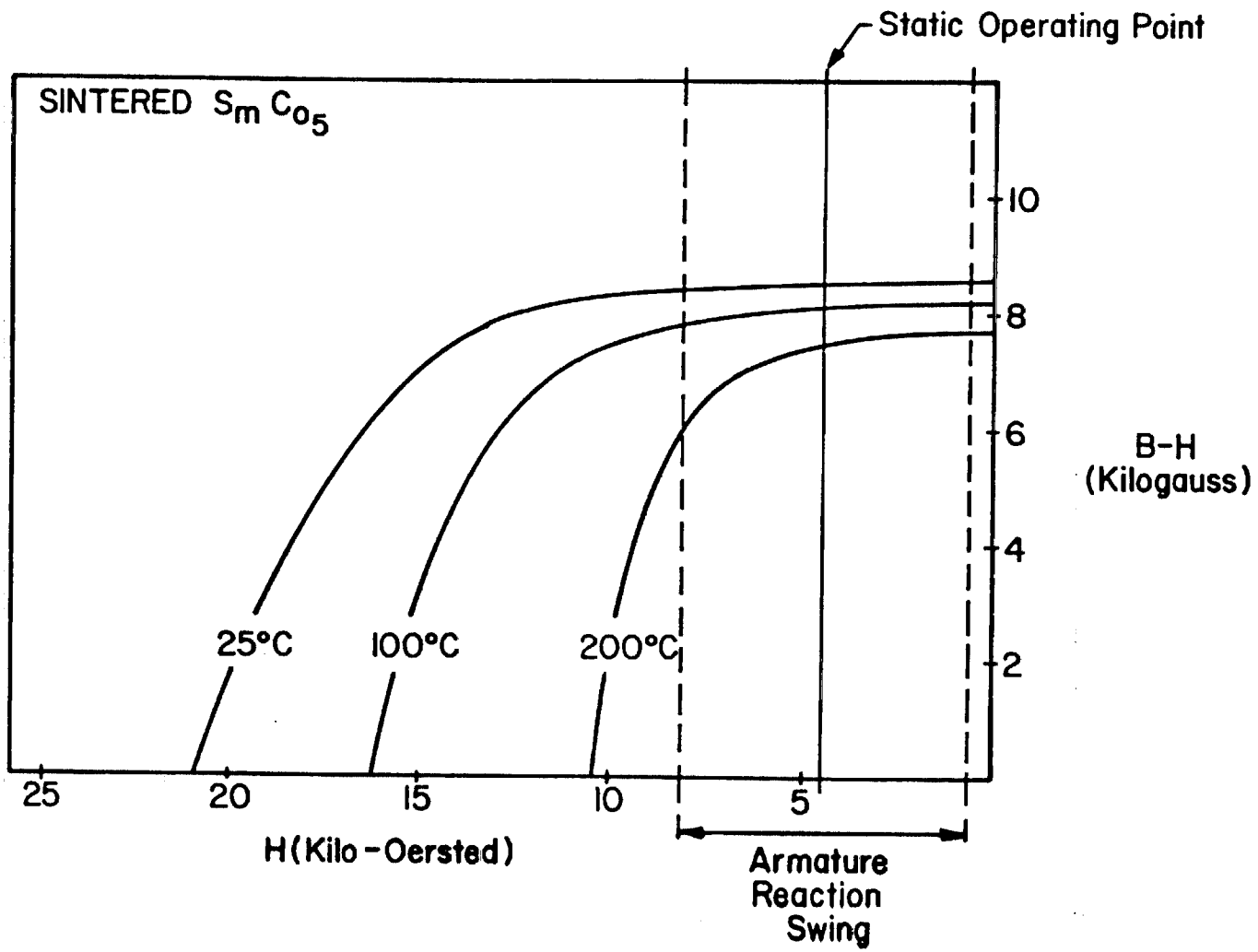

Figure 28: TEMPERATURE EFFECTS ON SAMARIUM-COBALT MAGNETS

overcome this problem, two approaches were considered: the first was to "can" the assembly in a metallic structure of low electrical resistivity (to reduce alternator losses) or, second, to use a reasonable conductive resin in the nonmetallic overwrap. The first approach has a number of fabrication issues involved with assembly of the metallic can around the magnet assembly but also has an additional advantage of keeping the potential contamination of the working gas from the composite magnet structure to a minimum. The composite assembly employing a conductive resin represents a more straightforward solution to the problem, but does leave the potential contamination problem. Since no clear decision could be made concerning the impact of the potential contaminants on the refractory components, it was decided that a composite assembly would be considered the prime design approach with a fall back based on the metallic can concept.

In the design of the current power module, the mass of the piston plays a significant role in determining the operating characteristics of the system. Since the amount of rare-earth magnets is essentially fixed once the operating stroke and frequency are selected, it is necessary to use materials of the lowest possible density to minimize overall piston mass. At the same time the construction material must have high resistance to fatigue cracking and high endurance strength. After an in-depth review, it was evident that only beryllium would meet the current engine requirements and, therefore, was used for the main piston body and its cylinder. The specific material employed is S-200E vacuum, not pressed, pure beryllium. Since it is probable that some contact between the piston and its cylinder will occur during start, the entire contact surface of both components is coated with chrome oxide and ground to final size. Due to the simple cylindrical shapes required and the stiffness of the beryllium, it is expected that the required clearances for the piston seal/bearing and the rear piston gas spring seal can be easily maintained during fabrication.

While not as critical in this design as the piston, the displacer mass also needs to be as low as possible while having to withstand temperatures well above those of the piston.

Beryllium is used for the main body of the gas spring and its associated seals, while Inconel is used for the remainder of the hot structure. The displacer shell represents the most critical component of the displacer from the point of thermal and fatigue considerations. With the 17 bar pressure amplitude within the engine, the shell would normally see a completely reversing load applied to it, since the internal space is maintained at essentially mean pressure via a small leak to the work space. To minimize this cyclic load, the shell can be internally pressurized to the highest point of the cyclic pressure through a one-way valve eliminating reversing pressure load.

Dynamic Balance Unit

From the viewpoint of existing hardware, the proposed active or adaptive dynamic balance unit employs the only conception in the current design that has not undergone actual testing. This concept uses variable stiffness gas springs to provide the necessary tuning of the balance unit to assure that the forces transmitted to the spacecraft are minimized.

The balance unit attached to the power module is highlighted in Figure 29. Since this unit represents an additional mass and is an extra moving component in comparison to the simple piston-displacer arrangement, a major attempt was made to integrate it into the overall power module. The goals are to use as much of the balance unit's structure as possible as a portion of the power module and minimize the possibility that the moving mass could be a life-limiting component.

The control scheme employed in the operation of the unit is shown in Figure 30. In operation the accelerometer mounted on the power module outputs a signal to the logic unit proportional to the net acceleration of the power module. If this value exceeds a specific set value, it would imply an excessive force is being transmitted to the spacecraft. Under these conditions the spring rates of the balance unit would be changed and, in turn, the natural

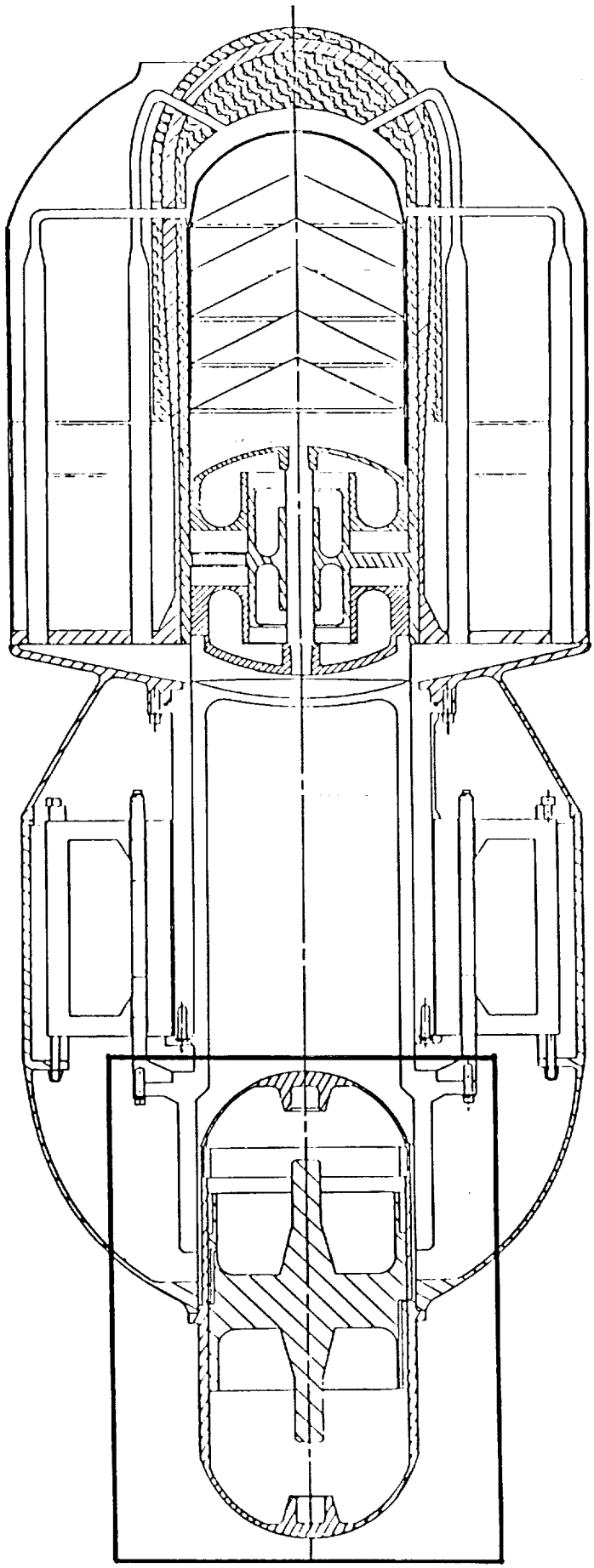

Figure 29: DYNAMIC BALANCE UNIT ATTACHED TO POWER MODULE

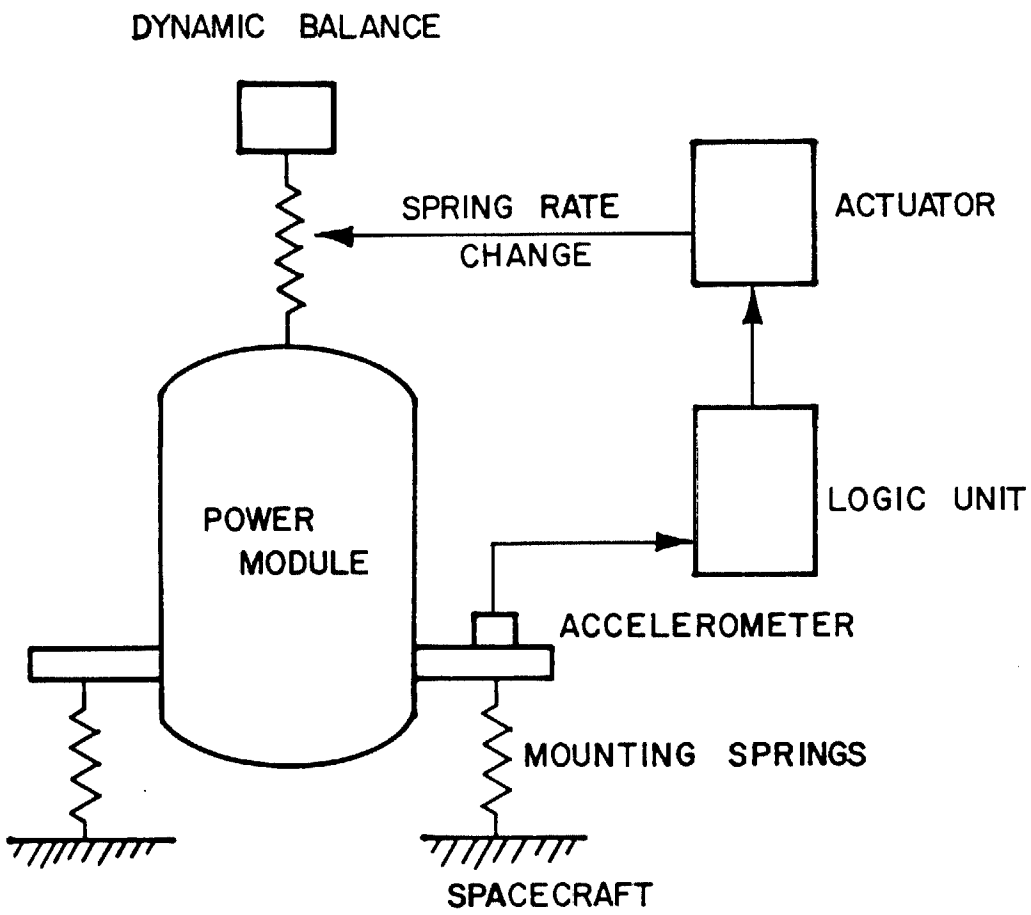

Figure 30: ACTIVE DYNAMIC BALANCE UNIT SCHEMATIC

frequency of the balance unit driven close to the operating frequency of the engine. Since it is expected that the necessary rate of change for the springs will be relatively low, either of the concepts proposed -- spring volume or pressure change -- will be more than adequate. Therefore, the decision on which concept to employ must be based on other criteria, such as reliability. In the case of the scheme using an incompressible fluid, some form of accumulator and valving system must be present. It is possible to use the engine pressure swing as a source of power for this system, but a hydraulic leak into the engine would cause the overall power module to fail. In comparison, the use of gas pressure changes as the controlling mechanism allows the use of the engine working gas itself instead of an auxiliary fluid. In this the springs would be pumped up by a valving system which would allow flow only into the gas spring cavities. In time the springs would be operating at the maximum pressure of the source of the gas, in this case the piston gas spring. Intermediate levels below the peak value would be controlled by a shut-off valve controlled by a separate valve into the bounce space of the engine. In both cases the valves would be placed on feed lines in such a way that if the valve were to fail to open, the pressure in the spring space would be that of the mean engine operating pressure and, as such, have very little pressure swing. This latter factor is one of the major advantages of this system in that it is not involved in the thermodynamic cycle. If it should totally fail, the net effect is an increase in the load transmitted to the spacecraft but the power module will continue to operate. The schemes with opposed pistons and displacers cannot operate at all if one of the four moving components fails, and may loose their net balance effect if the components begin to operate at off-design points.

Based on these considerations, a gas pressure variation scheme was employed to control the spring rate of the balance unit. The basic balance unit is shown in Figure 31 with its key components called out. The moving mass is a 6.5 kg piston enclosed in a pressure vessel which is located partially within the engine pressure vessel and also serves the purpose of a seal support for the piston gas spring. To maintain position of the balance

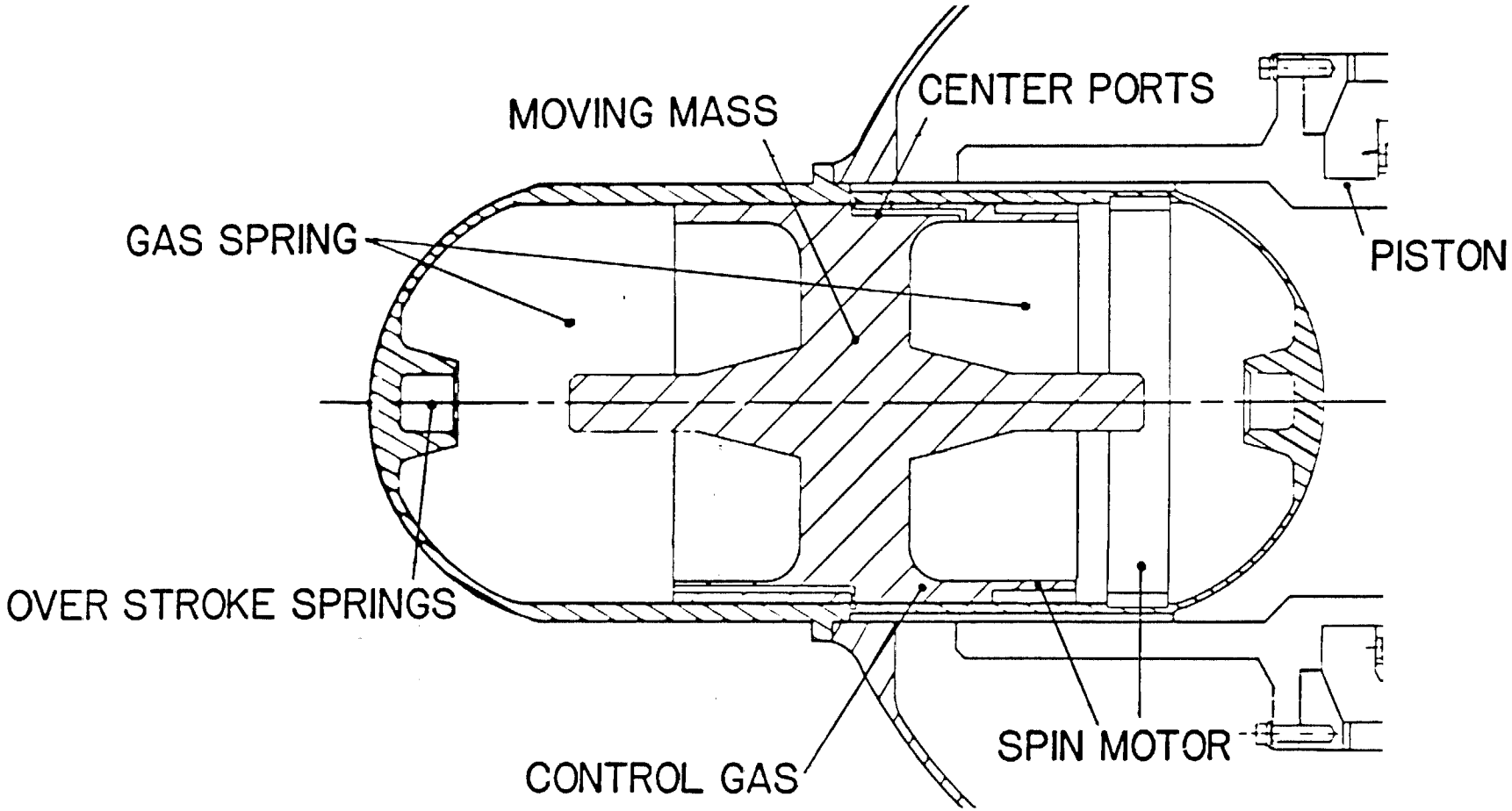

Figure 31: DYNAMIC BALANCE UNIT

mass, a simple center porting scheme is employed. Unlike the reciprocating components within the Stirling engine, there is no particular preferred drift direction unless the seal does not have symmetric leak characteristics. As a safety feature, overstroke is prevented by the addition of spring chambers, which are only active if the extension rod on the mass enters the cavity. Under these conditions, an extremely strong restoring spring force is generated.

To maintain a low balance unit mass, it is necessary to trade off piston mass and amplitude once a particular accelerometer accuracy is selected. For the current design, no major attempt was made to find the most accurate accelerometers available since a number of rugged stock units were available which had sensitivities in the range of 100 mV/g. This would allow adequate operation of the control system to maintain net forces well below the 100 newton goal. With the accelerometer characteristics known, a moving mass of 6.5 kg was selected, based on the desire to maintain a mass amplitude of 30 mm. While the seal requirements are relatively large due to the low pressure swing in the gas springs, the seal must also serve as a bearing for the balance mass. Due to the high operating frequency and stroke, only noncontact bearings can be employed. Based on the test rig results of the hydrodynamic spin bearing and their proposed use on the piston and displacer, it was decided to employ the same concept on the balance unit. In this case, since no gas forces are available to spin the mass, it is spun by a small induction motor mounted on the interior of the balance unit and on the balance mass itself. The estimated 25 watts to 40 watts of power is provided by the engine output.

The overall response of the balance unit is dependent on the amount of damping present. In the current power module, the two potential damper sources are the leaks past the seal and the hysteresis losses in the gas springs. In this particular design, the seal loss is negligible in comparison to those of the gas springs. To reduce the spring hysteresis losses to a minimum, a low $\Delta V/V$ design with a minimum surface area was employed with a resulting hysteresis loss of about 360 watts per spring. The impact of this damping is

shown in Figure 32b and can be compared to Figure 32a where no damping is present. It is also important to note that the gas spring hysteresis losses of the in-board spring must be added to the alternator, piston gas spring, and conduction heat loads which must be rejected by the alternator cooling system. This is a further inducement to minimize spring losses since, even in the current optimized design, the spring loss makes up about 20 percent of the cooling load. The overall operating characteristics of the balance assembly are shown in Table 16.

TABLE 16: BALANCE UNIT OPERATING CHARACTERISTICS

• Moving component mass	6.5 kg
• Amplitude	30 mm
• Transmitted force	80 N
• Tuning range (active)	88 Hz to 100 Hz
• Accelerometer	
• Does not affect cycle thermodynamics	
• Spinning mass concept based on existing technology	

Power Piston

The power piston represents the more massive of the two moving components. It is also the more complex from a structural viewpoint due to its support and driving of the magnet plunger assembly of the linear alternator. The overall power piston assembly was shown previously (Figure 22) in the alternator assembly and is briefly described below.

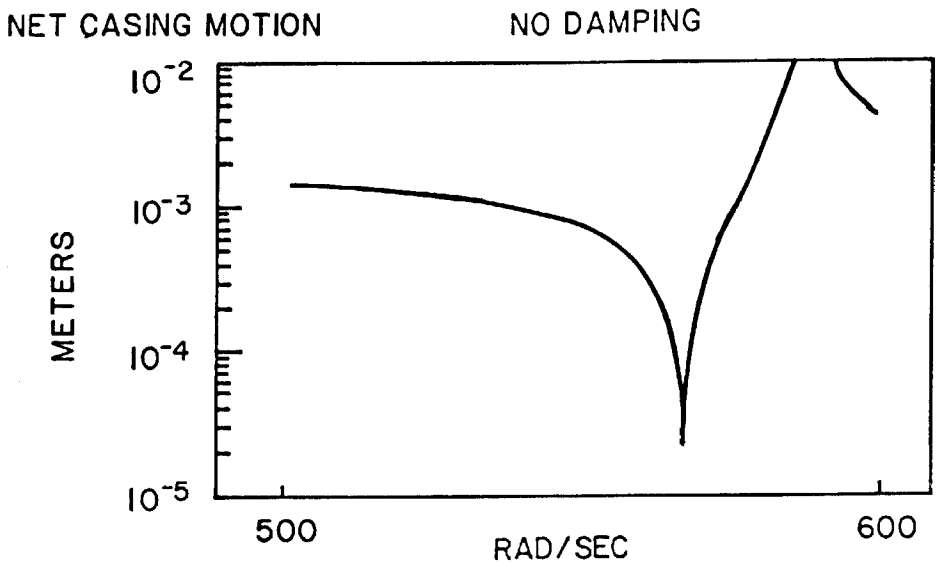

Figure a

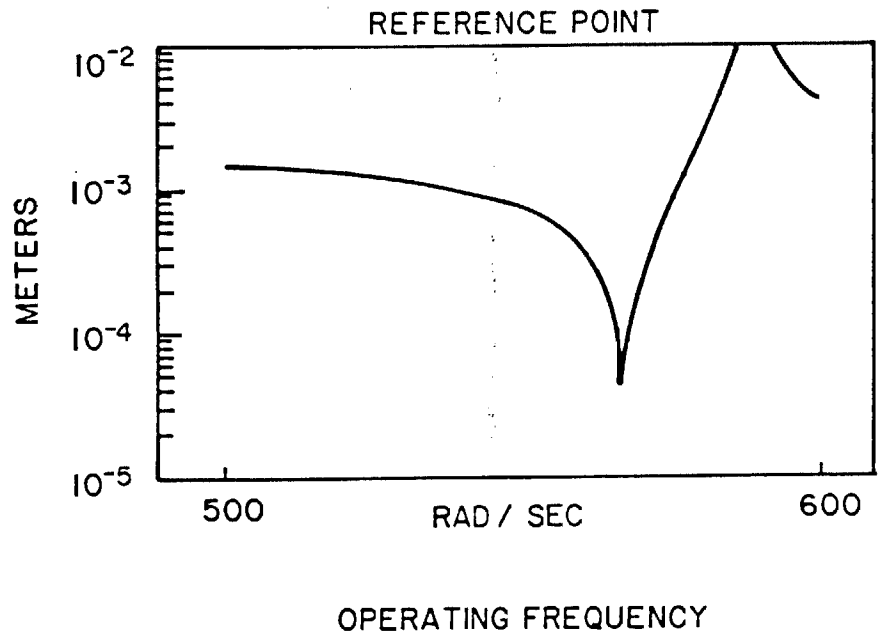

Figure b

Figure 32 a and b: BALANCE UNIT RESPONSE TO DAMPING

The major structural component is essentially an open-ended cylinder, fabricated from beryllium, which makes up the piston body with the necessary support structure to attach the magnet assembly. Sealing for the piston gas spring and the connection between the compression space and bounce space are provided by clearance seals which are hard-coated, precision-ground surfaces on the main piston body. A conventional center porting scheme is employed to maintain the piston at its center position while the engine is operating. An estimate was made of the losses occurring with the centering and seal system for various piston wall gaps. It was determined that the wall gap could range between 15 μm and 20 μm without excessive losses. These results were integrated into the design techniques for the spin bearing and a final gap dimension selected. Concurrently with this effort, the seal requirements of the piston gap spring assembly were reviewed. The desired seal gaps for the gas spring were essentially the same or somewhat larger than those used on the piston seal.

Attachment of the magnet assembly is via a titanium support ring which is bolted to the basic piston body. The magnet assembly is composed of a nonmetallic framework to properly space and support the magnets. Titanium support plates are employed on either end of the assembly as the tie-down points for a number of metallic reinforcements used to compress the magnet assembly prior to overwrap with a fiber-reinforced composite. Due to the potential for heat generation within the magnets themselves, a thermally conductive resin is used in this fabrication stage.

The engine power piston assembly, its cylinder, and the alternator are assembled as a single unit prior to installation in the pressure vessel and close-out via welding of the pressure vessel at the interface between the cylindrical sections of the rear shell.

Power Piston External Gas Spring

In an attempt to reduce the specific mass of the power module during the Task 1 Parametrics Study, it became evident that a reasonably large portion of the piston spring requirement would have to be provided by an external spring. This was due to the strong effect of the magnet assembly mean diameter and the piston diameter on overall weight of the power module. For the smaller values of this ratio used in the current design, the spring requirement was approximately 2.3 X 10^6 N/m which could not be provided by simply using the existing volume in the bounce space. After considering a number of possible variants, it was decided that the space within the power piston body represented a convenient volume for the required gas spring. However, this decision also required the use of an additional seal to separate this space from the remaining piston bounce space. In the present design, the seal is provided by a clearance seal employing the piston body and the in-board end of the balance unit. The general size of the balance unit provided more than adequate length for a reasonably sized gap but did introduce the complication of maintaining alignment between the piston and rear pressure vessel (and the balance unit seal surface) during assembly and final close out. The proposed assembly technique would address this problem by completely assembling the power module without the balance unit being installed. The balance unit would then be temporarily installed and an electrical continuity test performed to assure that no contact is present between the piston body and the balance unit. It may also be possible to spin the piston via an auxiliary gas supply attachment in the engine bounce space, which would be directed at a set of turbines located on the piston body in the area of the magnet assembly attachment point. Once noncontact is assured, the balance unit would be electron-beam welded to the rear pressure vessel flange, possibly with the noncontact checkout procedure continuing during the welding operation. While somewhat complicated, it is believed that this basic scheme will provide adequate alignment for the overall system.

A fall-back approach, based on the use of a metallic bellows assembly that is shown in Figure 33, was considered since it would not depend on a critical alignment between the various components. However, questions concerning the bellows' life at the high operating frequencies and amplitudes were not answered during this program and this concept was dropped. It is recommended that this concept receive further review in any follow-on efforts concerning this power module design.

This actual gas spring design was directed at a low $\Delta V/V$ arrangement to minimize hysteresis losses with the existing piston body size retained, if at all possible. Some compromise was required in this area since the balance unit design was much more sensitive to the combination of hysteresis losses and balance spring diameter than to the piston gas spring. This required a small step in the diameter of the piston gas spring seal, otherwise the gas spring volume is essentially a cylinder with an L/D of about two. The calculated hysteresis losses are 180 watts at the design point temperature and must be removed by the cooling system for the alternator space.

Impact of Heater Temperature Profiles

The initial Space Power Module designs developed in Task 1 employed relatively low temperature drops across the liquid-metal heat transfer fluids during their passage through the engine heater and cooler. This was primarily driven by the desire to minimize electromagnetic pump power requirements and maintain reasonable spacing between the individual heat exchanger modules so that the solidified liquid metal would thaw during initial heating. Under these conditions, heat pipes showed little or no advantages over pumped-metal loops, sodium seemed to be the preferred heater working fluid, and mercury for the cooler working fluid.

At the completion of Task 1, a number of changes occurred in the design requirements for application to Task 2, the detailed 25 kW design portion of the program. The majority of these affected the Stirling engine portion of the design from the viewpoint of

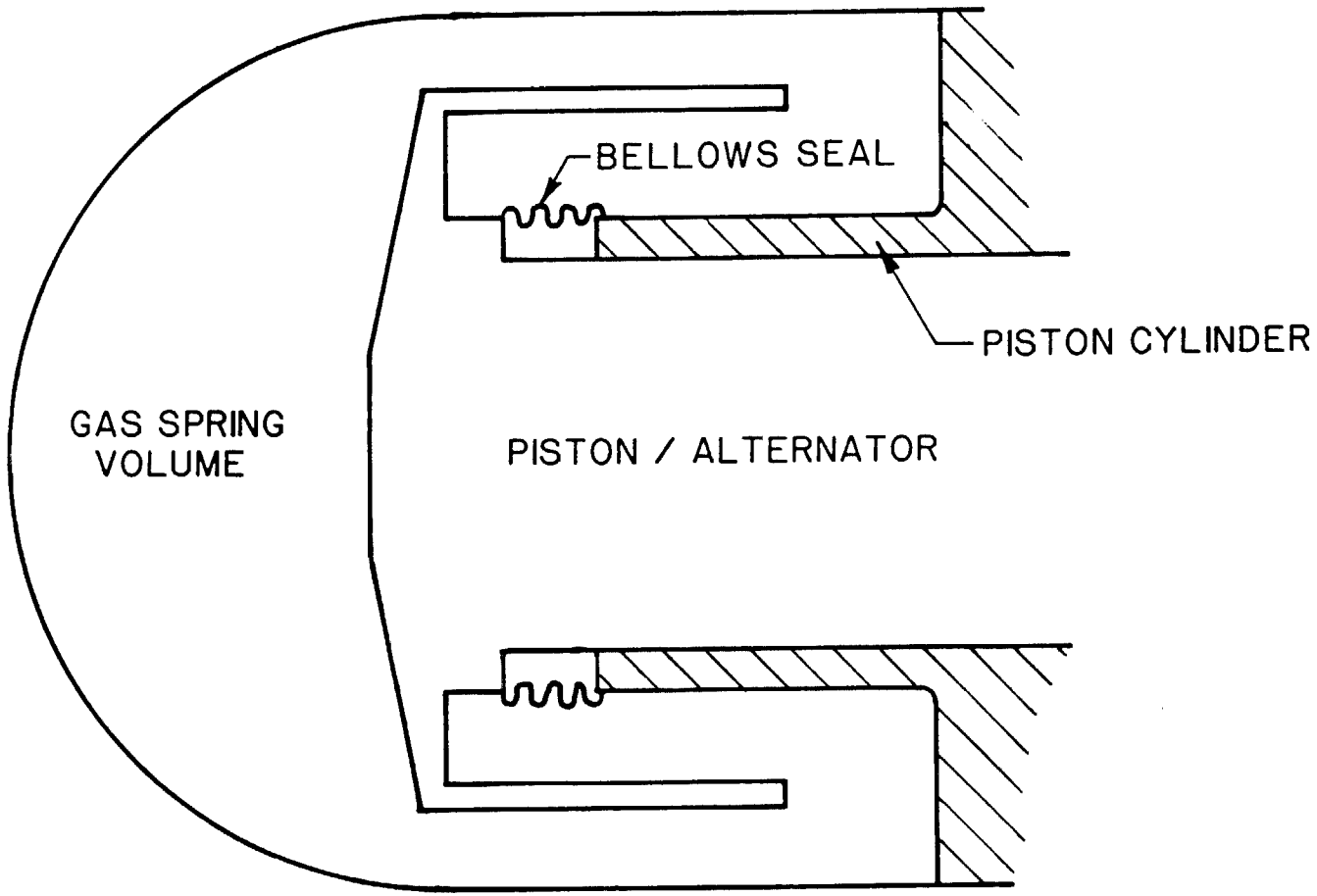

Figure 33: BELLOWS SEAL FOR POWER PISTON GAS SPRING (ALTERNATIVE APPROACH)

performance improvement. The primary exterior changes were the requirement for higher operating temperatures and, more importantly, the use of relatively low liquid-metal flow rates (and in turn high temperature drops) through the engine's external heat exchangers. This latter factor has a number of effects on the overall system (some positive, some negative) that are reviewed below. It is important to note that these effects have been investigated primarily from the viewpoint of a pumped liquid-metal loop. The application of heat pipes would have an impact on some of these factors since, in theory, this could significantly reduce the temperature gradients currently encountered.

Impact on Exterior Pumping Losses

The basic heat exchanger arrangement employed in the current design is a cross flow shell-and-tube type, employing baffles to direct the liquid metal over the tubes. For reasonable designs, entrance, exit, and edge effects are relatively minor in comparison to fluid friction and flow reversal effects on heat exchanger pressure drop. In the case of a specific design, the liquid metal to wall ΔT in the exterior heat exchanger area is played off against heat transfer coefficients which are highly dependent on flow velocity and, in turn, determine liquid-metal pressure drop. This velocity is determined primarily by spacing of the tubes and the number of baffles employed. The spacing of the tubes has a lower limit on the order of 3 mm to 7 mm to reduce the problems during start up, if the liquid metal is frozen.

Temperature Profile Impact on Stirling Engine Performance

Since the current design point has a temperature drop of approximately 80°C to 100°C in the liquid-metal loop, the question of which direction the temperature profile should have became important. Intuitively, the use of a profile with the hottest liquid-metal temperature toward the regenerator on the heater and the coldest temperature toward the regenerator on

the cooler will produce the higher thermodynamic performance. However, this arrangement also produces the highest temperature gradients across the regenerator assembly which increases conduction losses through the regenerator can and also requires a thicker wall on the hotter end of the can.

A series of simulations were run with the profiles mentioned above. All previous simulations employed a constant average wall temperature. From this relatively brief review, it is evident that the impact of the temperature profile on Stirling engine performance is quite sensitive to the specific design being investigated. On the current Task 2 engine, the existing temperature profile somewhat increases the engine thermodynamic performance; however, further decrease in mass flow will drive the temperature profile into the regime where performance will actually fall in comparison to a flatter temperature profile. This review does not consider the impact of the temperature profile on specific mass of the engine.

Temperature Profile Impact on Engine Mass

The impact of temperature profiles on engine mass only occurs in the heater portion of the heat exchanger assembly and the hot-end pressure vessel. The reason for this is the extreme sensitivity of the long-term usable strength of the candidate materials at the temperatures required. Figure 27 shows the 100,000 hour stress rupture life for the materials used extensively in the current engine as a function of temperature. To determine the impact of temperature profiles on the mass of the high temperature components, it was assumed that the sensitivity of the materials could be defined as the slope of the useful strength vs. temperature curve for the niobium-based materials and the Inconel. (Inconel could only be used in an insulated design.) From this approach it was determined that the heater assembly and hot portions of the heater head had a mass about 7 percent greater than that required if the wall were at a constant mean temperature. This mass penalty increases dramatically as the temperature profile is increased, due to the rapid nonlinear drop in usable strength for the niobium alloys.

Use of Lithium as a Heater Working Fluid

If the potential of material incompatibility is ignored, the use of lithium as a heater fluid makes considerable sense at the current design point. Not only is it a better heat transfer fluid than the NaK, but it also has the advantage of a higher boiling point, i.e., 1592 K vs. about 1100 K (standard conditions), which eliminates the possible onset of boiling due to some failure in the heat transport system. With the same mass flow as the current design the temperature gradient is reduced by a factor of about 4.4. However, the pumping power requirements will increase by nearly a factor of 2 at the same pressure drop and mass flow rate employed in the current design. Modification to the present heater tube spacing to take advantage of the better heat transfer characteristics available with lithium could counteract the majority of these increased pumping losses. The net effect should be a reduction of the temperature profile by a factor of 3 to 3.5 with little or no mass increase in the heat exchangers.

Task 3 Demonstration of a Displacer Hydrodynamic Gas Bearing

Background

The art of gas-lubricated bearing design is well advanced, with abundant literature available to guide the designer. For the purpose of application to long life free-piston Stirling engines, it is reasonable to consider conventional gas bearings in which the lubricating film is induced by spin, as is conventional practice in other machines. The problem is then confined to the design of the spinning mechanism, which may be done in many ways, including a conventional electric motor or a turbine designed to intercept the gas flow through the engine in such a way to induce a torque on the spinning elements. The requirement of the spin mechanism is that it be effective in driving the spinning element, and that it minimally affect the operation of the engine.

Bearing design analysis shows that the required driving power of a rotating gas bearing with conventional gaps and other dimensions characteristic of a space power module producing 25 kW power is very low, on the order of 10 W. The starting torque can also be very low since the side loads are small in zero gravity, and even in earth gravity.

However, it was recognized that the problem likely to be encountered was the maintenance of the required close bearing gaps (on the order of 10 to 20 micrometers) in the presence of thermal and stress-induced distortions.

Purpose of Investigation

This program was undertaken with the intent of investigating the feasibility of a turbine-spun gas bearing in a conventional free-piston Stirling engine (FPSE). The goal was limited to spinning the displacer, with the intent of extending it to spinning the piston in the event of success with the displacer. Table 17 outlines the experimental objectives.

TABLE 17: OBJECTIVES OF GAS BEARING EXPERIMENTS

- Demonstrate spinning of displacer by gas flow through cooler port
- Noncontact operation of displacer
- Minimal power loss due to bearing
- Operation at conditions scalable to SP-100 FPSE power module

Concept of Turbine Spin Technique

It happens that the maximum gas flow rate through the cooler port of a FPSE occurs at approximately the same time in the cycle that the displacer is fully out or away from the expansion space (schematic shown previously in Figure 23). This allows the use of a small turbine mounted on the outer end of the displacer to intercept the gas flow through the cooler port so as to induce a torque on the displacer and cause it to spin around its axis (Figures 34 and 35). The turbine must impart a torque sufficient to start the spin and maintain it at the speed necessary to induce the lubricating gas film. (See Figures 36 and 37.)

Description of the Test Rig

The test device was a modified Sunpower 1 kW FPSE, as shown in Figure 38. The turbine elements were mounted on the displacer (Figures 39 and 40). The test rig was then motored by its alternator so as to cause the gas flows required for the turbine. Two pairs of eddy current type proximity sensors – one pair at the top and one pair at the bottom of the bearing – were installed 90 degrees apart on the displacer rod to monitor the gap

Displacer passes cooler port near maximum port mass flow condition.

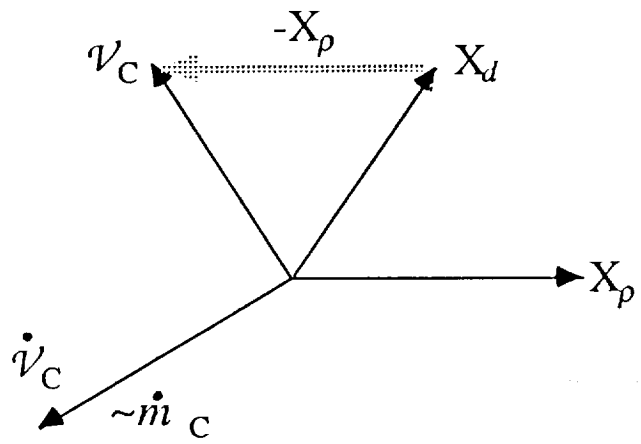

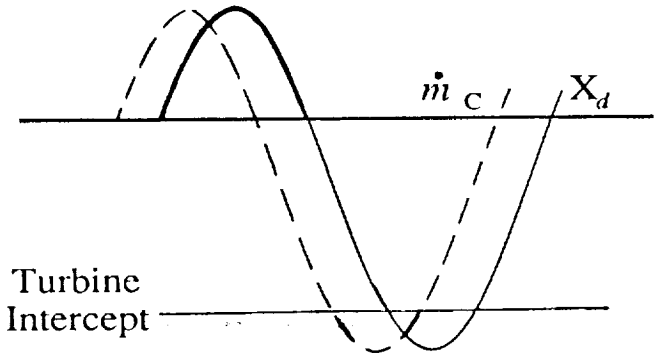

Interception of cooler port flow by turbine blades on displacer imparts angular momentum to displacer.

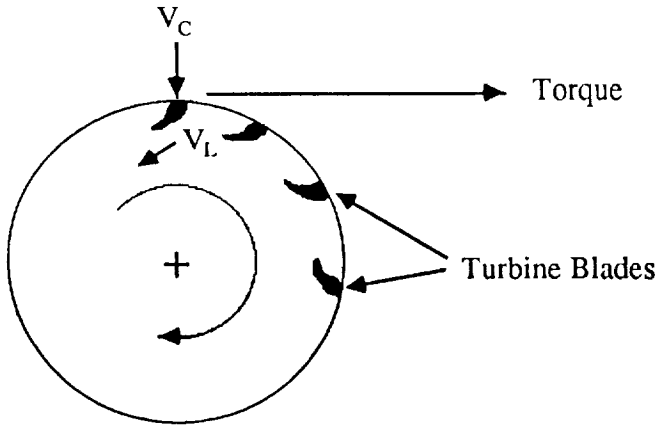

Rotating displacer induces dynamic film lubrication on displacer rod bearing, preventing contact.

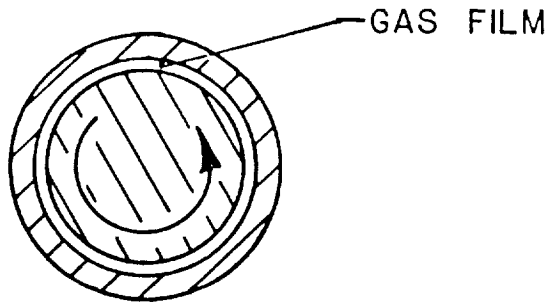

Terms

V – Velocity
$\mathcal{V}$ – Volume
$\dot{\mathcal{V}}$ – Volume time rate of change
$\dot{m}$ – Gas mass flow
X – Position

Subscripts

C – Compression space
L – Condition leaving turbine
ρ – piston
d – displacer

Figure 34: SPIN-BEARING CONCEPT

At displacer maximum out point (See Figure 34.), the time rate of change of the volume of the compression space is about maximum positive; thus, maximum flow into the compression space coincides with turbine alignment with the cooler port.

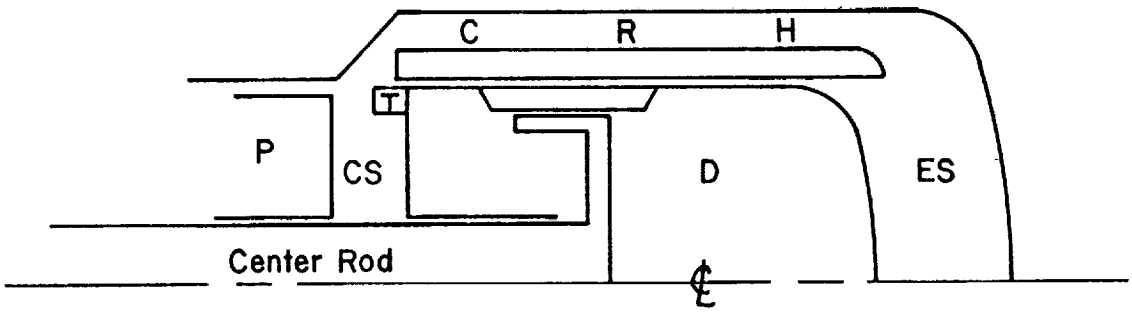

C – Cooler
R – Regenerator
H – Heater
T – Turbine
P – Piston
CS – Compression Space
D – Displacer
ES – Expansion Space

Figure 35: COOLER PORT FLOW RELATIONS

Impulse Turbine Characteristics

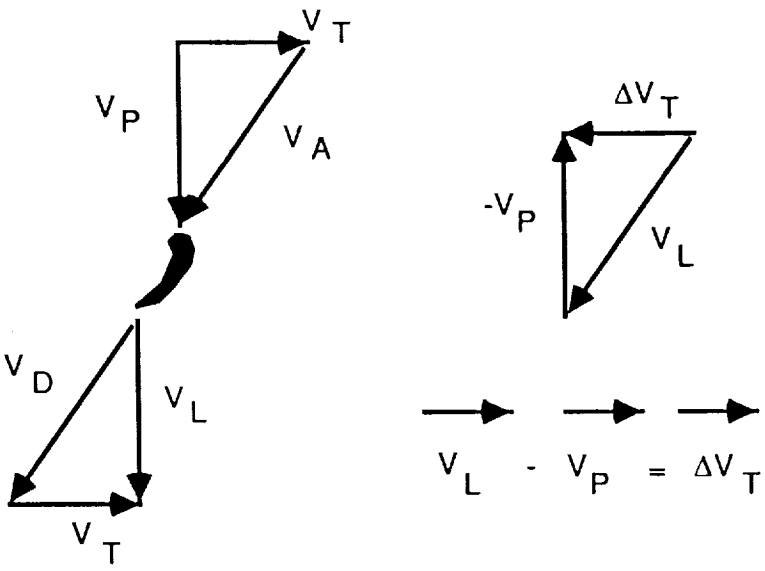

•Turbine Torque = $\dot{m}_\rho \Delta V_T \cdot D_T/2$ • Turbine Impulse = Torque * Time of Torque Application

•For Equilibrium, Turbine Impulse = -Bearing Drag Torque Impulse

Bearing Drag Relations

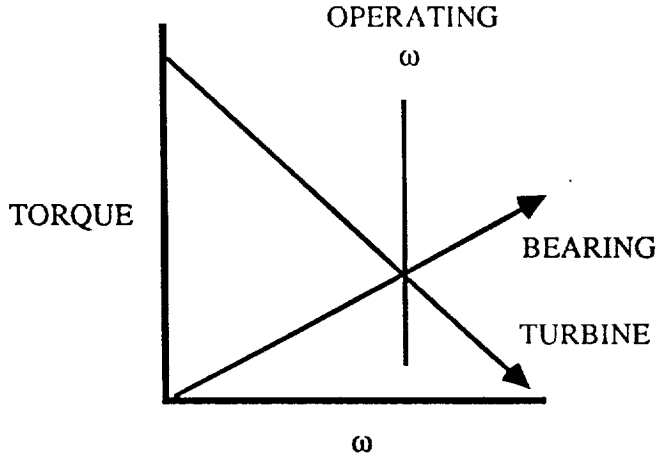

$$\text{Drag Force} = \frac{\pi\mu D^2 L\omega}{2C}$$

$$\text{Torque} = \text{Force}*\text{Radius} = \frac{\pi\mu D^3 L\omega}{4C}$$

$$\text{Power} = \text{Torque} * \omega = \frac{\pi\mu D^3 L\omega^2}{4C}$$

Terms

C	–	clearance between stator and bearing
D	–	diameter of bearing
L	–	length of bearing
V	–	velocity
m	–	gas mass flow
ω	–	angular velocity
μ	–	gas viscosity

Subscripts

A	–	approach to turbine
D	–	discharge
L	–	condition leaving turbine
P	–	cooler port
T	–	turbine
ρ	–	piston

Figure 36: OPERATING CHARACTERISTICS OF TURBINE AND BEARING

Λ – Bearing Number – $\dfrac{6\mu\omega}{P}\left(\dfrac{D}{2C}\right)^2$

Dimensionless Loading – $\dfrac{F}{PLD}$

ε – Eccentricity Ratio – Rotor Eccentricity/Clearance (≤ 1)

Stability Group – $\dfrac{F}{MC}$

Dimensionless Group Relations for Low Λ and Low ε

$$\frac{F}{PLD} = \beta\Lambda \qquad \beta = f(\varepsilon)$$

Stability Criterion for Plain Bearings

$$\omega_i = \xi\Lambda\left(\frac{F}{MC}\right)^{1/2} \qquad \xi = f(\varepsilon)$$

(Complete concentric bearings with ε equal to zero are unstable.)

Terms

- ω – angular velocity, rad/s
- ωi – angular velocity at which whirl instability occurs, rad/s
- μ – gas viscosity, N-s/m^2
- C – clearance between stator and rotor of bearing, m
- D – diameter of bearing, m
- F – force on bearing, N
- L – length of bearing, m
- M – mass of rotating component of bearing, kg
- P – pressure of bearing surroundings, N/m^2

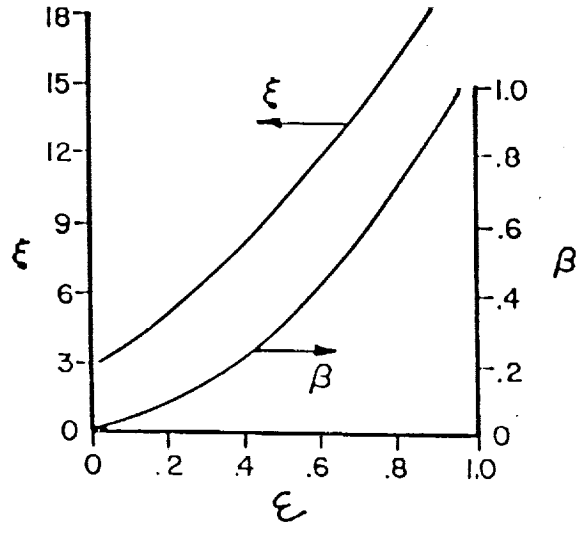

Figure 37: DIMENSIONLESS GROUPS FOR BEARING DESIGN

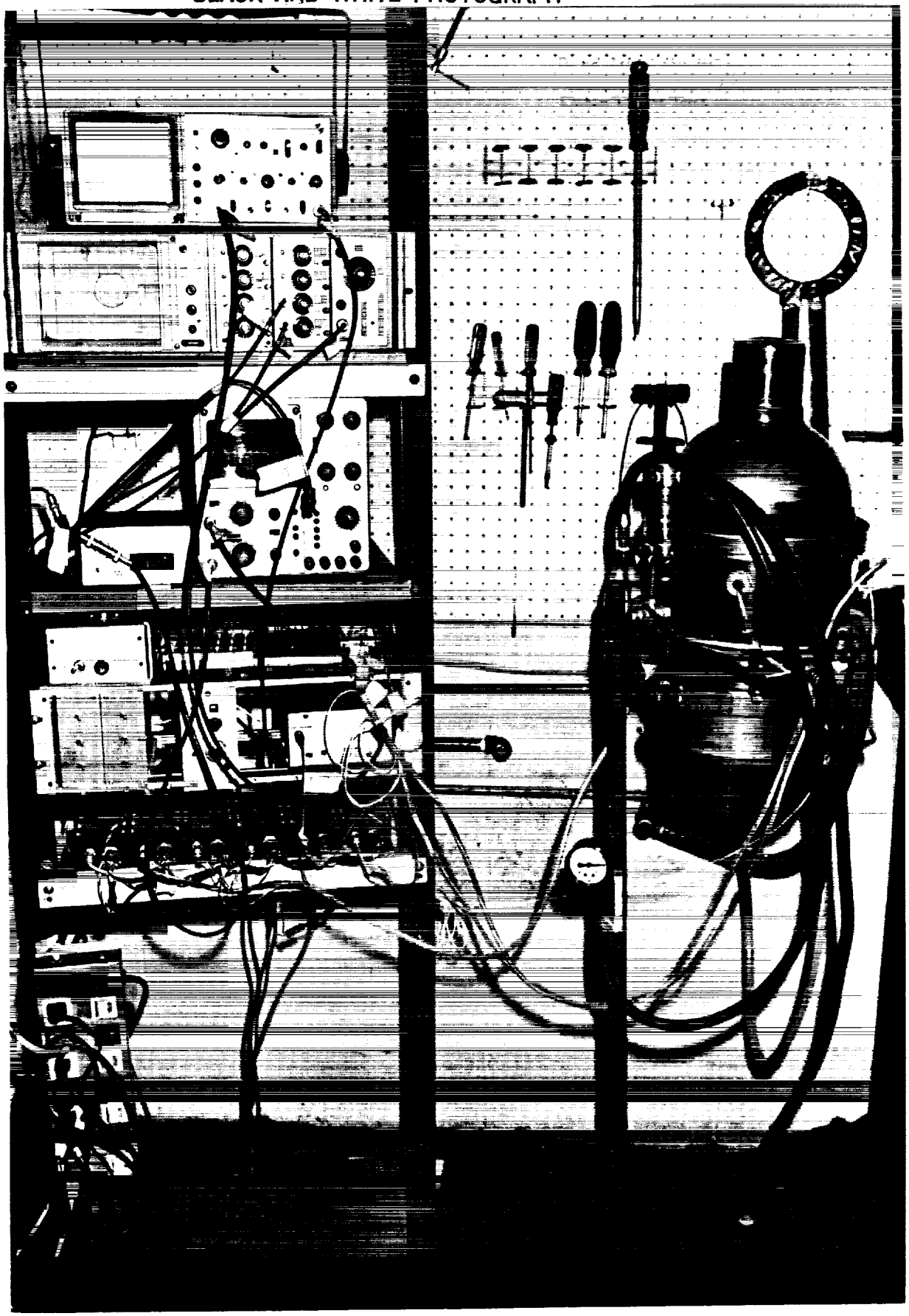

Figure 38: SUNPOWER 1 KW FPSE AND TEST EQUIPMENT FOR GAS BEARING TESTS

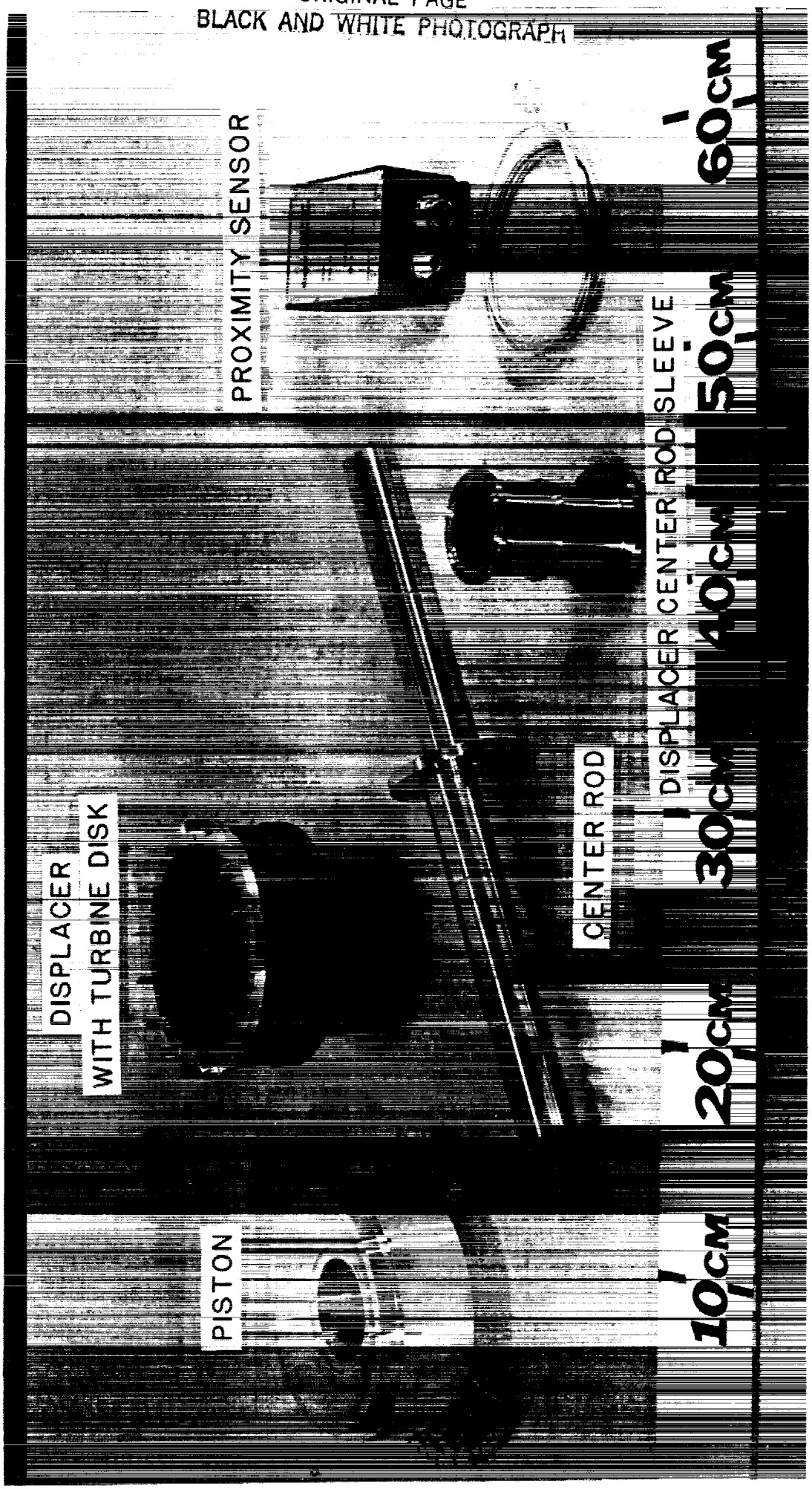

Figure 39: SPIN BEARING TEST COMPONENTS

Figure 40: DISPLACER AND TURBINE ELEMENTS

dimensions on the central bearing (Figure 41). The output of the instruments was displayed on an oscilloscope as the position of the central axis of the bearing within a circle representing the clearance between the bearing and its journal, typically about 20 microns. A number of turbine and stator elements were fabricated and tested with the intent of investigating their effect in inducing spin and noncontact operation, and their effect on the engine cycle.

Results of Experiments

With the first attempts at operation, it became apparent that the real problem of the program was going to be, not the spinning technique, but in the accuracy of alignment of the concentric components of the displacer and their dimensional stability. It was found that even with great care and persistence, the bearing components of this rig would not remain aligned, round, and concentric within the needed tolerances. The rig would occasionally operate as desired, with stable spinning and noncontact, but this operation would only be for a short time before some distortion or other mechanical difficulty interfered.

Some of the problems encountered were a result of fabrication stress relaxation in the steel central rod, distortion in that rod caused by mounting bolts at its inner end, thermal distortion in the aluminum displacer gas spring components as the test rig was motored and temperature gradients were set up, and stress deflections of the cantilevered central rod.

Another major problem was the establishment and maintenance of the necessary concentricity of the displacer drive elements.

The chief positive result of the test program was the demonstration for short periods of stable noncontact operation of the displacer spin bearing using turbine elements which intercepted cooler port gas flow having a tangential component from a stator blade ring

Figure 41: INSTRUMENTATION INSTALLED ON DISPLACER ROD

mounted in the cooler port. This was a partial stator, covering only a fraction of the cooler port (Figure 42). The spin frequency was about 10 hertz.

It was concluded that if the displacer was, in fact, free to rotate without interference from imperfections of the structure, then it would do so with very little torque from the turbine, and the turbine-stator combination seemed to have very little effect on the normal operation of the engine. Under successful operating conditions, no differences in displacer amplitude were measured compared to the base case with no turbine, stator, or spinning.

Unfortunately, the persistent problems caused by dimensional instabilities of the test rig prevented the accumulation of any quantitative data, since the periods of time in which the spin bearing actually operated properly were very brief. Subjective impressions were that the system would spin at the slightest provocation when the mechanism was sufficiently free to allow it. In fact, even without a turbine, the displacer would tend to rotate slowly in an erratic way when the engine was driven.

During the times that the displacer was spun successfully, there was no indication of whirl instability or other problems, and the bearing operated without evidence of contact.

In summary, the work done emphasized the need for high quality materials, design, and construction, but most of all, the choice of a simple, robust configuration which would be capable of fabrication and inherently resistant to distortion. The engine used as a test bed, the Sunpower SPIKE 1 kW FPSE, did not have these characteristics. The displacer elements were made of aluminum, and had three concentric close fits, the central rod, the displacer gas spring puck, and the displacer outer diameter seal. In order for the test rig to work properly, all three of these had to have gaps of the same order, about 20 to 30 microns; the fabrication accuracy required for the three concentric elements was beyond the capability of the model shop available. Further, the dimensions were not stable, and changed with stress and particularly with thermal cycling.

Full Port Stator

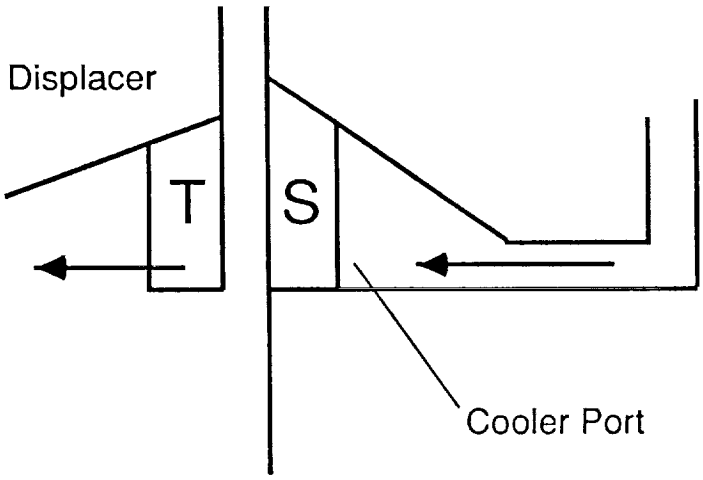

T – Turbine S – Stator

Gas must flow through stator going both in and out of compression space.

Results – Rapid spin, loss of displacer amplitude caused by flow obstruction of stator.

Partial Port Stator

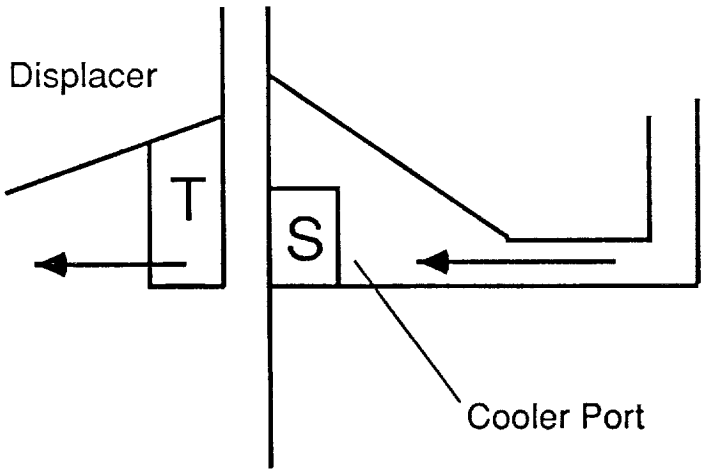

T – Turbine S – Stator

Flow through stator only during half cycle of flow into compression space.

Unobstructed flow out of compression space.

Results – Rapid spin, lower flow losses.

Preferred geometry

Figure 42: STATOR-TURBINE CONFIGURATION

It was concluded that in order for a spin bearing to work on a Stirling engine with the required close fits, the whole system must be designed with close attention to the requirements of dimensional stability. This requirement would suggest that the materials and configurations be chosen to avoid concentric close fits, cantilevered supports, thin walls, low stiffness, high thermal expansion, and any other characteristic inimical to such stability.

The spinning device itself does not seem to be difficult to implement, nor does its power requirement or other demands seem to have significant effect on the successful operation of the basic engine cycle.

Other Spin-Bearing Work at Sunpower

This displacer gas bearing work was followed by two other gas bearing efforts at Sunpower. These were a DOE-funded experimental effort to demonstrate spin on both the displacer and power piston of a test device equipped with a linear alternator (reference 5) and later implementations of spin operation with use of cooling machines intended for commercial production.

The DOE program to spin both the displacer and power piston also encountered difficulties in achieving and maintaining the close alignments and low distortion needed. A further problem was that of nonuniformity in the magnetic field of the alternator.

The previously encountered problems were overcome in a later program at Sunpower which used a turbine-spun displacer and motor-spun piston in a cooling machine. Additional elements contributing to this success were the use of long gas spring seals of simple design involving no concentric close fits, and the placement of critical fits outside of areas having large thermal gradients. The cooling machine demonstrated noncontact

operation over periods of hundreds of hours with no measurable degradation of thermodynamic performance attributable to the spin energy input, which was very small in relation to the gas power of the machine.

However, it must be pointed out that the successful operation of spin-induced noncontact operation on both displacer and piston of the cooling machine was achieved under circumstances of temperature, frequency, side loads, gap dimensions, and other relevant conditions much less demanding than would be faced in a space power plant. In particular, vertical orientation, low pressure, and low frequency of the cooling machine and its robust construction, low thermal gradients, and well supported bearings with large gaps made the spin task much easier than it would be in a highly stressed space power engine.

Lessons From Work Done

The essential lessons of the work done to date at Sunpower on spinning gas bearings can be summarized as follows:

1) The prerequisites for achievement of spinning noncontact operation of close fit seals are **correct choice of design, materials, and fabrication methods** so that the essential close fits are maintained under all operating conditions of temperature and loading. Such design should have no concentric or cantilevered close fits, high L/D ratios and as large gaps as permitted by the cycle losses, low thermal gradients, materials of high stiffness, stability and low thermal coefficients of expansion, and no deforming stresses on the close fit components. Labyrinth seals may be used in combination with larger gaps to keep leakage losses within bounds.

2) The required rate of spin to effect noncontact operation of the seals is quite low (on the order of 10 Hz); and, as long as the proper gaps are maintained by proper design and choice of materials, this **required spin rate is easily achieved by**

very low power turbines or other devices such as electric motors. The power required to maintain spin is negligible in proportion to the gas power of the cycle and does not significantly detract from the performance of the machine.

3) In the absence of gravity forces (vertical spin axis), **startup is readily achieved**, with a rate of increase of angular momentum consistent with an assumption of very low drag. This observation supports the hypothesis that axial oscillation alone tends to develop at least a partial fluid film which greatly reduces contact friction.

4) The magnetic circuit and the magnets themselves must be homogeneous in structure and magnetic properties around the perimeter of the magnet, otherwise there may be excessive toggling forces which both impede spin and induce electromagnetic losses. Further, the magnet must not change as a result of decay or other effects in operation in a nonuniform way which could induce drag on the spinning elements.

5) Proposed displacer drive configurations for space power, with a multiplicity of close fits, often concentric and cantilevered, and with low aspect ratios, appear to require extremes in material characteristics, accuracy of machining, assembly, and quality control. The lessons learned to date, cited above, suggest that these designs are suspect, and that effort should be expended in devising new displacer and piston configurations which make the bearing task easier and more likely to remain capable of noncontact operation over long periods. As mentioned already, the characteristics to be sought are geometrical simplicity, stiffness, and stability.

6) In the concentration on spinning as a means of achieving noncontact operation, it should not be forgotten that there are promising and as yet unexplored nonspinning means of providing gas lubrication. Also, there are promising contact sliding pairs, the properties of which should be investigated for use in long life in free-piston Stirling engines.

Task 4 Dynamic Balance Demonstration

The dynamic balance system concept demonstrated in Task 4 was employed on the engine designs of the Task 1 Parametric Study as a means to reduce forces transmitted to the spacecraft structure. Depending on the specific force limitations imposed, the mass of the absorber can vary from a relatively insignificant amount in comparison to the overall mass of the engine to values on the order of 15 percent, if extremely small forces are required.

During Task 1 no specific values were imposed on the transmitted force, rather the goal was to reduce casing motions to small fractions of those occurring in an engine without an absorber unit. The basic trend in dynamic balance system specific mass is shown schematically in Figure 43 for a passive balance system. Also shown in this figure is the power variation of a representative engine module with changes in frequency. Two critical points are evident in this figure. One, the engine types developed in Task 1 are extremely fine-tuned systems, which are very sensitive to operation at off-design points; for example, frequency variation of less than 5 percent result in power variations of 20 percent or more. Two, the specific mass of the dynamic balance unit increases rapidly as the required casing motions are decreased and as the necessary operating band width is increased. In the case of the Task 1 engine design, a 5 percent frequency variation required an absorber mass in the range of 6 percent to 14 percent of the power module mass for vibration amplitudes of 0.15 and 0.075 mm, respectively.

Under Task 4 of the contract, a passive dynamic absorber was demonstrated on the RE-1000 free-piston Stirling engine at NASA Lewis. The dynamic absorber for this demonstration used mechanical springs for tuning. The absorber is shown in Figures 44a and 44b. The mass of the absorber was 26.5 kg; two additional rings, each with a mass of about 1 kg, could be added to vary the natural frequency of the balance system. The natural frequency of the absorber with one additional mass ring was 30 hertz. This could

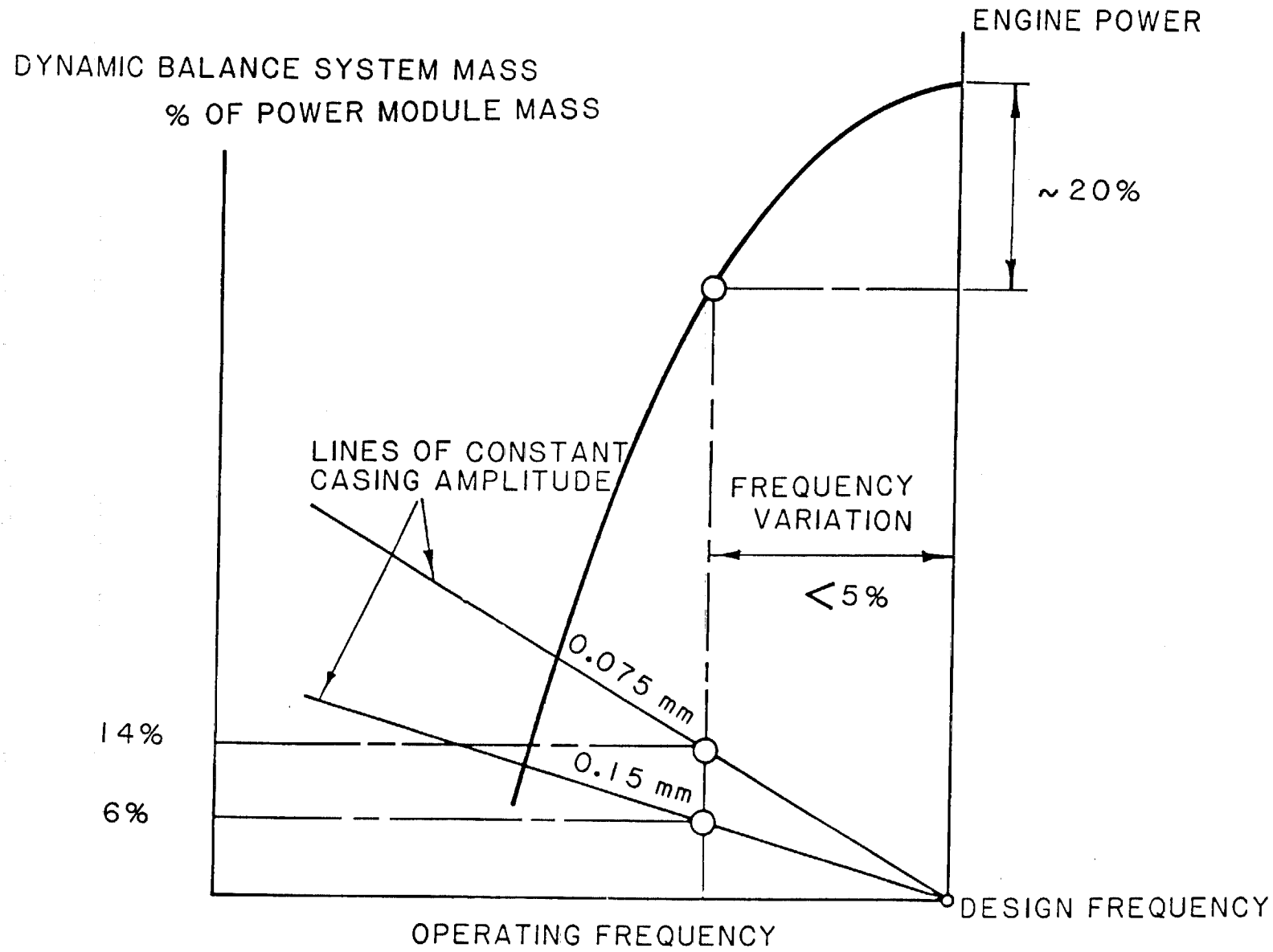

Figure 43: DYNAMIC BALANCE SYSTEM MASS

NASA
C-84-5210

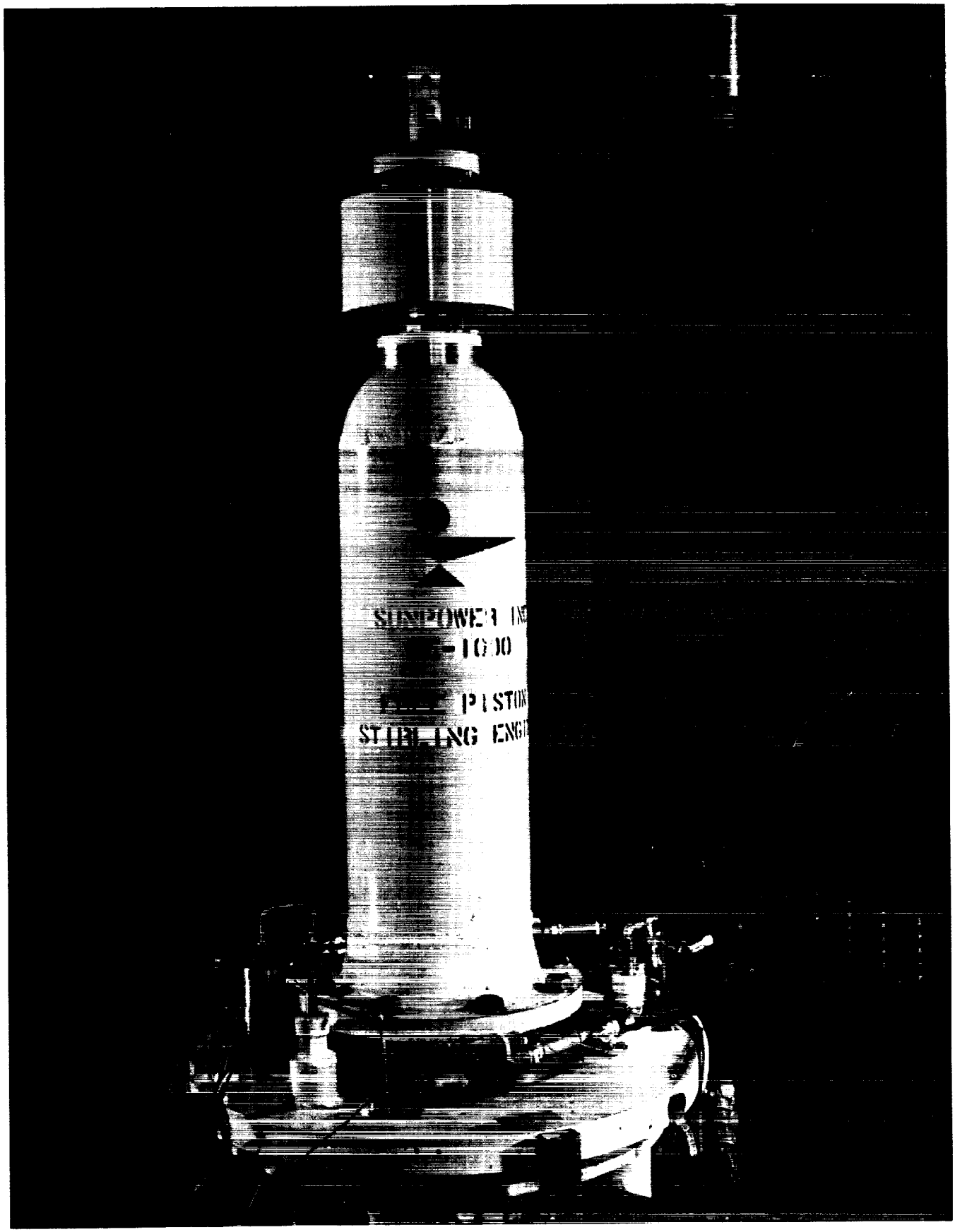

Figure 44a: BALANCE UNIT INSTALLED ON NASA-LEWIS RE-1000

ORIGINAL PAGE
BLACK AND WHITE PHOTOGRAPH

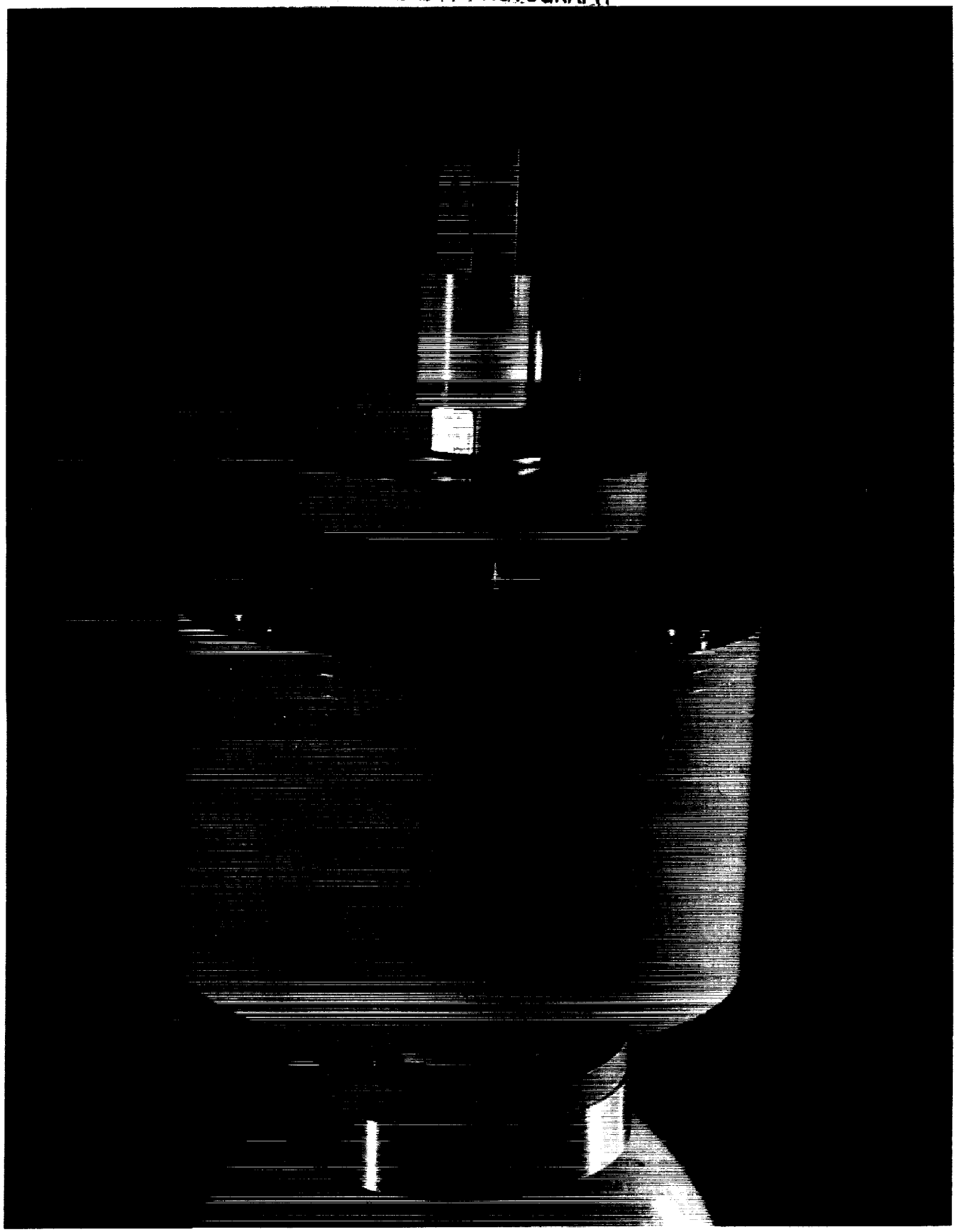

Figure 44b: BALANCE MASS

be varied by ± 0.5 hertz by removing or adding a mass ring. The mass of the engine power piston was 6.2 kg and the mass of the displacer was 0.4 kg. The total sprung mass solidly coupled to the engine housing was approximately 200 kg.

The test results with the passive dynamic absorber on the RE-1000 are shown in Figures 45 through 47. Figure 45 shows vibration amplitude measured on the engine housing as a function of engine frequency and absorber mass. The frequency of the engine was varied by changing the engine mean pressure level. Also, shown is the vibration amplitude of the unbalanced engine (no absorber). Figure 46 is a plot of the amplitude of the absorber (with respect to the housing) and the housing amplitude. Finally, Figure 47 compares the test data with theoretical values of the housing amplitude. The lowest measured values of housing amplitude were within the accuracy of the instrumentation used to make the measurements; the instrumentation accuracy was about ± 0.03 mm.

The test results from this demonstration clearly indicate that the basic concept of the dynamic absorber can be employed to radically reduce casing motion and internal forces transmitted to the spacecraft. Since the spring rates of the passive balance unit cannot be changed during operation, the natural frequency of the balancer is fixed; this requires a design band width equal to the full range of possible engine operating frequencies (Figure 48). With an adaptive dynamic absorber, the required operating band width, due to engine frequency variation, is immaterial since the balance unit can drive its natural frequency to a point very close to the operating frequency of the engine.

Figure 49 shows a comparison between a passive and adaptive balance unit and its impact on the specific mass of a power module. The engine used as a reference is the T_H/T_C = 875 K design from the parametric study, which has a frequency of about 100 hertz and a specific mass of 5.5 kg/kW(e) without the absorber unit. It is assumed that the mounting springs between the power module and the spacecraft have a natural frequency of

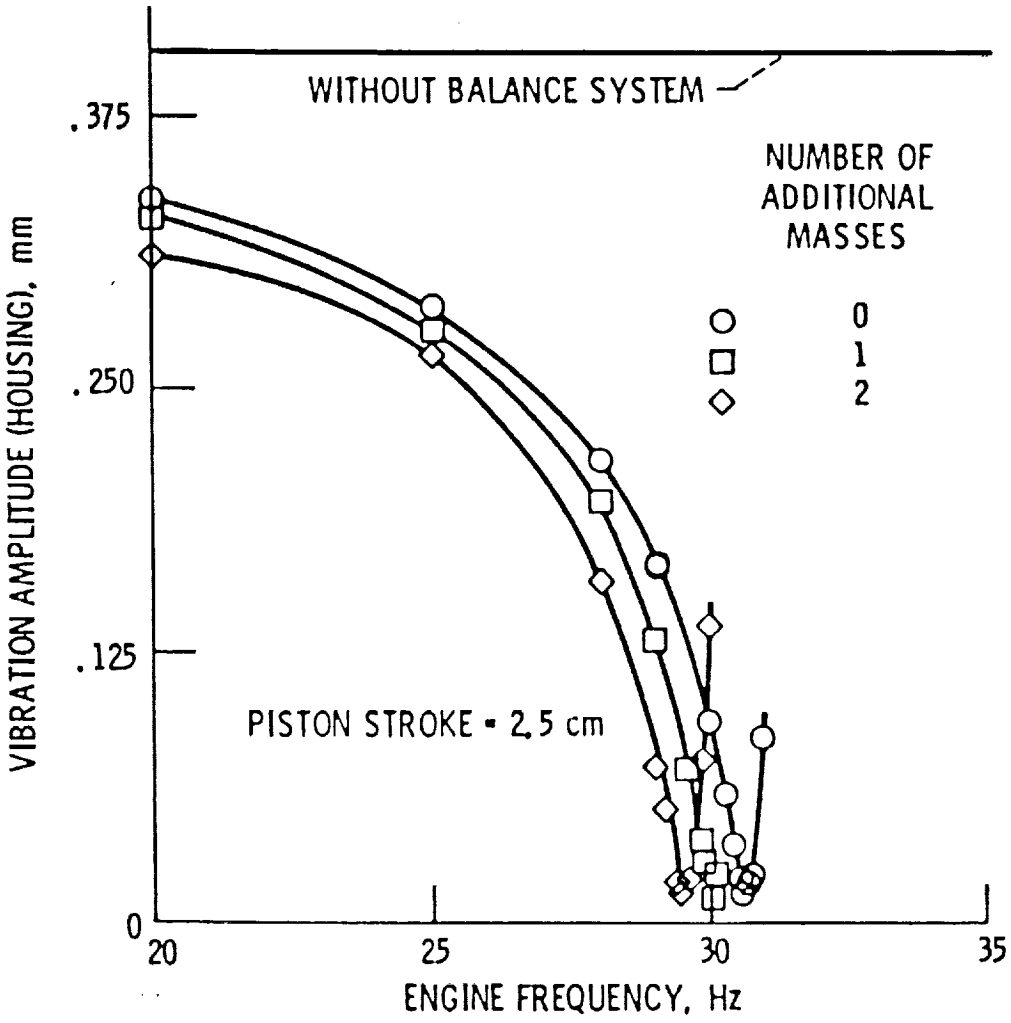

Figure 45: RE-1000 ENGINE VEBRATION AMPLITUDE VS. FREQUENCY WITH AND WITHOUT BALANCE SYSTEM

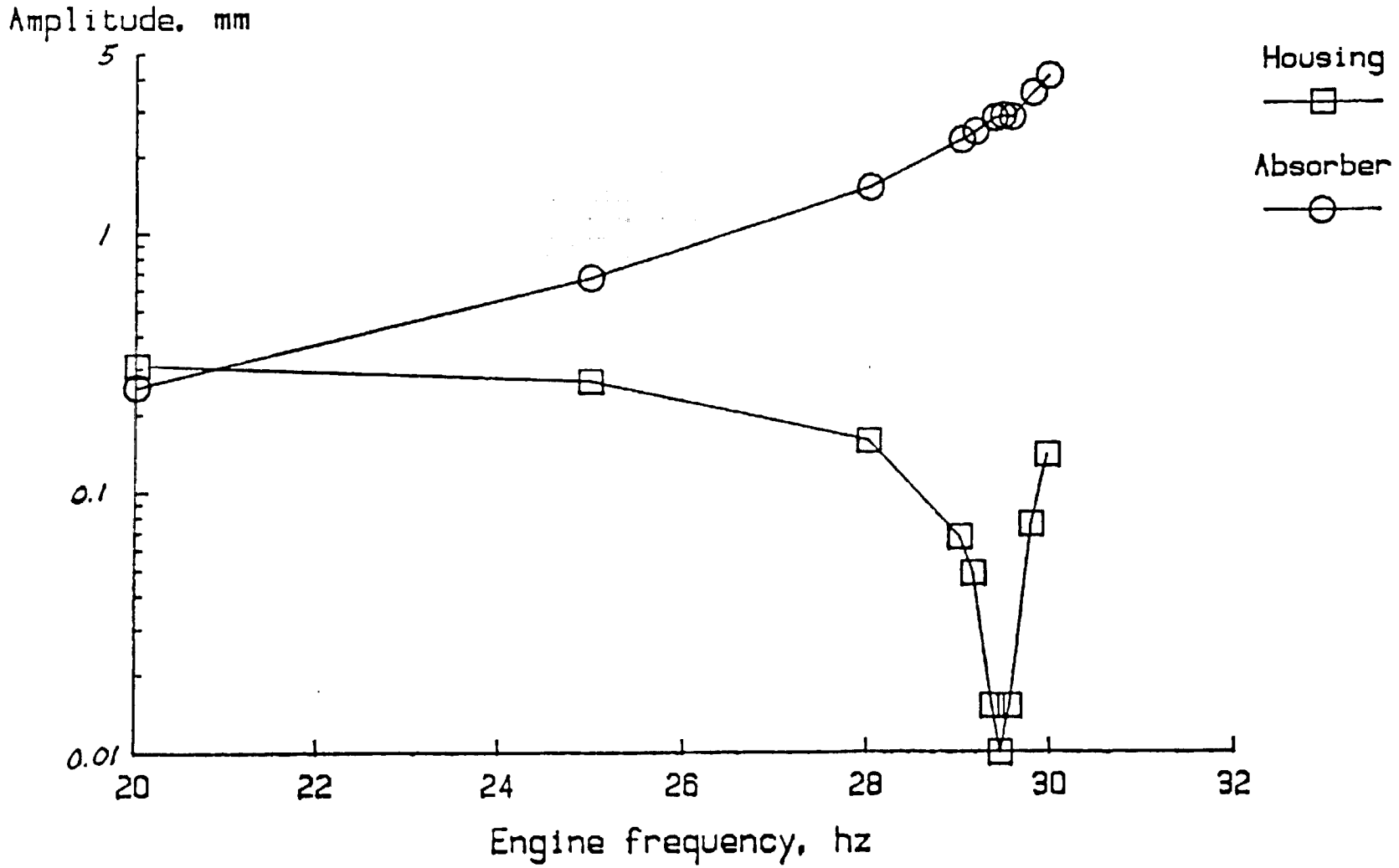

Figure 46: RE-1000 ABSORBER AND HOUSING AMPLITUDES VS. FREQUENCY

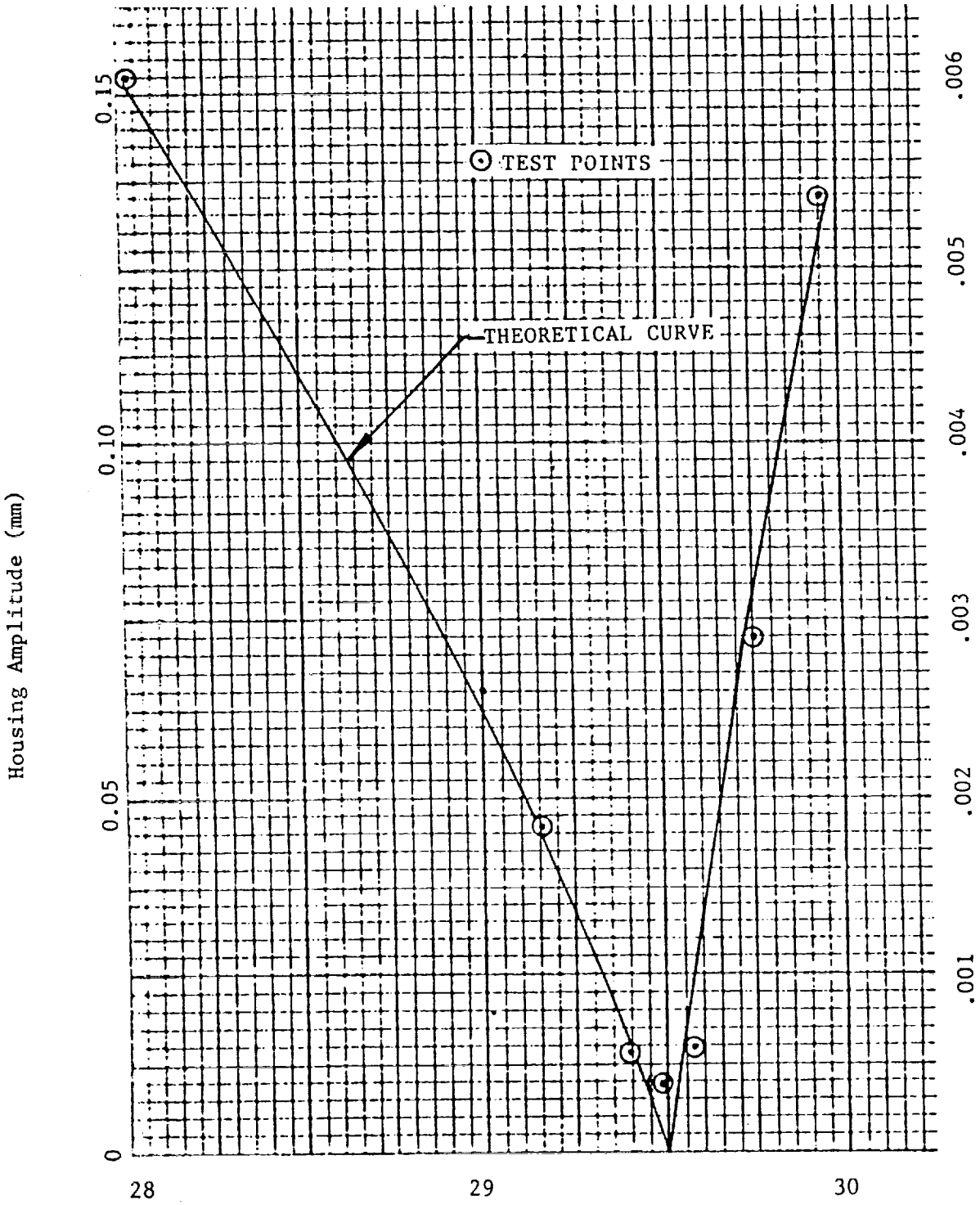

Figure 47: RE-1000 HOUSING AMPLITUDE COMPARED TO THEORETICAL VALUES

(2.5 CM PISTON STROKE WITH TWO ABSORBER MASS RINGS)

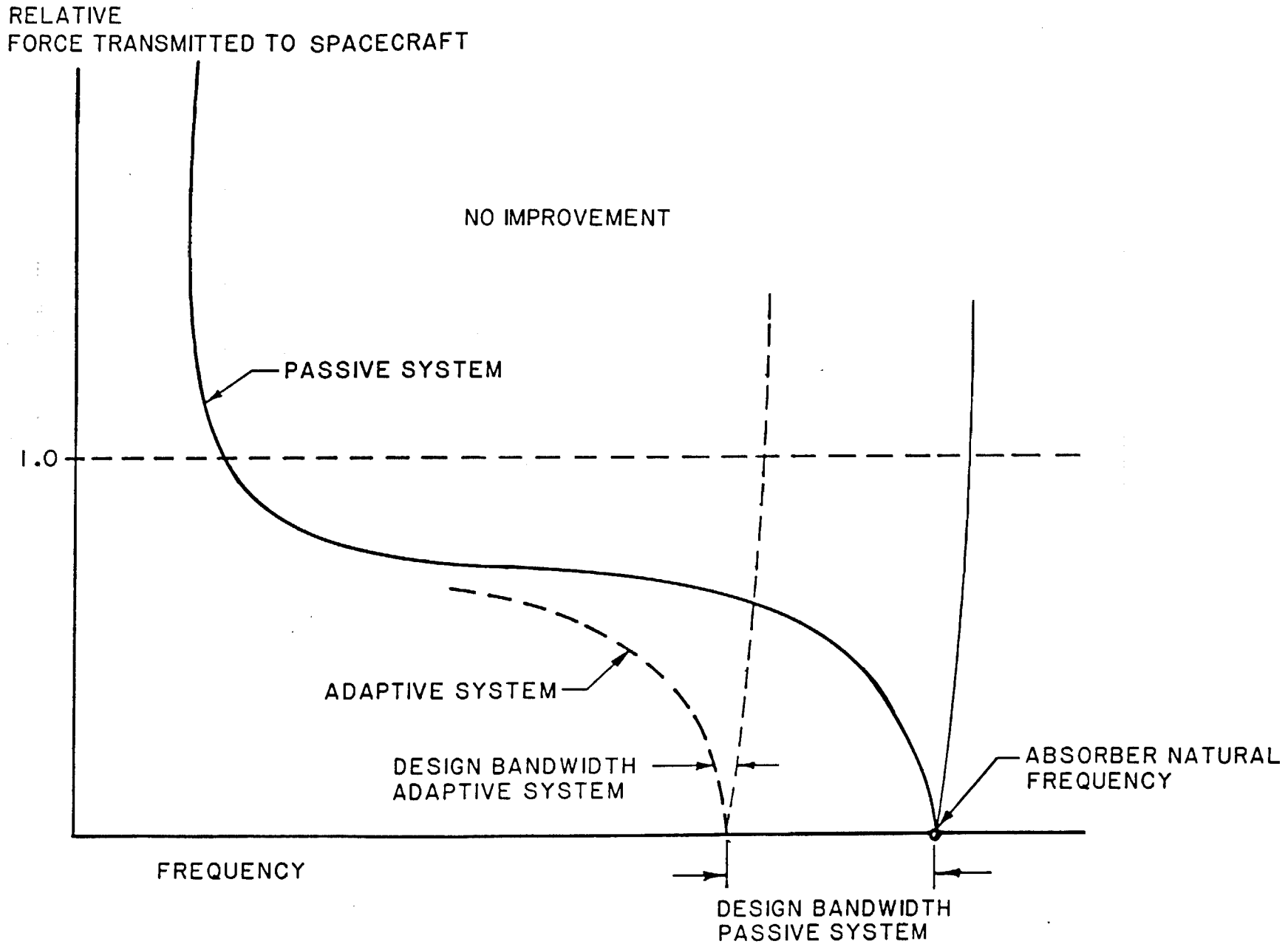

Figure 48: DYNAMIC BALANCE SYSTEM OPERATING CHARACTERISTICS

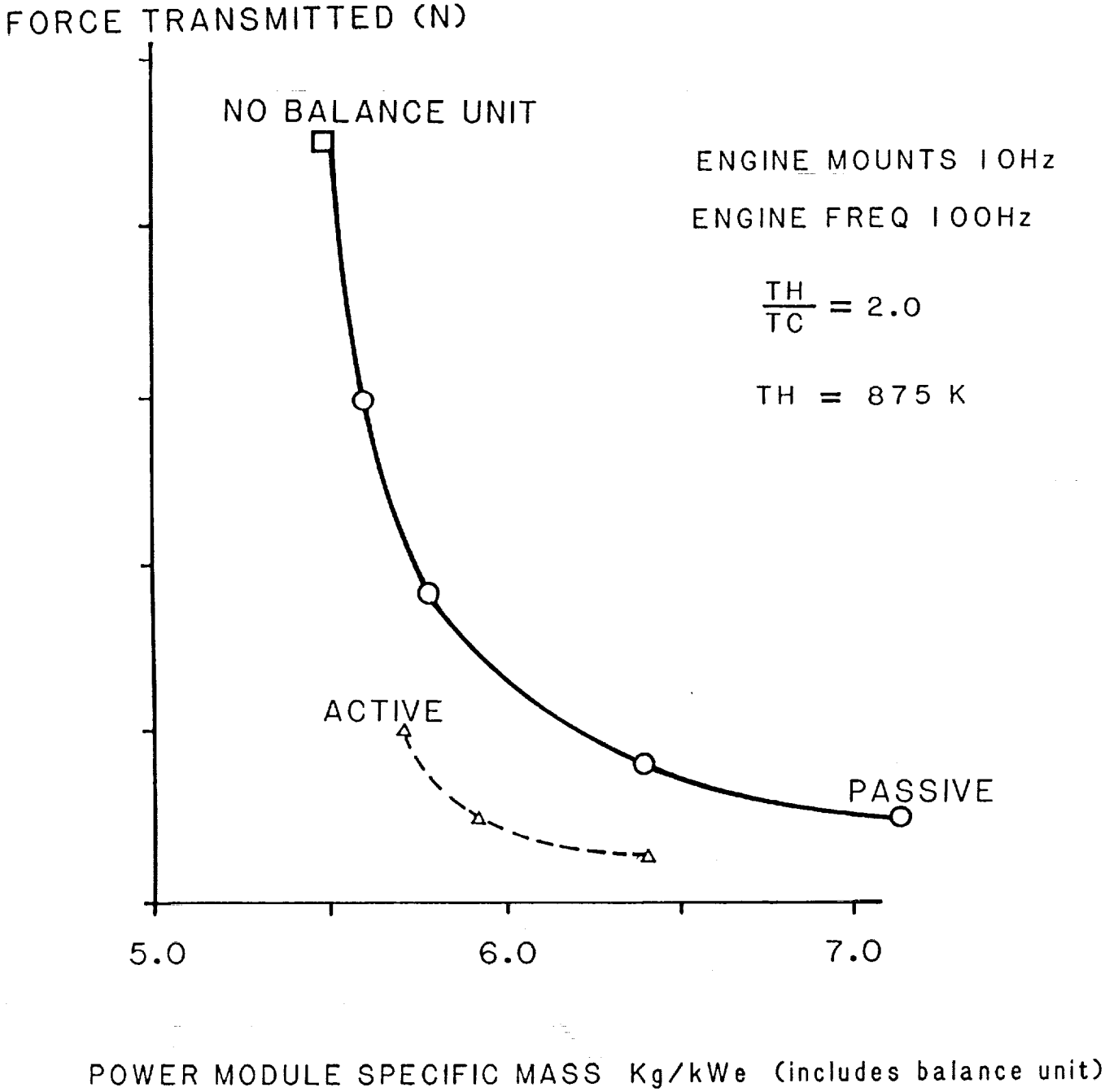

Figure 49: IMPACT OF PASSIVE AND ADAPTIVE BALANCE UNITS ON POWER MODULE SPECIFIC MASS

10 hertz. This value can be adjusted within a reasonably wide range if necessary to avoid spacecraft-power module interactions without affecting the results to any significant degree.

The baseline passive balance unit previously investigated increased the specific mass of the engine module to 6.4 kg/kW(e) and reduced the transmitted force to about 1/6 that of the unbalanced engine. An adaptive unit transmitting an equivalent force is estimated to increase the module specific mass only to 5.7 kg/kW(e) or reduce the transmitted force to 1/18 that of the unbalanced unit at a specific mass of 6.4 kg/kW(e). The basic arrangement of such a system was shown previously in Figure 30. The logic system in this case simply tries to drive the measured casing acceleration to zero by varying the spring rate of the balance unit. The design band width for the adaptive balance unit employed in these calculations assumed a value of 0.5 hertz which is quite conservative based on existing instrumentation capabilities. Since gas springs would be employed, either the spring pressure, cross sectional area, or volume can be changed to vary the spring rate. Over the range of operating frequencies that cause a 25 percent variation in power output of the engine, spring parameters would have to undergo changes of only 4 percent from their nominal values. The most reasonable configurations vary either pressure or volume, as shown in Figure 50.

One interesting situation that the control logic must deal with is determining which "side" of the natural frequency of the absorber the engine is operating, see Figure 47. Normally the engine should operate below the absorber natural frequency ("left side"). If, however, it gets on the "right side," the sensitivity to minor frequency changes is extremely high and could lead to a major increase in forces transmitted to the spacecraft.

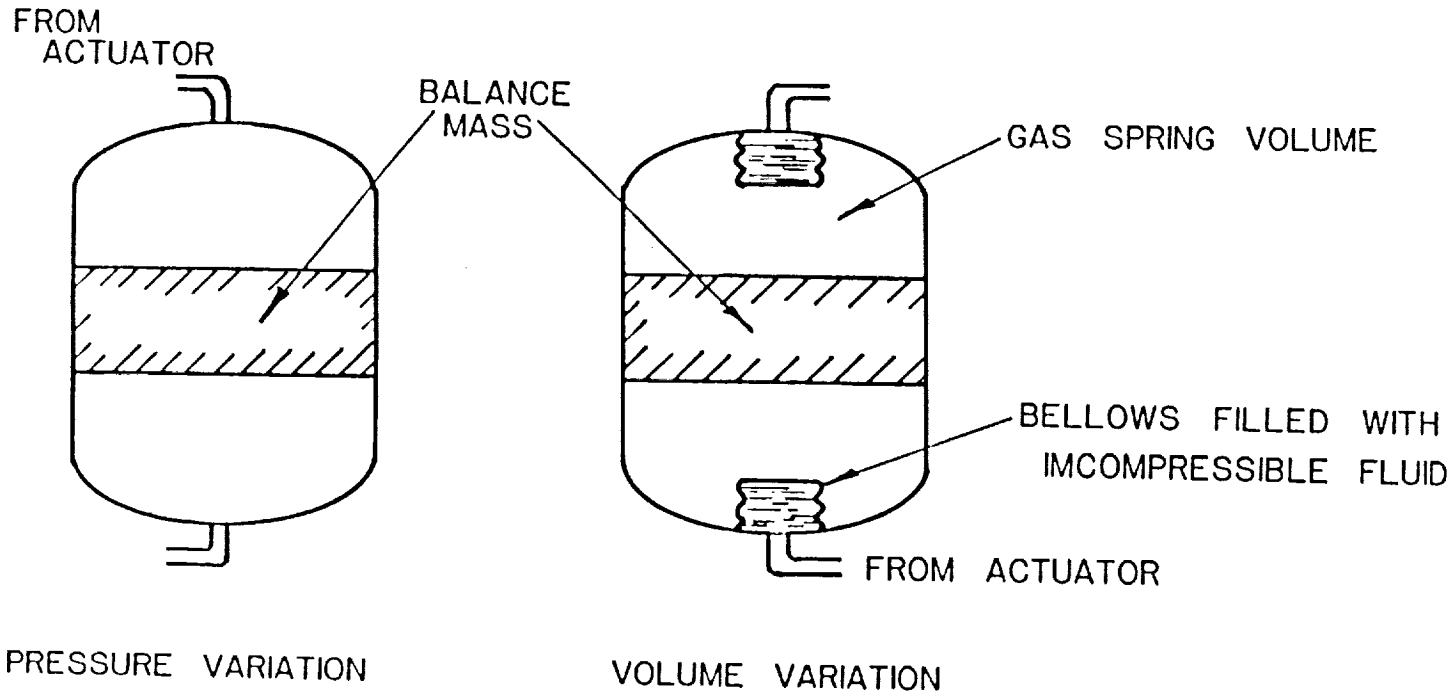

Figure 50: VARIABLE GAS SPRING CONCEPTS

Conclusions

The results of the Task 1 parametric review represent a realistic assessment of the performance and specific mass potential of the FPSE/LA concept when directed toward the SP-100 power module requirements. However, the results were somewhat conservative due to the nature of the design constraints employed in the development of these reference engines. Thus, the original work was followed by an estimation of the growth potential of the designs.

It is felt that improvements on the order of 10 percent for the specific mass of the engines can be expected with refinements to the designs. From the viewpoint of engine performance, more uncertainty exists as to the potential improvements. This is primarily due to unique loss mechanisms which are aggravated by the simultaneous requirements of high performance and low engine specific mass. Until these loss mechanisms are better understood, either by further analysis or actual experimental tests, questions will exist on the potential growth of these designs.

Based on the Task 1 results, specific mass values in the range of 6 kg/kW(e) can be attained without major material or structural problems for the lower temperature designs (T_H = 875 K). At the higher operating temperature (T_H = 1075 K), material joining technology problems might compromise the specific mass; these should be resolved in a reasonable power module development program. All other materials employed in components which have a significant impact on specific mass are within current materials technology. Selection of the materials for the high performance linear alternator, running at reasonably high operating temperatures (above 475 K), however, will require very careful review. This is particularly true for the rare earth magnets.

It is also clear that reducing the operating temperature ratio to 1.5 caused the engine designs to enter a regime quite different from that encountered at temperature ratios of 2.0 and 1.75. In all cases, the engine performance became extremely sensitive to relatively small changes in the basic engine operating characteristics which were being varied to reduce specific mass. This made selection of a clear optimum design at this temperature ratio questionable; therefore, caution should be employed if this information at temperature ratios of 1.5 is used for systems analysis.

The Task 2 design effort produced a conceptual design of a 1080 K FPSE/LA with a temperature ratio of 2.0 to match the requirements of the overall Stirling power systems designs being considered at that time. An insulated heater head concept allowed the use of superalloy materials throughout most of the hot end. The refractory metal, Nb-1Zr, was used for the heat exchanger modules which are in contact with liquid metal. The efficiency, including the linear alternator, was 28.5 percent and the specific mass, including an adaptive dynamic balance unit, was 5.8 kg/kW(e); these values agree well with the growth estimates for this temperature ratio from the Task 1 parametrics.

Compatibility and joining characteristics of the refractory alloy are one of the principal issues in the design. In particular, a question exists as to the effect of contamination of the refractory metal by materials transported by the working gas from other parts of the engine. A second issue concerns the impact on engine mass and efficiency of the large temperature drops across the engine heater in the liquid-metal pumped loop. The large temperature drops are a result of the low liquid-metal mass flow rates chosen to match the values determined from the overall power system design. The use of a heat pipe in future designs of the hot end may offer significant reductions in the temperature gradient currently encountered.

The design work was supported by the hardware demonstration of two of the component concepts. The first demonstrated noncontact operation of the displacer

hydrodynamic gas bearing; this was achieved by spinning the displacer by impacting the cycle gas flow on turbines mounted on the base of the displacer. The spin rate was about 10 hertz. There was no evidence of bearing instability nor any obvious decrement of the engine performance.

During the gas bearing program, it became evident that the primary problem was in maintaining the very small gaps in the concentric displacer components operating in an environment of high thermal gradients and thermally induced deflections. During the brief times that the necessary fits and alignments were actually achieved, the displacer was easily spun with very low power input from the turbine, and the bearing worked well without contact. From this, it was concluded that the concept of a turbine-spun noncontact gas bearing was viable. Potential solutions to the problem of maintaining the rigidity of the basic structure include the use of stiff materials with low thermal expansion and designs which avoid high thermal gradients in the bearings area and, as possible, avoid concentric close fits.

In the second hardware demonstration, a passive dynamic balance unit tested on the RE-1000 engine at NASA Lewis showed that radical reductions in the vibration amplitudes could be achieved. The mass penalty for a passive balance unit as employed in the Task 1 parametric designs was on the order of 10 percent to 15 percent of the total engine mass. For an adaptive balance unit, as used on the Task 2 engine design, the penalty becomes much smaller, with the moving balance mass representing only about 4 percent to 5 percent of the total engine mass.

References

1. Brown, Alec T.: *Space Power Demonstrator Engine, Phase 1 Final Report.* NASA CR-179555, MTI 87TR36, 1987.

2. Slaby, Jack G.: *1988 Overview of Free-Piston Stirling Technology for Space Power at the NASA Lewis Research Center.* NASA TM 100795, 1988.

3. Penswick, L. Barry: *1050 K Stirling Space Engine Design.* NASA CR-182149, 1988.

4. Boser, O.: *The Stirling Engine as a High Temperature Pressure Vessel.* Engineering Aspects of Creep. Vol. II, 1980.

5. Brunson, Gordon and Beale, William: *Develop Lube Gas Bearing for FPSE with Linear Alternator, Final Report.* DOE Phase II DE-ACQ2-85ER80268, 1989.

NASA
National Aeronautics and Space Administration

Report Documentation Page

1. Report No.	2. Government Accession No.	3. Recipient's Catalog No.
NASA CR-182168		

4. Title and Subtitle	5. Report Date
Free-Piston Stirling Engine Conceptual Design and Technologies for Space Power Phase I—Final Report	January 1990
	6. Performing Organization Code
7. Author(s)	8. Performing Organization Report No.
L. Barry Penswick, William T. Beale, and J. Gary Wood	None
	10. Work Unit No. 586-01-11
9. Performing Organization Name and Address	11. Contract or Grant No.
Sunpower, Inc. 6 Byard St. Athens, Ohio 45701	NAS3-23885
	13. Type of Report and Period Covered Contractor Report Final
12. Sponsoring Agency Name and Address	14. Sponsoring Agency Code
National Aeronautics and Space Administration Lewis Research Center Cleveland, Ohio 44135-3191	

15. Supplementary Notes

Project Manager, Lanny Thieme, Power Technology Division, NASA Lewis Research Center. L. Barry Penswick and William T. Beale, Sunpower, Inc. J. Gary Wood, Consultant, 3996 Marion Johnson Rd., Albany, Ohio 45710.

16. Abstract

As part of the SP-100 program, Sunpower, Inc. completed under contract for NASA Lewis a phase I effort to design a free-piston Stirling engine (FPSE) for a space dynamic power conversion system. SP-100 is a combined DOD/DOE/NASA program to develop nuclear power for space. This work by Sunpower was completed in the initial phases of the SP-100 program prior to the power conversion concept selection for the Ground Engineering System (GES). Stirling engine technology development as a growth option for SP-100 is continuing after this phase I effort. Following a review of various engine concepts, a single-cylinder engine with a linear alternator was selected for the remainder of the study. The relationships of specific mass and efficiency versus temperature ratio were determined for a power output of 25 kWe. This parametric study was done for a temperature ratio range of 1.5 to 2.0 and for hot-end temperatures of 875 K and 1075 K. Sunpower then completed a conceptual design of a 1080 K FPSE with a linear alternator producing 25 kWE output. This was a single-cylinder engine designed for a 62,000 hour life and a temperature ratio of 2.0. The heat transport systems were pumped liquid-metal loops on both the hot and cold ends. These specifications were selected to match the SP-100 power system designs that were being evaluated at that time. The hot end of the engine used both refractory and superalloy materials; the hot-end pressure vessel featured an insulated design that allowed use of the superalloy material. The design was supported by the hardware demonstration of two of the component concepts—the hydrodynamic gas bearing for the displacer and the dynamic balance system. The hydrodynamic gas bearing was demonstrated on a test rig at Sunpower. The dynamic balance system was tested on the 1 kW RE-1000 engine at NASA Lewis.

17. Key Words (Suggested by Author(s))	18. Distribution Statement
Stirling engine Heat engine Space power Gas bearings Dynamic balance system	Date for general release January 1992 Subject Category 20

19. Security Classif. (of this report)	20. Security Classif. (of this page)	21. No. of pages	22. Price*
Unclassified	Unclassified	139	A07

NASA FORM 1626 OCT 86